THE GEOCHEMISTRY AND ORIGIN OF PEGMATITES CHEROKEE-PICKENS DISTRICT, GEORGIA

Alexander J. Gunow
and
Gregory N. Bonn

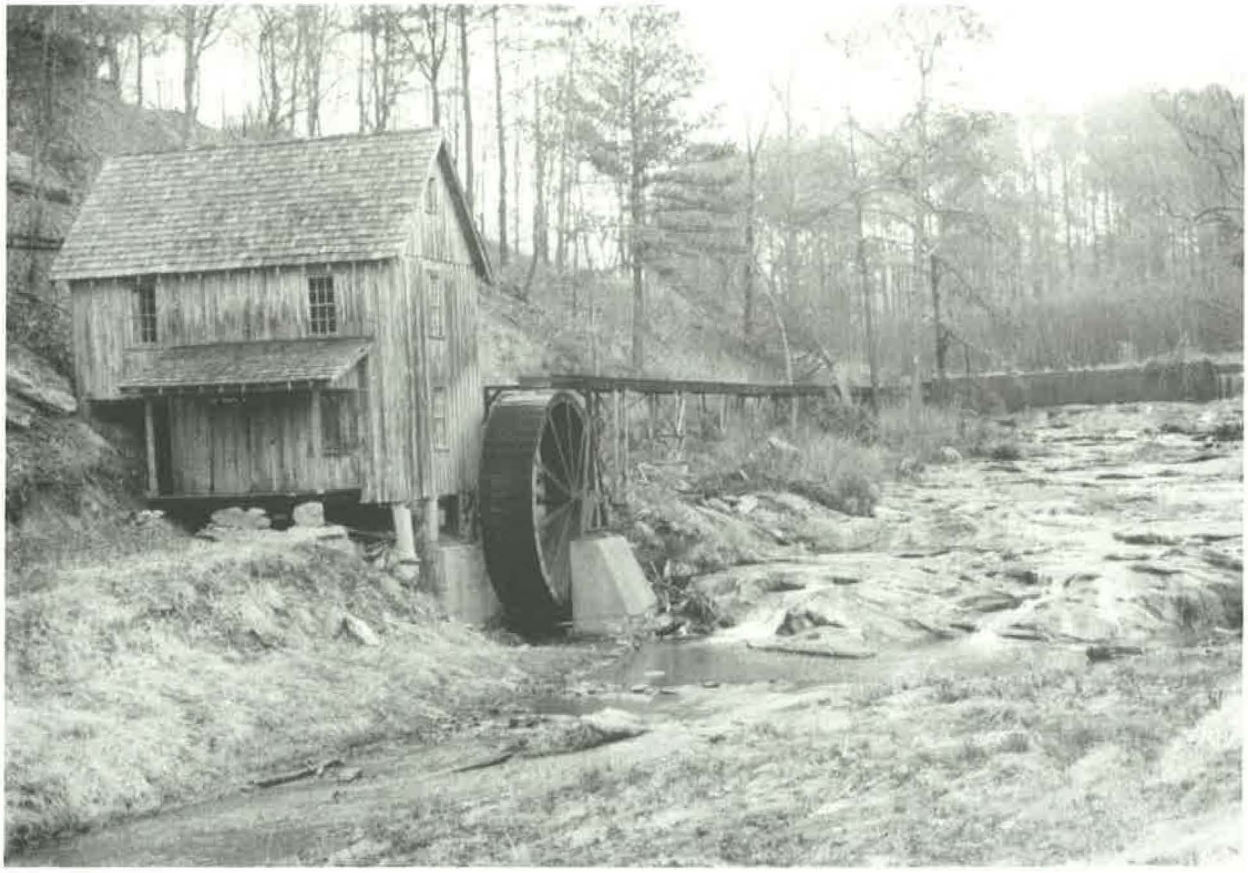

DEPARTMENT OF NATURAL RESOURCES
ENVIRONMENTAL PROTECTION DIVISION
GEORGIA GEOLOGIC SURVEY

BULLETIN 103

Cover photo: Pegmatites in the stream bed of Toonigh Creek, Cherokee County.

THE GEOCHEMISTRY AND ORIGIN OF PEGMATITES CHEROKEE-PICKENS DISTRICT, GEORGIA

Alexander J. Gunow
and
Gregory N. Bonn

Georgia Department of Natural Resources
J. Leonard Ledbetter, Commissioner

Environmental Protection Division
Harold F. Reheis, Assistant Director

Georgia Geologic Survey
William H. McLemore, State Geologist

Atlanta
1989

BULLETIN 103

TABLE OF CONTENTS

LIST OF FIGURES

LIST OF PLATES

LIST OF TABLES

THE GEOCHEMISTRY AND ORIGIN OF PEGMATITES CHEROKEE-PICKENS DISTRICT, GEORGIA

Alexander J. Gunow
and
Gregory N. Bonn

ABSTRACT

The pegmatites of the Cherokee-Pickens district of Georgia occur in two major pegmatite fields contained within late Precambrian to early Paleozoic metasedimentary and metaigneous host rocks. The regional metamorphism is characterized by kyanite-grade, Barrovian-type facies (middle amphibolite facies). The pegmatite fields (Holly Springs and Ball Ground) are located within separate thrust sheets defined by the major northeast-trending faults of the district, and are separated by the Allatoona thrust sheet which is barren of pegmatites. The barren thrust sheet is anomalous in that the regional metamorphic grade is generally lower than the surrounding sheets. The Dahlonega gold belt coincides with the Allatoona thrust sheet.

The pegmatites of this district are generally concordant with host rock foliation along north to northeast trends and several exhibit internal zonation features. The pegmatites of the Holly Springs field lack tourmaline and beryl, whereas all of the pegmatites of the Ball Ground field contain tourmaline ± beryl. None of the pegmatites observed within the district appear to contain significant rare earth element (REE) or columbite mineralization.

Comparison of trace element analyses of muscovite from these pegmatite fields indicate relatively low values and ratios for incompatible trace elements within the Holly Springs field (Li < 50 ppm, F < 2,000 ppm, Be < 7 ppm, Nb < 100 ppm, and Rb ppm/K% < 50). The tourmaline-bearing, beryl-poor pegmatites of the Ball Ground field exhibit trace element values similar to that of the Holly Springs field but Rb ppm/K% ratios are generally higher (32-94). The tourmaline and beryl-bearing pegmatites of the Ball Ground field exhibit significant enrichment in several incompatible trace elements (Nb > 200 ppm, Be > 20 ppm, Rb ppm/K% > 100). These trends suggest that the beryl-bearing pegmatites are more strongly fractionated than other pegmatites of the district and that rare element mineralization within the beryl-bearing pegmatites coincides with the extent of pegmatite differentiation.

Based on the geochemical data and field observations of this study, the Cochran pegmatite is the most strongly differentiated pegmatite of the district. Muscovite analyses from this deposit indicate anomalous enrichment in incompatible trace elements (Nb > 275 ppm, Be > 24 ppm, Li > 150 ppm, F > 2,700 ppm, and Rb ppm/K% > 150). The Cochran pegmatite is a zoned pegmatite, which contains abundant feldspar, sheet muscovite, and beryl. It exhibits wall rock tourmalinization and internal replacement features. A sample of muscovite from this deposit yields a K/Ar apparent age date of 356±20 m.y., suggestive of a postpeak metamorphic age for this pegmatite. The Cochran pegmatite is deeply saprolitized and contains powdery microcline ± kaolinite to a depth of at least 10 meters. Based on outcrop exposures, the Cochran pegmatite contains at least 250,000 tons of pegmatite as proven reserves; 550,000 tons of probable reserves, and possible reserves of 1.2 million tons, assuming a significant northwest extension from the present workings.

All of the pegmatites within the Cherokee-Pickens district belong to the muscovite class of Cerny (1982a). However, the beryl-bearing pegmatites of the district show a geochemical affinity to the rare element class of pegmatites.

Variations in incompatible element enrichment for pegmatites within the district is attributed to differences in the level of pegmatite emplacement relative to the differentiation history of a presumed parental granite magma. Processes contributing to differentiation within the parental granite may include partial melting, vapor fractionation, crystal fractionation, liquid state diffusion, and thermogravitational diffusion.

The role of volatiles may be of particular significance in enhancing differentiation by lowering melt viscosity and crystallization temperature. In this regard, boron may have played an important role by promoting differentiation in the tourmaline-bearing pegmatites of the Ball Ground field.

The results from this study indicate that muscovite is excellent material for use in geochemical exploration for rare element-enriched pegmatites in the southeastern

United States. Muscovite provides a ubiquitous and correlative medium to assess geochemically the rare element potential of pegmatites and to determine the relative extent of differentiation among pegmatites of a district.

ACKNOWLEDGEMENTS

This pegmatite project is an outgrowth of the work set forth by many former and present members of the Georgia Geologic Survey. The comprehensive study of the Georgia pegmatite deposits by A.S. Furcron and K.H. Teague provided the initial background to an understanding of the character and distribution of pegmatite deposits within the district. The Atlanta Regional Map by K.I. McConnell and C.E. Abrams provided a recent geologic framework for this study. The field and laboratory studies of the pegmatite project were significantly assisted by staff of the Georgia Geologic Survey. L.M. Wampler of Georgia Tech performed the K/Ar analyses and provided the age determinations for muscovite from the Cochran Mine and the Hillhouse pegmatite.

The authors thank J.M. German, R.L. Atkins, B.J. O'Connor, E.A. Shapiro and P.C. Perley for their helpful suggestions and review. Outside technical review of the manuscript was performed by W.B. Size, D.A. Vanko, and J.A. Whitney. Finally, the authors extend thanks to Jack Parkman, owner, for allowing access to the Cochran deposit.

INTRODUCTION

Purpose

Numerous pegmatite occurrences are known within the Blue Ridge and Piedmont physiographic provinces of the Southeast. These pegmatites vary from minor dikes, sills and pods to large deposits up to several hundred meters long and over 30 meters wide. Most of the productive pegmatites have been mined as a source of mica or feldspar, but some contain associated minerals enriched in rare elements. The associated minerals, if present in sufficient quantity, provide a viable resource for some important rare elements. Examples include beryl for Be, columbite-tantalite for Nb and Ta, spondumene for Li, and monazite, allanite or titanite, as sources for rare earth elements (REE).

Pegmatite districts in the Blue Ridge physiographic province extend from northwestern North Carolina to northern Georgia in a 65 km wide belt (Figure 1). The Blue Ridge physiographic province contains the well-known Spruce Pine pegmatite district of North Carolina. The pegmatite districts in the Piedmont physiographic province are more widely distributed in a 160 km wide belt extending from Central Virginia to eastern Alabama. The Li-enriched pegmatite districts of Amelia, Virginia, and Shellby-Hickory (Kings Mountain), North Carolina, are notable examples of rare element pegmatites in the Piedmont province (Glass, 1935; Kesler, 1961, 1976). In the past, most major pegmatites in Georgia were mined as a source of muscovite (Furcron and Teague, 1943). To date, there has not been a study in Georgia that investigated the rare element potential of pegmatites. As a consequence, the byproduct[1] and strategic mineral[2] potential of these pegmatites are relatively unknown.

A pegmatite project has been initiated by the Georgia Geologic Survey to investigate this potential. In its entirety, the pegmatite project involves a comprehensive geochemical investigation of the major pegmatite districts in Georgia. Specific districts of interest include the Cherokee-Pickens, Troup, Thomaston-Barnesville, Hartwell and North Georgia districts (Figure 1).

The present study concerns an investigation of selected pegmatites from the Cherokee-Pickens district. It provides a convenient method for assessing the rare element potential of pegmatites within the district, and presents a geologic framework for understanding the nature and origin of rare element enrichment in pegmatites.

Province Classification, Terminology, and Location

There is an important distinction between physiographic and lithologic classifications of the Piedmont and Blue Ridge provinces. According to the physiographic divisions shown in Figure 1, all of the pegmatites within the Cherokee-Pickens district are considered to be within the Piedmont Province. In contrast, the lithologic province classification presented by McConnell and Abrams (1984) shows the Allatoona fault as the boundary between the Blue Ridge and northern Piedmont provinces in northern Georgia. For clarity, the lithologic classification will be used in reference to provinces within this paper, unless otherwise stated. Thus, the Cherokee-Pickens district is located in the extreme southwestern corner of the Blue Ridge province with a small portion of the district extending into the northern Piedmont province (Figure 2).

Throughout this paper reference will be made to grain size within individual pegmatites or pegmatite zones. In conformance with grain size terminology of pegmatites developed by the U.S.G.S. (Jahns and others,

[1]A secondary or additional product.

[2]Minerals essential to national defense for which, during war, a nation could become wholly or partly dependent upon outside sources, and for which strict distribution and conservation measures are required.

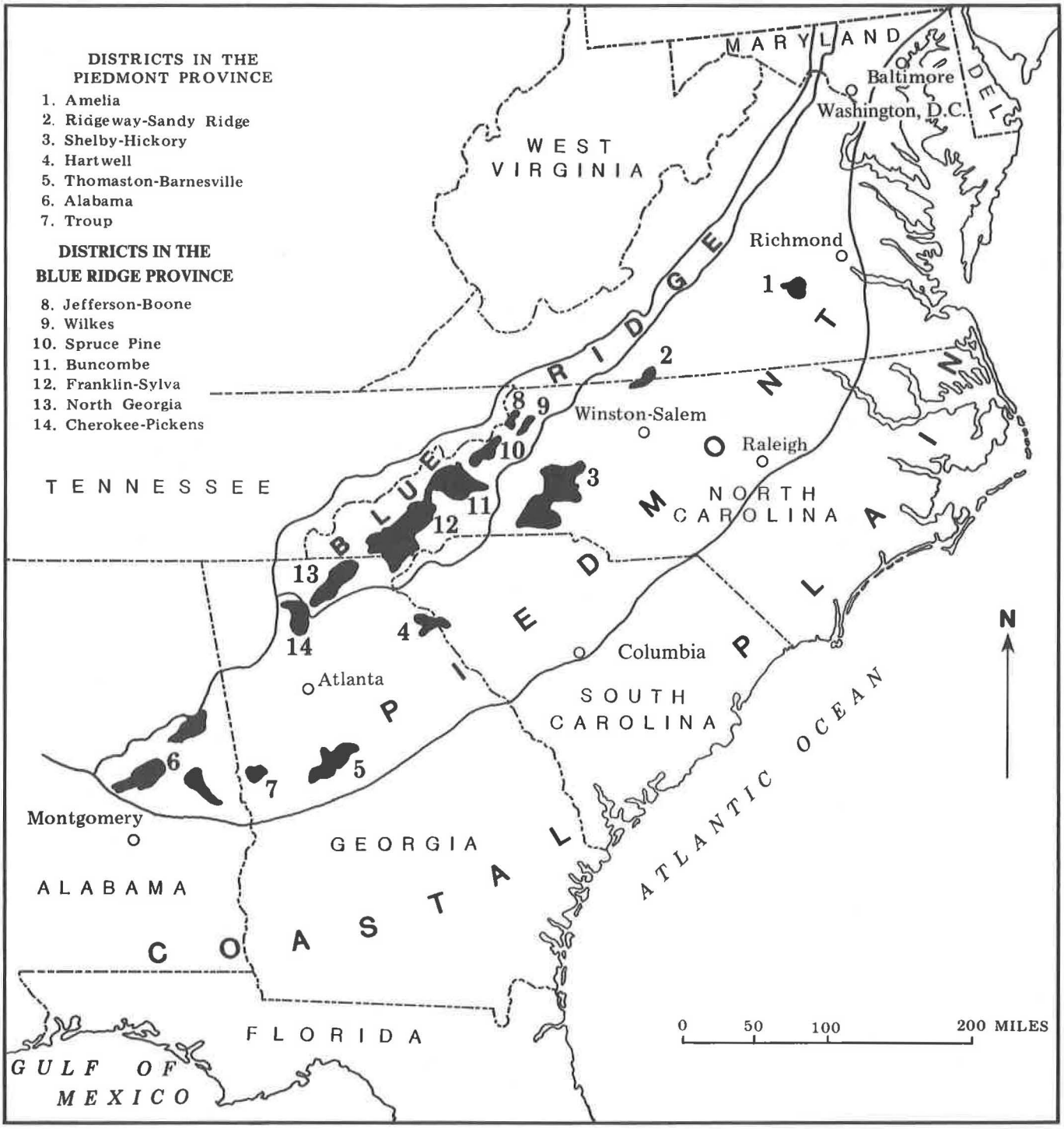

Base From U.S. Geological Survey
1:7,000,000 United States Contour Map, 1975

Modified from Jahns, Griffitts, and Heinrich (1952)

Figure 1. Index map of the southeastern United States showing the location of the main pegmatite districts in the Piedmont and Blue Ridge physiographic provinces.

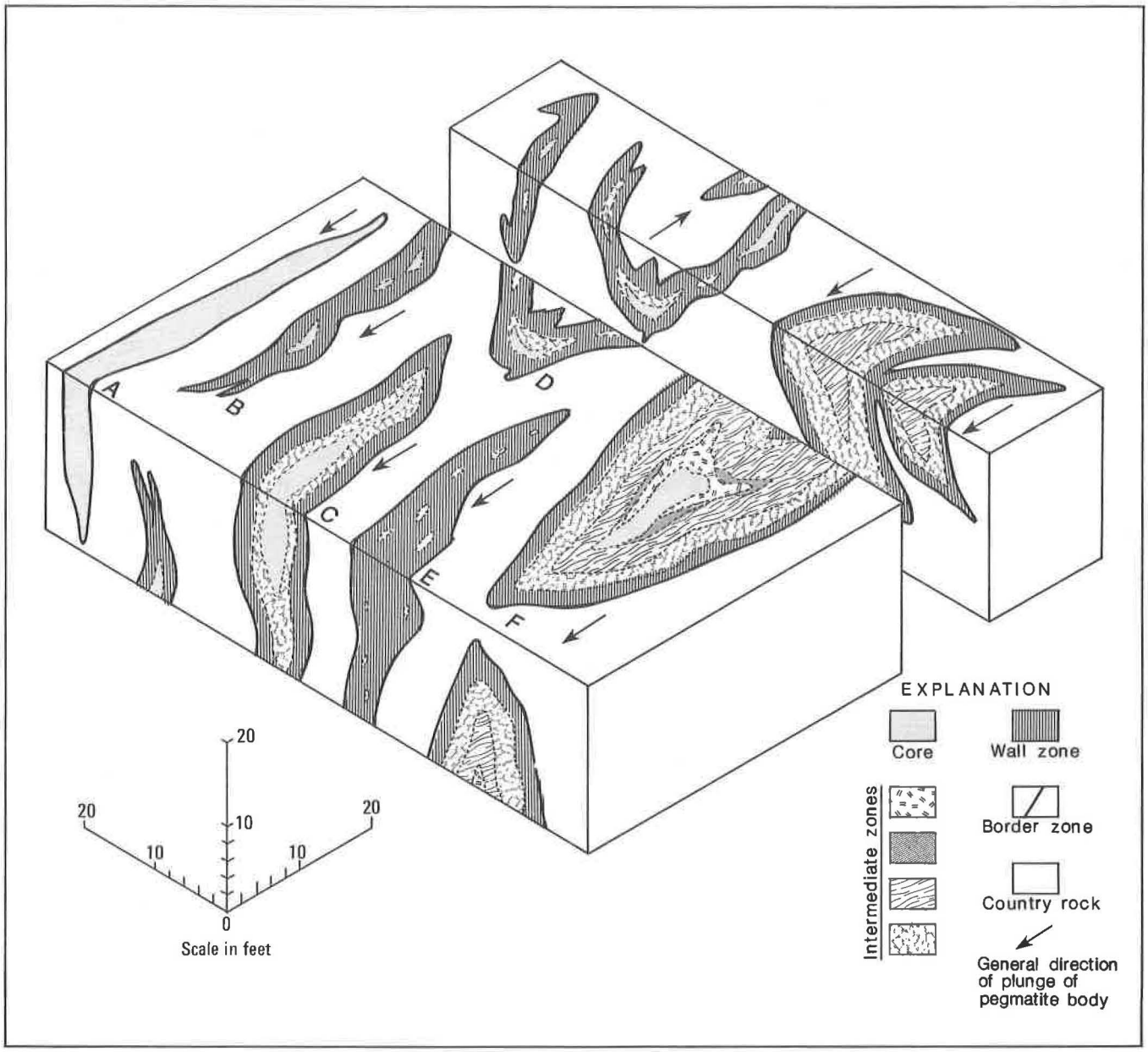

Figure 2. Exploded isometric block diagram, showing the characteristic distribution of completely and partly formed zones in pegmatite bodies. (A) Typical simple bizonal pegmatite. (B) Simple pegmatite with lenticular core. (C) Simple pegmatite with continuous intermediate zone. (D) Troughlike pegmatite with lenticular core and intermediate zone. (E) Simple pegmatite with pod-shaped core segments. (F) Large forked polyzonal pegmatite (Jahns and others, 1952).

1952); fine-grained refers to less than 2.5 cm in diameter; medium-grained refers to 2.5-10 cm; and coarse-grained refers to 10 cm-30 cm.

Pegmatites of the district are divided into two distinct pegmatite fields utilizing the classification of Cerny (1982a). Each is associated with individual thrust sheets of distinct lithologies. In this paper the term pegmatite field refers to a territory of pegmatite bodies having similar economic potential (barren, muscovite- or rare element-rich) with a common geologic-structural environment, age and a presumed common igneous or anatectic source.

Pegmatites of the Cherokee-Pickens district which are within the Blue Ridge province are distributed as a cluster of pegmatites within a 23 km radius of Ball Ground, Georgia, encompassing northeastern Cherokee County and southeastern Pickens County. These pegmatites are designated as the Ball Ground pegmatite field. Those pegmatites within the northern Piedmont province are distributed in a 5 km wide northeast trending group that extends from the Cherokee-Cobb county line through Holly Springs to Lathemtown. These pegmatites are designated as the Holly Springs pegmatite field.

The terrain throughout these pegmatite-bearing regions is rough and hilly with elevations ranging between 300-500 meters above sea level. Most of the mines and prospects within this terrain are accessible by automobile to within 500 meters of the deposits.

Production History

The earliest record of pegmatite mining within the Cherokee-Pickens district is at the Dean Mine, where work dates back to 1889 (Furcron and Teague, 1943). Mica from this deposit was ground on the premises, but the precise use of this mica at this early date is unknown (Galpin, 1915).

From the early 1900's to 1941, several pegmatites were mined for sheet mica and ground mica for use in electrical insulation. From 1941-1944, during World War II, a large subsidy was given to the mica industry by the Federal Government. With the help from this subsidy, pegmatite mining increased in Georgia and the Colonial Mica Corporation, a branch of the Metals Reserve, was established as a purchasing agent for mica. During this period the Colonial Mica Corporation maintained an office in Thomaston, Georgia. This subsidy was removed in early 1945, at which time nearly all mica mines ceased operation.

Renewed interest in pegmatite mining was generated from 1952-1957, as the need for mica and lightweight Be-Cu alloys became crucial. During this period, the General Services Administration attempted to stockpile Be for strategic purposes and agreed to accept up to 25 tons of beryl, per year, from individual domestic producers until June 30, 1957 (Reno, 1956). During this interval over 4,000 lbs of beryl was removed from the Cochran Mine in northeast Cherokee County and slightly over 1,500 lbs of beryl was mined from the Denson Mine in southern Pickens County (Furcron, 1959). During 1985 minor sheet mica, scrap mica and beryl was produced from the Cochran Mine as the result of a small hand-cobbing operation.

Future Production

Future production within the district will depend upon the demand for feldspar, kaolinite, mica, and rare element mineral byproducts such as beryl or columbite-tantalite. The largest pegmatites within the district, those with the greatest near-surface exposure and those enriched in potential byproduct minerals, possess the greatest possibility for future production.

Previous Geologic Studies

One of the earliest studies concerning the pegmatite deposits of Georgia was published by the Georgia Geologic Survey in the early 1900's (Galpin, 1915). This report was largely descriptive and gave the location and geologic features of feldspar, mica, and pegmatite deposits for producing counties in Georgia. Galpin (1915) noted that the host rocks for the granitic pegmatites in Cherokee and Pickens Counties consist of metamorphosed Paleozoic units. He also noted that pegmatites within Cherokee and Pickens Counties are located several miles to the northwest of major granitic outcrops. At the time of Galpin's report, only eight pegmatite mines or prospects were known to exist in Cherokee and Pickens Counties, half of these belonging to the Holly Springs field. Sterrett (1923) summarized the geology of major pegmatite deposits in the United States and documented the geographic distributions and geologic framework of pegmatite deposits in the Southeast. His study provided the first significant compilation of pegmatites throughout the continental United States. McCallie (1926) reviewed the mineral resources of Georgia and mentioned the rise in pegmatite mining activity in the Holly Springs area in the early 1920's. He noted that most pegmatite deposits were not sheared, suggesting a postdeformational age for these pegmatites. Furcron and Teague (1943), in a comprehensive study, documented the occurrence of pegmatite mines and prospects throughout the state of Georgia. Their study included descriptions of mines and prospects within the Cherokee-Pickens district and presented the production history, size, mineralogy and general geologic features of these deposits.

During the early 1940's a coordinated effort by the U.S. Geological Survey (U.S.G.S.) and the U.S. Bureau of Mines was initiated to characterize the major pegmatite

deposits of the Southeast. This effort resulted in detailed maps and drill core data for some of the major pegmatite deposits in Georgia. Within the Cherokee-Pickens district only the Amphlett pegmatite was selected for subsurface exploration, which included five diamond drill holes, all less than 200 feet deep. Beck (1948) published the core log data from the Georgia pegmatite program.

Subsequently, Jahns and Lancaster (1950), Jahns and others (1952), Griffitts and Olson (1953), and Heinrich and others (1953) published the results of the comprehensive U.S.G.S. investigation concerning pegmatite deposits of the Southeast. These publications provide details of the physical characteristics of pegmatitic muscovite, the general features of mica-bearing pegmatites (including their internal structure and mineralogy) and a synthesis of ideas regarding the origin of pegmatites.

With respect to the pegmatites of the Cherokee-Pickens district, Heinrich and others (1953) summarized the findings of Furcron and Teague (1943) and presented the results of the field mapping and diamond drill programs for the Amphlett pegmatite in Cherokee County. As interest in Be increased during the 1950's the beryl-bearing pegmatites in Georgia became more significant. Consequently, Furcron (1959) documented the occurrence of beryl-bearing pegmatites in Georgia. In this paper several beryl-bearing pegmatites were specifically noted in Cherokee and Pickens Counties.

Some of the regional geologic studies relevant to the geology of the Cherokee-Pickens district include those of Bayley (1928), Fairley (1965), Fairley (1969), Costello (1978), McConnell and Costello (1984), and McConnell and Abrams (1984). The regional geologic overview and the accompanying geologic maps presented herein are based on the interpretations given by McConnell and Costello (1984), McConnell and Abrams (1984) and Fairley (1965).

GENERAL GEOLOGIC SETTING

Structure and Stratigraphic Setting

Late Precambrian to early Paleozoic rocks of the Cherokee-Pickens district are divided into two major geologic provinces: the Blue Ridge, north of the northeast-trending Allatoona fault and the Northern Piedmont, south of the Allatoona fault (Plate 1). The Allatoona Fault is interpreted as a thrust fault separating late Precambrian, predominantly metapelitic rocks of the Ocoee Supergroup to the north, from metavolcanic, metasedimentary and metaplutonic rocks of the New Georgia Group to the south (McConnell and Abrams, 1984). Between 6-15 km south of the Allatoona Fault, a second major northeast trending thrust fault, the Chattachoochee fault, separates the New Georgia Group to the north from predominantly metasedimentary rocks of the Sandy Springs Group to the south. Both the Allatoona and Chattahoochee faults are major northeast-trending thrust faults that dip to the Southeast. The New Georgia Group which lies between these two faults is interpreted as a folded and faulted nappe that was overturned and thrust over rocks of the Blue Ridge Province (McConnell and Abrams, 1984). Units of the Sandy Springs Group are believed to be thrust over rocks of the New Georgia Group. The combined effect of imbricate thrusting produced significant crustal shortening (McConnell and Costello, 1979).

The thrust sheet north of the Allatoona fault, within the Blue Ridge lithologic province and in the Cherokee-Pickens district, is referred to in this report as the Great Smoky thrust sheet. The thrust sheet between the Allatoona and Chattahoochee thrust faults is referred to as the Allatoona thrust sheet and the thrust sheet south of the Allatoona fault is referred to as the Chattahoochee thrust sheet. The relative age and sequence of rocks within the district, compared to rocks north of the district, is shown in Table 1.

Corbin Gneiss Complex

The oldest rocks in the Cherokee-Pickens district crop out in the western portion of the district and consist of the Precambrian Corbin Gneiss Complex (Plate 1). This basement complex forms the core of an anticlinorium referred to as the Salem Church anticlinorium. The Corbin Gneiss consists of orthogneiss, generally of quartz monzonite composition, but varying from granite to granodiorite in normative composition (McConnell and Abrams, 1984; Martin, 1974). The Corbin Gneiss Complex experienced granulite facies metamorphism during the Grenville Orogeny, accounting for an age date of the Corbin Gneiss in excess of 1.0 b.y. (Odom and others, 1973).

Pinelog and Wilhite Formation

The Pinelog Formation rests nonconformably upon the Corbin Gneiss Complex and forms the overturned, western limb of the Salem Church anticlinorium. It is a Precambrian sequence of interlayered metaconglomerate, metasandstone, carbonaceous metasiltstone and metashale. The Pinelog Formation is believed to have been directly derived from the Corbin Gneiss by detrital processes (Hayes, 1901).

Conformably overlying the Pinelog Formation are graphitic phyllites, metaconglomerates and siliceous marbles of the Precambrian Wilhite Formation. Locally the Wilhite Formation is in contact with the Corbin Gneiss Complex due to a series of echelon faults within

Table 1. Relative age and sequence of rocks within Cherokee-Pickens district compared to rocks north of district.

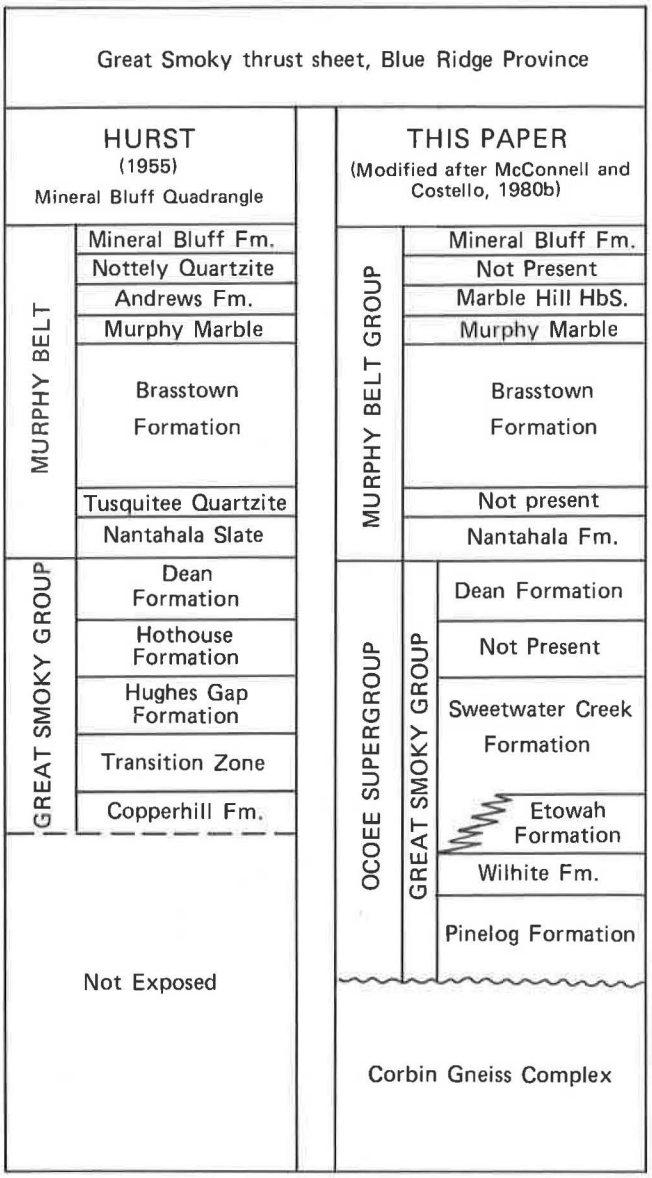

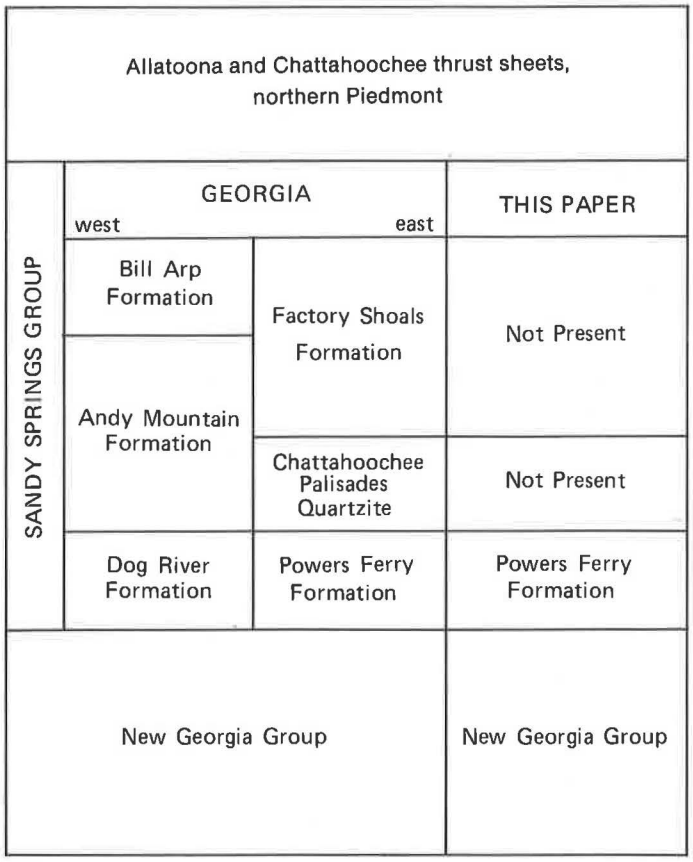

the eastern limb of the Salem Church anticlinorium (McConnell and Abrams, 1984). Both the Pinelog and Wilhite Formations belong to the lower portion of the Ocoee Supergroup (McConnell and Costello, 1980). The Corbin Gneiss and Ocoee Supergroup units are not hosts to significant pegmatite deposits in the Cherokee-Pickens district. Production records do not indicate any pegmatite mining activity within the Salem Church anticlinorium (Furcron and Teague, 1943; McConnell and Costello, 1984).

Great Smoky Group

Based upon areal extent, the Great Smoky Group comprises a significant proportion of the exposed rocks within the north and northwest portions of the Cherokee-Pickens district (Plate 1). These late Precambrian rocks of the Ocoee Supergroup overlie the earlier Ocoee units of the Salem Church anticlinorium. The Great Smoky Group can be divided into three lithologic formations: the Etowah Formation, the Sweetwater Creek Formation and the Dean Formation.

The Etowah Formation is composed of an interlayered sequence of metasandstones, biotite gneiss and sericite phyllite with small lenses of calc-silicate granofels. The Etowah Formation is distinguished from the Wilhite Formation by the paucity of carbonate and graphite in the layered sequence. The Etowah Formation overlies the Wilhite both lithologically and structurally (Plate 1). The Etowah grades upward into the Sweetwater Creek Formation.

The Sweetwater Creek Formation consists of a metaconglomeratic metasandstone, interlayered with graphitic and sericite phyllite. The conglomerate contains pebble-size clasts of quartz and feldspar, and lithic clasts of slate up to 0.3 meters in length (McConnell and Abrams, 1984).

The Dean Formation is the uppermost unit of the Great Smoky Group. This unit is characterized by a quartz-pebble metaconglomerate with interlayered beds of metasandstone and sericite phyllite. The metaconglomerate of the Dean Formation differs from that of the Sweetwater Creek Formation by exhibiting better sorting characteristics and containing fewer mafic minerals. The metaconglomerate of the Dean Formation contains detrital plagioclase, perthitic microcline and tourmaline. It should be noted that all of the formations of the Great Smoky Group are known to contain accessory tourmaline (McConnell and Abrams, 1984; Fairley, 1965). Some of the most interesting and complex pegmatites of the district are within the Great Smoky Group.

Murphy Belt Group

Conformably overlying the Dean Formation of the Great Smoky Group are the metasedimentary rocks of the Murphy belt group of probable Paleozoic age (Pzmu, Plate 1). The Murphy belt group outcrops in a 1.5-9.5 km wide belt in the north-central portion of the district and is located in the axial portion of the Murphy Synclinorium. From oldest to youngest, the Murphy belt group consists of the Nantahala formation, the Brasstown Formation, the Murphy Marble, the Marble Hill Hornblende Schist and the Mineral Bluff Formation (McConnell and Abrams, 1984; Fairley, 1965).

The Nantahala Formation conformably overlies the Dean Formation and is characterized by carbonaceous phyllite and dark-colored argillites interbedded with medium-grained metagraywacke. Traces of tourmaline are commonly observed within the various units of the Nantahala (Hurst, 1955; Fairley, 1965). The Nantahala Formation is best exposed on the western limb of the Murphy Syncline, in contrast to the eastern limb where this formation is not well exposed. As a consequence, the actual contact between the Ocoee Supergroup and Murphy belt group rocks is poorly defined within the Ball Ground and Marblehill areas. Based on available maps, the Ocoee-Murphy contact shown in Plate 1 is identical to that designated by McConnell and Abrams (1984) and McConnell and Costello (1984) except within the Marblehill and Ball Ground fields where the contact is taken from the mapping defined by Fairley (1965).

The Brasstown Formation rests above the Nantahala Formation and is composed of an interlayered sequence of gray biotite schists and micaceous quartzites. Tourmaline is a common accessory constituent of the Brasstown Formation, varying from 0-0.6% by volume (Fairley, 1969).

The Murphy Marble overlies the Brasstown Formation. It is a conspicuous unit composed of fine- to medium-grained calcite and dolomite with minor graphitic layers. Powers and Forrest (1973) documented the detailed stratigraphy of the Murphy Marble and suggest that this unit originated in a reef or carbonate bank environment. At present, the Murphy Marble is a significant source for high purity calcium carbonate, as well as dimension and crushed stone.

Grading upward from the Murphy Marble is the Marble Hill Hornblende Schist, a sequence of interbedded impure marble and calcareous hornblende schist. Overlying the Marble Hill Hornblende Schist and forming the core of the Murphy synclinorium is a thick sequence of garnet-quartz-sericite schist interbedded with sericite schists, referred to as the Mineral Bluff Formation.

Numerous pegmatites are found as concordant or discordant intrusions within the Murphy belt group. Within the district, Paleozoic host rocks for pegmatites include the Brasstown Formation and the Marble Hill Hornblende Schist. A gray dolostone unit exposed immediately northwest of the Cochran Mine adjacent to Long Swamp Creek also contains minor pegmatite dikes.

Pegmatite-hosting rocks in the Ocoee Supergroup crop out immediately south and southeast of the Murphy belt group. These units extend southward where they are truncated by the Allatoona fault, and the rocks of the northern Piedmont province are encountered.

New Georgia Group

Within the study area, the New Georgia Group consists of units south of the Allatoona fault but north of the northeast-trending Chattahoochee fault. The New Georgia Group is composed of metavolcanic, metasedimentary and metaplutonic schists and gneisses, amphibolites and banded iron formations (German, 1985).

In the southwest corner of the district, the New Georgia Group consists of felsic to intermediate metavolcanic and metaplutonic gneisses. McConnell and Abrams (1984) interpreted the protolith for this gneiss as being a premetamorphic intrusive-extrusive complex. The felsic gneisses are characterized by low alkali contents and paucity of potassium feldspar.

Premetamorphic mafic intrusions of the New Georgia Group are also located in the southwest corner of the district. Principal lithologies include concordant garnet amphibolite and metagabbro. Rocks within the New Georgia Group are associated with volcanogenic gold and massive sulfide deposits forming the Dahlon-

ega gold belt (Abrams and McConnell, 1984; German, 1985). Granitic pegmatites are conspicuously absent within the New Georgia Group (German, 1985). A more detailed description of the stratigraphy of the New Georgia Group is given by McConnell and Abrams (1984) and German (1985).

Sandy Springs Group

South of the Chattahoochee fault, the New Georgia Group is truncated and overthrust by metasedimentary and metavolcanic rocks of the Sandy Springs Group. Within the study area, the Powers Ferry Formation is the dominant unit in the Sandy Springs Group.

The Powers Ferry Formation consists of interlayered gneiss, schist, amphibolite and banded iron formation. Numerous pegmatites are hosted by the Powers Ferry Formation within 2 km of the Chattahoochee fault, in the vicinity of Holly Springs. McConnell and Abrams (1984) note that the Chattahoochee fault served as a migmatitic front characterized by an abundance of pegmatites and aplites south and east of the fault and little or no apparent anatectic material north or west of the fault.

Other Premetamorphic Intrusions

The Laura Lake Mafic Complex is a premetamorphic mafic complex which crops out south of the Chattahoochee fault (Plate 1). This intrusive and extrusive complex is elongate to the northeast paralleling the regional fabric and consists of migmatitic garnet amphibolite with minor pyroxene-bearing metagabbros, meta-quartz diorites, meta-ultramafics and banded iron formations. McConnell and Abrams (1984) note that the Laura Lake Mafic Complex bears similarity to the amphibolites of the New Georgia Group. The outcrop pattern suggests that the Laura Lake Mafic Complex represents a small portion of the New Georgia Group rocks that overthrust other units of the New Georgia Group along with the Sandy Springs Group. Alternatively, the Laura Lake Mafic Complex may simply represent a premetamorphic complex which intruded the Sandy Springs Group. Granitic pegmatites are not present within the Laura Lake Mafic Complex.

An outcrop of uralitized metagabbro and amphibolite is located approximately 1.5 km east of Marble Hill. This northwest-trending body measures approximately 2.5 km by 1.5 km in outcrop extent. A smaller outcrop is exposed immediately south of Marble Hill, along the East Branch. Evidence that this gabbro may have intruded during the late stages of deformation is suggested by the elongation of the gabbro parallel to cross-folding in the surrounding schists of the Brasstown Formation (Fairley, 1965). However, the actual age of these mafic bodies is unknown.

Metamorphism

At least one regional metamorphic event has affected the Precambrian and early Paleozoic rocks of the Cherokee-Pickens district. Based on K-Ar and Rb-Sr mineral ages and accounting for argon retention during cooling, Dallmeyer (1978) suggests that peak metamorphism in the southern Piedmont occurred as late as 365 m.y. ago. Abrams and McConnell (1981) and German (1985) have interpreted that this age of regional metamorphism is applicable to rocks of the northern Piedmont province. If this interpretation is correct, then this age of regional metamorphism is probably applicable to the Cherokee-Pickens district as well.

Regional metamorphism within the district is characterized by kyanite-grade rocks (Barrovian-type or middle amphibolite facies) containing garnet, kyanite ± staurolite as index minerals. Smith and others (1969), Hurst (1973) and McConnell and Abrams (1984) show metamorphic isograd maps that encompass various portions of the district. These maps indicate that kyanite-grade metamorphism is dominant throughout most of the district, and that the grade of metamorphism increases from greenschist facies to amphibolite-grade facies toward the southeast.

A conspicuous low-grade metamorphic zone is inferred for the Allatoona thrust sheet on the basis of a lack of kyanite but an abundance of garnet. German (1985) reports that lithologies within the northeastern portion of the New Georgia Group are characterized by quartz-muscovite-almandine-biotite-plagioclase and staurolite-bearing assemblages for pelitic rocks and assemblages of hornblende-plagioclase-almandine ± epidote in mafic rocks. Exceptions to these assemblages include local chlorite coexistent with hornblende from basic rocks, and kyanite in only the most aluminous pelitic rocks. Given these assemblages, German (1985) concludes that the regional metamorphic grade within the New Georgia Group is the lowest amphibolite grade and corresponds to the staurolite-almandine subfacies of Turner and Verhoogen (1960). It should be emphasized that this anomalous thrust sheet, characterized by a relatively weak regional metamorphic grade, also exhibits few pegmatites.

Premetamorphic to Synmetamorphic Intrusions

Pre- to synmetamorphic intrusions that retain penetrative deformation fabrics are present only locally within the Cherokee-Pickens district (Holly Springs field). However, south of the district several synmetamorphic intrusions of granitic to quartz monzonitic composition have been reported. These units typically exhibit deformation fabrics and are located in crestal areas of regional folds. They are characterized by higher potassium values relative to the premetamorphic felsic intrusions of the New Georgia Group (McConnell and Abrams, 1984).

Postmetamorphic Intrusions

All intrusions that postdate peak regional metamorphism (365 m.y.) are classified as postmetamorphic intrusions. McConnell and Abrams (1984) identified two subdivisions of postmetamorphic intrusions within the Greater Atlanta Region based on available K-Ar age dates. These include intrusions dated between 300-325 m.y. and those dated between 180-230 m.y.

Based upon field relations and two apparent K-Ar determinations for muscovite from the Cochran pegmatite and the Hillhouse pegmatite in Cherokee County (350 ± 20 m.y., and 338 ± 5 m.y., J.M. Wampler, personal communication), these pegmatites appear to have formed during or subsequent to the peak of regional metamorphism. Assuming that most pegmatites of the Ball Ground field have an age similar to that determined for the Cochran pegmatite, the earliest postmetamorphic intrusions within the district are related to pegmatite emplacement. These pegmatites are generally concordant to the local foliation but lack the regional deformation fabrics of earlier intrusions. Most of the pegmatites exhibit rotated host rock inclusions, indicative of emplacement rather than in situ origin, and several show wall rock alteration features (tourmalinization).

During or subsequent to pegmatite emplacement numerous sills, dikes and plutons of felsic composition were emplaced outside the study area. Within the Greater Atlanta Region, these simple to composite intrusions include the Stone Mountain and Panola plutons, both with radiometric ages near 325 m.y. (Atkins and others, 1980). Stone Mountain is a tourmaline-bearing two mica quartz monzonite (Grant and others, 1980, Higgins and Atkins, 1981); whereas, the Panola pluton is a biotite-bearing granite (Higgins and Atkins, 1981). Large felsic plutons are not reported within the Cherokee-Pickens district.

The youngest known postmetamorphic intrusions emplaced within the Cherokee-Pickens district are diabase dikes of the Mesozoic age. These dikes are most abundant south of the district in the southern Piedmont and tend to strike in a northwest direction, crosscutting the regional deformation fabrics (Dooley and Wampler, 1983).

Within the district, one diabase dike was observed cutting the Amphlett pegmatite. This diabase dike is discordant with the local foliation and strikes northwest. Based on K-Ar ages corrected for excess argon, the diabase dikes within the Georgia Piedmont and Blue Ridge are believed to have formed approximately 180 m.y. ago (Dooley and Wampler, 1983). The diabase dikes of Georgia show several similarities with the Liberian diabase dikes reported by Dalrymple and others (1975). They have discordant ages due to excess ^{40}Ar, and are believed to belong to an early Mesozoic system of dikes in North America, South America and Africa that formed during incipient rifting and formation of the Atlantic Ocean (Dooley and Wampler, 1983).

PEGMATITE DEPOSITS

General Characteristics

Granite pegmatites of the Cherokee-Pickens district are fine to medium-grained and composed primarily of microcline, perthite, albite or oligoclase, quartz and muscovite. These pegmatites occur as irregular, tabular or lenticular bodies of variable width (<1 meter, up to 30 meters) and extend from 5 meters to over 600 meters along strike. In most cases, the pegmatites are concordant with host rock foliation and deformation structures.

Pegmatite textures vary between and within individual deposits. The most common textures include graphic granite, perthitic, equigranular, and seriate. Aplitic textures are locally observed in some pegmatites, particularly in the most complex pegmatites of the district. An unusual texture, termed "burr rock" or "mica conglomerate" is characterized by an abundance of randomly oriented muscovite books in a matrix of white quartz. In some cases the muscovite appears to be poikilitically enclosed within the quartz. This texture is most common within the Holly Springs pegmatite field.

The most common accessory minerals of this district include garnet, tourmaline, biotite and sericite. Individual pegmatites may contain other accessories including beryl, magnetite, ilmenite, spodumene, columbite, apatite, pyrite, pyrrhotite, chalcopyrite, and malachite (Heinrich and others, 1953). The rare earth minerals monazite and xenotime have not been observed within the district. Several pegmatites are deeply saprolitized resulting in kaolinite after feldspar.

The locations of pegmatites noted in this study are shown in Plate 1. Most occurrences consist of individual prospects and mines with poor outcrop exposures. In several cases, only pegmatite dump material remains as evidence of past mining activity. Although some of the pegmatites occur as small exposures, others are more extensive. For example, the Holly Springs pegmatites tend to be confined to a north-east-trending zone, forming a swarm of dikelets and northeast-trending dikes of pegmatitic granite and pegmatite within a restricted area. The northeast trend of the larger pegmatite within this pegmatitic field suggests that a common structure has guided their emplacement. The Amphlett pegmatite in northeast Cherokee County consists of at least three pegmatite exposures which have a combined northeast strike length of over 600 meters.

Pegmatite Fields

The Holly Springs pegmatite field in the Chattahoochee thrust sheet is contained within metapelitic schists and gneisses of the Powers Ferry Formation. These pegmatites generally trend N30° to N60° and dip 45-66° southeast and are concordant with host rock foliation and regional structures. The average of these pegmatites is generally less than 3 meters. The pegmatites of this field are characterized by a simple mineralogy of feldspar, quartz and muscovite ± garnet ± biotite. Tourmaline and beryl are absent. The most common texture is that of "burr rock" although graphic, equigranular and seriate textures are locally present. Massive quartz or quartz lenses have been observed at the Hillhouse prospect and the Wacaster Mine.

The Cook Mine pegmatite, although not aligned directly along the trend of the Holly Springs field, is within the same thrust sheet and is thus part of the same pegmatite field. The country rock of this deposit is biotite gneiss intruded by granite and granitic gneiss. This pegmatite also exhibits "burr rock" textures.

The Ball Ground pegmatite field is contained within the Great Smoky thrust sheet, which is characterized by metapelitic rocks (schists, phylites, metagraywacke) and gneisses associated with the Ocoee Supergroup, or Paleozoic metasedimentary host rock of the Murphy Belt group. Pegmatites of the Ball Ground field typically trend N10° to N75°W, generally dip to the south or southeast and are usually concordant with the enclosing host rocks. The average width of these pegmatites is generally less than 2 meters, but individual pegmatites may be over 25 meters in width. The pegmatites of this field are boron-enriched and have a relatively complex mineralogy consisting of microcline, perthite, albite or oligoclase, muscovite, tourmaline ± garnet ± biotite. Beryl is associated with several of these pegmatites.

Many of the Ball Ground pegmatites are mineralogically zoned with several exhibiting quartz cores. The most common textures include graphic, equigranular, and fine- to medium-grained pegmatite.

Pegmatite Zonation

Although many pegmatites consist of a texturally homogenous assemblage of feldspar and quartz ± muscovite (simple pegmatite), several authors have noted that productive pegmatites exhibit concentric margin to core, mineralogic and textural zonation patterns (Landes, 1933, Cameron and others, 1949, Jahns, 1955). These concentric patterns are generally interpreted as the result of progressive crystallization in a pegmatite melt. Jahns (1982) suggests that pegmatite zonation progresses from margin toward core as evidenced by crystal growth structures with growth orientations toward the central core.

Jahns and others (1952) note that many of the productive pegmatites of the southeastern U.S. exhibit four zones: border, wall, intermediate and core (Figure 2). The border zone forms thin (<10cm) concentric selvages of: (1) aplitic or fine-grained pegmatite, possibly representing a chilled margin, (2) "burr rock" or (3) muscovite pegmatite, characterized by muscovite growths exhibiting a preferred orientation in which cleavage planes are oriented perpendicular to the pegmatite-host rock contact.

The wall zone forms interior to the border zones and is characterized by the presence of plagioclase, quartz and muscovite ± perthite ± biotite. Common accessories include garnet, beryl and apatite. The texture of the pegmatite in this zone usually consists of fine- to coarse-grained granular intergrowths but graphic granite and perthitic textures are common. The wall zone is normally the thickest zone of the pegmatite.

The intermediate zone forms interior to the wall zone and possesses the same characteristics as the wall zone but differs by a greater abundance of potassium feldspar (microcline) relative to sodic plagioclase. Both the wall and intermediate zones may contain large crystals of beryl, garnet and tourmaline.

The core zone forms a central lenticular quartz-rich zone or a series of discontinuous quartz-rich lenses. The core generally consists of massive white quartz but may include milky or smoky quartz and may contain large crystals of beryl, garnet or tourmaline.

Within the Cherokee-Pickens district, the Cochran, Amphlett, Denson, Jones and the Marblehill pegmatites are the major complex pegmatites of the district. They contain a central core of quartz; an intermediate zone assemblage of feldspar-quartz-muscovite with accessory garnet and tourmaline; and a discontinuous border zone composed of an aplitic or fine-grained assemblage of feldspar-quartz and muscovite. Recognition of other pegmatite zonation features within the district is difficult due to poor exposures and deep saprolitization which prevents feldspar identification.

Beryl is associated with all of the major zoned pegmatites except Marblehill. At Marblehill, the quartz core is intergrown with large tourmaline crystals up to 2 cm long and rare gem-quality garnet crystals up to 1 cm in diameter.

Mineralization (General Features)

As a consequence of rare element accumulation, some pegmatites possess an unusual abundance of exotic minerals, making the study of pegmatites a fascinating endeavor for mineral collectors, researchers and those interested in specialty metals.

Common pegmatite minerals of potential economic value include muscovite, feldspar and kaolinite.

Less common types of mineralization range from strategic or rare element minerals enriched in Ta, Li, Cs, Be, Nb, Sn or rare earth elements to gem minerals such as topaz, aquamarine and rubellite. Because of the wide spectrum of potential mineral products within pegmatites, a common nomenclature has developed to indicate the type of mineralization associated with a pegmatite. Thus, there are lithium pegmatites to indicate a pegmatite containing significant spodumene or lepidolite, and tantalum pegmatites to indicate a pegmatite enriched in tantalite or other Ta-bearing minerals.

In this paper the principal varieties of pegmatite are: (1) barren pegmatites (no apparent commercial value; (2) muscovite pegmatites (pegmatite possessing potentially commercial muscovite); (3) rare element-enriched pegmatites (those pegmatites enriched in one or more of the rare metals, but in uneconomic concentrations); and (4) rare element pegmatites (those pegmatites possessing potentially economic concentrations of any of the strategic or rare metals).

A common characteristic of rare element pegmatites is that most of these unusual pegmatites are enriched in several of the specialty metals rather than one specific metal. Some of the most significant rare element pegmatites in North America include: (1) the Kings Mountain district in North Carolina and the Amelia district in Virginia as a source for Be and Li; (2) the Tanco deposit at Tanco, Manitoba as a source for Ta, Li, and Cs; (3) the Black Hills region of South Dakota for Be, Li and Cs; (4) and the Harding pegmatite in New Mexico for Ta, Be and Li (Norton, 1973).

Endocontact Mineralogic Features

Several mineralogic features within pegmatites provide evidence for either internal differentiation during pegmatite crystallization or internal alteration due to the development of an exsolved hydrothermal fluid. These features include compositional zonation, mineral replacement and fracture-filling.

There are numerous examples of compositional zonation features in pegmatite minerals. Studies by Jolliff and others (1986), Brock (1974), and Cerny and others (1986) have demonstrated significant enrichment of incompatible[3] trace elements at the edges of zoned accessory minerals in differentiated pegmatites. The zoned minerals include tourmaline, muscovite, lepidolite, and Nb and Ta oxides. Assuming that these zonation features are primary, they suggest that the fluids that equilibrated with these minerals were undergoing physiochemical reequilibration or evolution throughout pegmatite crystallization. As such, changes in chemical activity, fugacity, temperature or pressure may have influenced trace element partitioning during the crystallization of these pegmatites.

Evidence for compositional zonation is observed on a larger scale by comparing the chemistry of a given mineral from various regions within a zoned pegmatite. Staatz and others (1955), in a study of the Brown Derby pegmatite, document that the color and composition of tourmaline varies with respect to location within the pegmatite. Within the border zone the tourmaline is black to dark green, whereas within progressively internal zones the tourmaline varies from blue to light green to pink. These color changes correspond to a decrease in Fe and Ti and enrichment in the incompatible elements Rb, Li and Cs. Similar findings by Jolliff and others (1986) indicate trace element differences at the Bob Ingersoll pegmatite, South Dakota. These authors note a general trend of Mn, Li and Sn enrichment, accompanied by Mg, Ti, and Fe depletion in tourmaline, from country rock to the core of the pegmatite. Staatz and others (1965) report that beryl from interior regions of zoned pegmatite is generally enriched in Rb but depleted in Ti, Cr, Mg and Fe relative to beryl from adjacent exterior zones.

Based on the above data, it appears that compositional trends from zoned minerals and the compositional trends of a given mineral from different pegmatite zones show similar trace element patterns. The general pattern is one of volatile and incompatible element enrichment during pegmatite crystallization. Heinrich (1953) notes that late fluid-rock interaction in pegmatite results in systematic compositional variation of successive generations of mineral species. With decreasing age of formation, plagioclase is enriched in Na; potassium feldspar and mica are enriched in Rb; and garnet, tourmaline, columbite-tantalite and micaceous minerals show a decrease in the Fe/Mn ration. He attributes these compositional trends to fractional crystallization processes.

The relative importance of volatile exsolution or other hydrothermal features on trace element partioning is an important consideration. Mineral replacement features indicate relative differences in mineral stability and chemistry resulting from metasomatic processes. Examples of mineral replacement in pegmatite include pseudomorphic or fine-grained aggregate replacement of spodumene by muscovite or albite and the replacement of tourmaline by muscovite, lepidolite or other phyllosilicates (Jahns and Ewing, 1976; Jahns, 1982; London and Burt, 1982).

---

[3]Elements that are typically dispersed in igneous rock which, because they are not easily accommodated in the common rock-forming minerals, will preferentially enter any liquid phase resulting from partial fusion, and will preferentially enter into a fluid phase generated by magmatic gases, metamorphically derived solutions, or circulating groundwater.

Further evidence of a late fluid phase during pegmatite crystallization is provided by fracture-fillings. Examples of fracture-filling include quartz veins cross-cutting pegmatite or pegmatitic minerals. Quartz veining is common in the intermediate and core zones of several pegmatites including those within the Amelia district of Virginia (Glass, 1935). Other vein minerals noted in pegmatites of the Southeast include sericite, yellow-green muscovite, and minor carbonate and sulfide minerals (Jahns and others, 1952).

Recent evidence regarding the evolution and nature of late-stage hydrothermal fluids in pegmatite is documented by Stern and others (1986). Their study of the Little Three pegmatite in San Diego County, California, indicates that centrally-located pockets within the pegmatite are zones of late crystallization in which volatiles, Mn and several incompatible trace elements were concentrated. These compositional changes resulted in the crystallization of a pocket mineral assemblage of muscovite, F-rich lepidolite, F-rich topaz and Mn-rich elbaite.

The general conclusion from these endocontact observations is that in certain pegmatites a silica, manganese and incompatible element-enriched hydrous fluid reacts with previously crystallized pegmatite in the late stages of pegmatite crystallization. Some of the most productive complex pegmatites exhibit notable endocontact features.

Within the Cherokee-Pickens district only the beryl-bearing and largest pegmatites of the district (Cochran and Denson pegmatites) show evidence for significant compositional zonation in minerals. At the Cochran deposit compositional zonation is evidenced by comparing the composition of muscovite from the border zone of the pegmatite with that of muscovite from interior portions of the pegmatite. In contrast, compositional zonation at the Denson deposit is evidenced by the presence of color zoned muscovite within the pegmatite.

Exocontact Features

Wall rock alteration is a common exocontact feature of productive pegmatites. Although alteration aureoles rarely penetrate greater than 20 meters from most pegmatites, they are usually distinctive features and are attributed to exsolution of fluids from a volatile enriched granitic melt (Jahns, 1982; Shearer and others, 1986). Varieties of wall rock alteration include albitization, tourmalinization, sericitization, silicification and biotitization (Page and others, 1953; Hanley and others, 1950; Norton and others, 1962; Staatz and Trites, 1955; Makrygina, 1977; Shearer and others, 1986). The most common alteration aureoles consist of either tourmaline-rich assemblages due to introduction of boron into wallrock by exsolution of a fluid phase from pegmatite or by a series of retrograde metamorphic assemblages resulting from reequilibration of primary metamorphic assemblages (Shearer and others, 1986). The presence or variety of alteration in a given district is dependent upon an interplay of several features including: (1) the presence of a volatile-saturated pegmatite melt, (2) the reactivity of the host relative to the composition of the pegmatitic melt or hydrous fluid, and (3) the permeability and porosity of the host rock for fluid-rock interactions.

Within the Cherokee-Pickens district few pegmatites exhibit significant exocontact alteration. Only the Cochran Mine displays obvious tourmalinization within the contact aureole. Here, secondary tourmaline extends as much as 10 meters from the pegmatite hanging wall and is characterized by the development of quartz-muscovite-tourmaline lenses within the mica schist host rocks.

The following chapters in this report describe the trace element characteristics of pegmatites and associated alteration aureoles from the Cherokee-Pickens district. Emphasis is placed on the importance of mica geochemistry as a means of distinguishing between barren and rare element enriched pegmatites. Table 2 gives a summary of descriptive data for some individual pegmatites of the Cherokee-Pickens district. The data are compiled from recent observations and from descriptions given by Furcron and Teague (1943). A detailed description of selected pegmatites including the Cochran pegmatite is given in Appendix A.

EXPLORATION FOR PEGMATITES

Assessing the Rare Element Potential of Pegmatites

The mineralogy of a given pegmatite provides a basis for identifying rare element pegmatites in the field. Unfortunately, pegmatite exploration in the Southeast is hindered by poor outcrop exposures and deep saprolitization which often masks the outcrop extent and mineralogy. In several cases, the only evidence for an underlying pegmatite is indicated by zones of kaolin containing coarse-grained muscovite. Whole rock geochemical techniques are not reliable for trace element exploration work because of the inherent inhomogeneity of most pegmatites due to zoning and the large grain size of pegmatites. Given these limitations and considerations, a geochemical sampling program involving muscovite sampling and analysis was initiated to determine the relative trace element characteristics of pegmatites within the Cherokee-Pickens district.

Table 2. Characteristics of pegmatites from the Cherokee-Pickens district.

(Chattahoochee thrust sheet)

Name	Host Rock	Width (meters)	Dip (°)	Strike (°)	Length (meters)	Type	Accessory Minerals
Kuykendall prospect	pfu	2	90	N45E	10	simple	
Dean Mine	pfu	5	SE ?	N40E	30	simple	
Hause Mine	pfu	5	77SE	N23-50E	100	simple	
Cole Mine	pfu	5	82SE	N34E	20	simple	
Wacaster Mine	pfu	4-8	60-67SE	N35E	20	simple	
Cook Mine	pfu	4	45-65SE	N30-35E	20-25	simple	
Hillhouse Mine	pfu	2-3	60-80SE	N40-50E	20-30	complex	

(Great Smoky thrust sheet)

Hendrix prospect	pGgs (Dean Fm.)	8	?	N70E	100	complex	Be,Tm,Gnt
Amphlett prospect	pGgs (Etowah Fm.)	1-7	32-45SE	N50E	600	complex	Tm,Gnt,Bt Be ?,Ap
Cochran Mine	pGgs (Dean Fm.)	22-25	45-55SE	N70-80E	600	complex	Be,Tm,Gnt
Revis prospect	pGgs	1-2	SW	N78W	100	simple	Tm
Densmore prospect	pGgs	2	70SE	N10W	30	simple	Tm
Bennett Mine	pGgs	2-3	39SE	N15E	100	simple	Tm,Be
Carney prospect	pGgs	2	57SE	N57E	10	simple	Tm
Denson Mines	pGgs	2	15-47SE	N15-63E	400	complex	Tm,Be,Gnt
Cagle Mine	pGgs	3	55SE	N15-20E	100	complex	Tm,Gnt
Fowler-Freeman prospect	pGgs	2	?	N35W	100	simple	Tm
Jones Mine	Pzmu	2	40SE	N60E	300	complex	Tm,Be,Bt
Reynolds Mine	Pzmu	3-4	90	N35E	20	complex	Tm,gnt
Davis prospect	Pzmu	2	40SE	N45E	20	simple ?	Tm
Howell Mine	Pzmu	2	45-60SE	N45E	20	simple	Tm
Wilkie prospect	pGgs	1-3 ?	?	N34W	10	simple	Tm
Worley prospect	pGgs	1	?	N60W	5	simple	Tm
Poole Mine	pGgs	2	12-35E	N-15-35E	400	simple	Tm
Partain prospect	Pzmu	1	45SW	N75W	?	simple	Tm
Marblehill prospect	Pzmu (hornblende schist)	1	17SE	N78W	?	simple	Tm,Bt,Gnt
Marblehill prospect	Pzmu (Brasstown Fm.)	2	25SE	N6-70E	500	complex	Tm,Bt,Gnt
Foster prospect	Pzmu	5	36-39SE	N58E	40	complex	Tm,Bt,Gnt
Mullinax prospect	pGgs	2	?	?	5?	complex	Tm,Be

Pfu = Powers Ferry Formation, pGgs = Great Smoky Group, Pzmu = Murphy Belt group
Be = Beryl, Tm = Tourmaline, Gnt = Garnet, Bt = Biotite, Ap = Apatite

Muscovite Chemistry

Muscovite is an ideal mineral to determine relative trace element characteristics of pegmatite because the muscovite stability field extends from the igneous environment, through most metamorphic environments, and into the deuteric environment. Furthermore, the crystal structure of muscovite allows for a diversity of trace element substitutions (Belyankina and Petrov, 1983; Bailey, 1984). Prerequisite to the formation of the micaceous minerals is the presence of volatiles such as H_20, F and Cl.

The crystal structure of mica may be described as composite sheets of alternating layers of tetrahedrally and octahedrally coordinated cations. The ideal muscovite structure is a central layer of octahedrally coordinated cations (primarily Al) layered between $(Si, Al)0_4$ tetrahedra. Each layer is linked by a plane of large interlayer cations (K, Na, Ca). Hydroxyl radical, fluorine and chlorine anions enter into the mica structure essentially coplanar to the apical sites of the tetrahedral layers (Hazen and Burnham, 1973). However, these hydroxyl site anions form bonds which are exclusively linked to the octahedral cation. For this reason the composition of the anion site is intimately related to the cationic composition of the octahedral layers. This is demonstrated by the strong effect that Li and Mg have on the partitioning of F in micaceous minerals (Munoz, 1984).

Elements with similar ionic radius and charge can easily substitute for one another in sites having the same coordination. Given a diversity of site characteristics in mica including octahedral cation, tetrahedral cation, interlayer cation, and hydroxyl site anion, it is not surprising that several trace elements with diverse radius and charge characteristics are capable of substituting into the muscovite structure. Table 3 demonstrates some of the common substitutions in muscovite. Many of these substitution schemes require a coupled substitution involving different sites within the muscovite structure. Several potential substitution schemes are presented by Speer (1984). Micas are capable of accommodating elements of unusually large ionic radius into interlayer sites or elements of high ionic charge into octahedral sites because of the diversity of coupled substitutions. Thus, micas provide excellent sites for accommodating several incompatible trace elements from silicate melts.

Trace Element Chemistry

Because micas are scavengers of many incompatible trace elements, their trace element characteristics can indicate the rare element potential of the parent pegmatite.

A useful criterion is a comparison of the extent of Rb substitution in micas between barren pegmatites and spodumene-bearing pegmatites. Trueman and Cerny (1982) demonstrate that the Rb content of associated mica increases from less than 500 ppm in barren pegmatites to as much as 1-2% in spodumene- and lepidolite-spodumene-bearing pegmatites. Studies by Gordiyenko (1971) show similar results indicating a strong positive correlation between Rb and rare element-enriched pegmatites.

The Be and Nb content of mica in pegmatite is highest in those pegmatites containing beryl or columbite. Within the Franklin-Sylva district of North Carolina only 0.6% of the pegmatites contain columbite. The corresponding micas from the district average only 0.1 ppm Be and 9.4 ppm Nb. In contrast, in the Petaca district of New Mexico approximately 67% of the pegmatites contain beryl and 87% contain columbite. The corresponding micas from the district average 5 ppm Be and over 400 ppm Nb (Heinrich, 1962). Furthermore, spectrographic studies of muscovite within the tin-spodumene belt in North Carolina (Griffitts, 1954) indicate that spodumene-bearing pegmatites of the district contain Be-enriched mica relative to mica associated with the spodumene-poor pegmatites of the district.

Several authors have noted a strong, positive correlation between F and Li-enriched micas (Foster, 1960; Nemec, 1969; Nieva, 1975). Their results suggest that fluorine is an additional element that can be utilized to indicate rare element-enriched pegmatites. This correlation can be attributed, at least in part, to the strength of the F-Li bond (Munoz, 1984). The mobility of fluorine due to reequilibration processes is an additional consideration (Gunow and others, 1980; Guidotti, 1984).

The Cs and Li content of muscovite also provide a measure of the rare element potential of pegmatites. Gordiyenko (1971) and Cerny and Burt (1984) demonstrate a significant enrichment of these elements in rare element pegmatites by comparing the muscovite chemistry associated with barren pegmatite; muscovite pegmatite enriched in Be, Nb, and Ta; and pegmatites enriched in Li (spodumene and spodumene-lepidolite pegmatites). The Li-enriched pegmatites exhibit the highest Cs and Li content. Other trace elements in muscovite which show enrichment in rare element pegmatites include Ga, Sn, Ti and Zn (Cerny and Burt, 1984).

These studies indicate that a suite of elements in muscovite can be utilized to distinguish barren from rare element-enriched pegmatites. Thus, several elements within the mica structure can be used in conjunction to make an assessment of an individual pegmatite or pegmatite zone for its rare element potential.

SAMPLING AND ANALYTICAL PROCEDURES

Sampling Procedure

Several muscovite samples were collected from twenty-nine pegmatite deposits throughout the Chero-

Table 3. Trace element substitutions in muscovite.

Site	Dominant Ion (radius)*	Substituting Ions (radius)
Octahedral Cations	Al^{3+} (0.57)	Fe^{2+} (0.80), Fe^{3+} (0.67), Mg^{2+} (0.74), Ti^{4+} (0.64), Mn^{4+} (0.52), Li^{+} (0.68), Nb^{5+} (0.66), Ta^{5+} (0.66), Sn^{4+} (0.67).
Tetrahedral Cations	Si^{4+} (0.39)	Al^{3+} (0.57), Be^{2+} (0.34), B^{3+} (0.20), P^{5+} (0.35).
Interlayer Cations	K^{+} (1.33)	Na^{2+} (0.98), Ca^{2+} (1.04), Sr^{2+} (1.20), Rb^{+} (1.49), Cs^{+} (1.65), Ba^{2+} (1.38).
Hydroxyl	$(OH)^{-}$ (1.40)	F^{-} (1.33), Cl^{-} (1.81)

*All radii in Angstrom units (Bloss, 1971).

kee-Pickens district. Most samples were collected from mine dumps or available outcrop exposures and one sample was obtained from a diamond drill hole at Marblehill (John Hinton, Georgia Marble Company).

All samples were selected on the basis of mineral paragenesis, location with respect to internal zoning within a pegmatite, mineral clarity, color, and lack of significant clay alteration or organic staining. In even the most strongly weathered deposits relatively fresh muscovite (containing few inclusions and lacking significant staining) could be easily obtained. The largest crystals (> 2cm) were preferentially sampled for analysis. In some of the larger, complex pegmatites a variety of muscovite samples were collected from each of the pegmatite zones and from different locations along the strike of the pegmatite. Where available, samples of biotite-muscovite pairs were collected in order to determine trace element partitioning characteristics. A complete list of all samples is given in Table 4, according to their location, paragenesis and physical properties. Specific locations of mica samples from the Cochran and Amphlett mines are indicated on the detailed maps presented in Appendix A.

Sample Preparation

Mica samples were examined for their physical characteristics including thick section color, secondary cleavage, striations ("A-structure"), color zoning, staining, and abundance and variety of inclusions. The report of Jahns and Lancaster (1950) is an excellent reference regarding the physical characteristics of muscovite. The identification of mineral inclusions and variety of oxide staining was determined using a standard petrographic microscope.

Kaolinite is the dominant mineral inclusion, occurring as mottled white-gray aggregates of poor transparency. Other inclusions include pseudohexagonal, pleochroic plates of biotite, rutile, zircon, tourmaline (Figure 3), and garnet. The dominant stains consist of manganese oxide and iron oxide, occurring as mottled blebs between mica cleavage plates. These oxide stains commonly show dessication cracks. All black oxide stains were tentatively identified as manganese oxide and all yellow, orange, red or reddish-brown stains were tentatively identified as iron oxides.

Single crystals or portions of a crystal containing the fewest stains of mineral inclusions (<0.5%) were selected for detailed X-ray and trace element analysis.

Conventional X-ray powder diffraction pattern techniques, using fluorite as an internal standard for line calibration, were utilized to determine the polytype of each mica sample. Polytype identification was determined from the diagnostic diffraction lines given by Bailey (1984).

A 5 gram split was submitted to a commercial laboratory for detailed geochemical analysis. The elements and corresponding analytical methods and detection limits are shown in Table 5. All trace element analyses are within 10% of the reported value and all major elements are within 2% of the reported value (Michael Volosin, Skyline Labs, personal communication, 1986).

Micas that were too small or too fine-grained for analysis by the above methods were prepared for microprobe analysis. For these samples only Rb and K were analyzed. These analyses include biotite-muscovite pairs and samples of muscovite associated with selected rocks.

Table 4. Characteristics of muscovite and biotite samples, Cherokee-Pickens district.

Sample #	Location	Type	Color	Paragenesis	Inclusions
P-1	Cochran	mu	yl-grn	be-qtz-mu	rt,kl
P-5	Cochran	mu	yl-grn	feld-mu-qtz	rt,kl
P-7*	Cochran	mu	yl-grn	tm-feld	FeO,MnO ,kl
P-10	Cochran	mu, (contact zone)	brn-gry	qtz-tm	FeO,MnO ,kl
P-11*	Cochran	mu, (from schist)	yl-grn	qtz-mu-tm	
P-12	Cochran	mu	yl-grn	qtz-feld	kl,FeO,MnO,z
P-14	Cochran	mu	yl-grn	tm-be-feld	kl,FeO,MnO
P-16	Cochran	mu	sv	tm-qtz	kl,FeO,MnO
P-17*	Cochran	mu (from schist)		mu-qtz-tm	
P-19*	Cochran	mu, (from schist)		mu-bt-qtz	
P-26	Cagle	mu	sv		kl,FeO,MnO
P-26A	Cagle	mu (burr rock)	grn-brn	qtz	kl,FeO,MnO
P-33*	Cochran	mu, (secondary veinlet)	brn-grn	tm	
P-36	Howell	mu	sv-grn	qtz	kl,FeO,MnO
P-37	Jones (north)	mu	brn-grn	qtz-feld	kl,FeO
P-40A	Jones (north)	mu	gry-brn	qtz-feld-tm	FeO,MnO
P-44A	Jones (south)	mu	sv-grn	qtz-feld	kl,FeO,MnO
P-44B	Jones (south)	mu	grn-brn	qtz-feld	kl,FeO,MnO
P-46	Wacaster	mu, (burr rock)	gry-brn	qtz-feld	kl,FeO,MnO
P-47	Wacaster	mu	gry	qtz	bt,MnO
P-48	Wacaster	mu	gry-brn		bt,MnO,FeO
P-49	Cochran	mu	yl-grn	qtz	kl,MnO,FeO,z
P-49B	Cochran	mu	yl-grn	qtz	kl,MnO,Tm,z
P-50	Cole	mu	gry	kl-qtz	kl,FeO,MnO
P-51	Hillhouse	mu	gry-blk	qtz-feld	kl,FeO,MnO
P-54	Amphlett	mu	cinnamon	qtz-kf	kl,FeO,MnO
P-55	Amphlett	mu	cinnamon	qtz-kf-tm	kl,FeO
P-56	Toonigh Cr	mu	sv-grn	qtz-feld	kl,chl,MnO
P-76	Marblehill	mu (border zone)	gry-brn	feld-qtz	kl,FeO,MnO
P-77	Marblehill	mu (core zone)	sv-grn	qtz-tm	kl,MnO
P-81	Jones-Howell area	mu	sv-grn	qtz-feld-gnt	kl,FeO,MnO
P-82a	Jones-Howell area	mu	sv-grn	qtz-feld	kl,MnO
P-82b	Jones-Howell area	bt	brn-blk	qtz-feld-gnt	kl,FeO
P-85	Denson	mu	sv-grn	qtz-feld-tm	kl,MnO
P-87	Denson	mu	sv-grn	qtz-gnt	MnO,kl,FeO
P-88a	Denson	mu (center)	sv-grn	qtz	kl,MnO
P-88b	Denson	mu (edge)	sv-brn	qtz	FeO,kl,MnO
P-90	Carney	mu	sv-grn	qtz-feld	kl,MnO
P-95b	Amphlett	mu	cinnamon		kl,MnO
P-95g	Denson	mu	sv-grn	qtz-feld	kl,FeO,MnO
P-98a	Amphlett	mu	cinnamon	qtz-kf-bt-tm	kl,FeO,MnO
P-98b	Amphlett	bt	brn-blk	qtz-kf-mu	kl,FeO
P-100	Mullinax	mu	sv-grn	qtz-feld	kl,MnO
P-106b	Hendrix	mu	sv-grn	qtz-feld-tm	kl,FeO
P-107	Hendrix	mu	sv-grn	qtz-feld	kl
P-108	Cook	mu	sv-grn	qtz-feld	kl,MnO
85-13-79*	Marblehill	mu	sv-grn	qtz-feld-bt-tm	kl

* = Microprobe samples, all others by wet-chemical methods.

qtz = quartz, kf = potassium feldspar, feld = feldspar, tm = tourmaline, mu = muscovite, bt = biotite, kl = kaolinite, chl = chlorite, rt = rutile, gnt = garnet, FeO = iron oxide, MnO = manganese oxide, z = zircon, be = beryl, yl = yellow, grn = green, gry = gray, brn = brown, blk = black, sv = silver

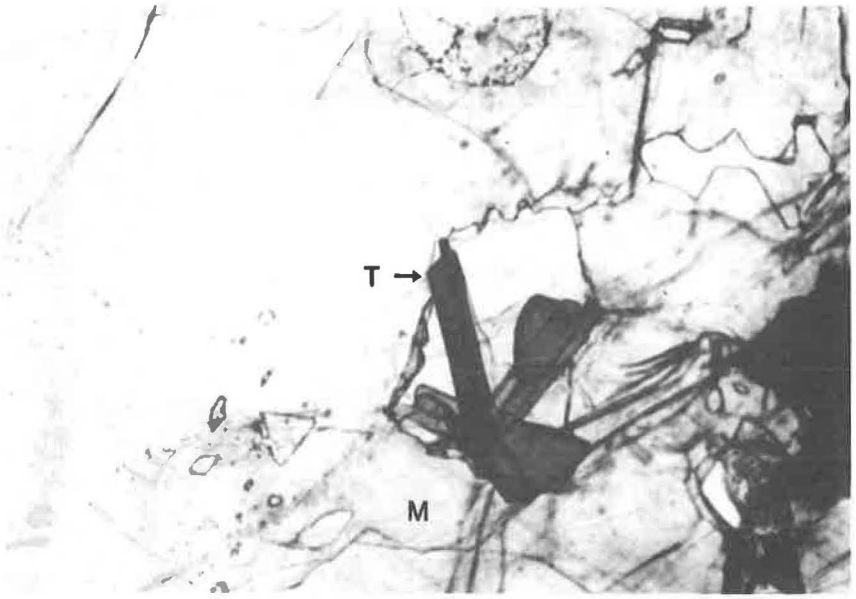

Figure 3. Photograph of tourmaline inclusions (T) in muscovite (M). From the Cochran pegmatite, sample P-49A, transmitted light, 40x. Width of field is 2.1 mm.

Table 5. Analytical methods for phyllosilicate analyses, Cherokee-Pickens district.

Element	Method	Detection Limit (ppm).
Si	ICP	200
Al	ICP	20
Fe^{2+}	ICP	20
Fe^{3+}	AA & ICP	20
Mg	ICP	20
Nb	ICP	20
K	ICP	200
Na	ICP	200
Ti	ICP	20
P	ICP	50
Mn	ICP	10
Sr	ICP	10
Li	ICP	5
Rb	AA	50
Ba	ICP	10
Be	AA	2
V	ICP	10
B	ICP	20-50*
Cs	ICP	10-20*
Ta	ICP	20
F	SIE	100
Cl	SIE	200

*Detection limit is dependent upon the quantity of sample analyzed.

Methods: ICP = Inductively Coupled Plasma

AA = Atomic Absorption

SIE = Selective Ion Electrode

ANALYTICAL RESULTS

X-Ray Analyses

Results from X-ray powder patterns of all sampled micas were compared to the pattern produced by the four muscovite polytypes utilizing the expected interplanar spacings. The results indicate that all of the pegmatitic muscovites within the study area are 2M1 polytypes.

Geochemical Analyses

Detailed mica analyses from the sample suite provide excellent comparative data concerning: (1) trace element differences among pegmatites throughout the district, (2) differences in trace element chemistry as a function of pegmatite zonation, (3) trace element variation within zoned micas, and (4) trace element comparisons in biotite-muscovite pairs. Regarding trace element differences among pegmatites, the selected sample suite is specially useful for comparing and contrasting the trace element characteristics of beryl-poor pegmatites of the Holly Springs field with beryl-bearing pegmatites of the Ball Ground field.

A list of the trace element characteristics for pegmatites in the district is given in Table 6. Complete structural formulae for all micas are provided in Appendix B. The results of the microprobe analyses are presented in Table 7.

Trace Element Comparison of Pegmatite Fields

A comparison of trace element analyses for pegmatitic muscovite within the district demonstrates anomalous enrichment of incompatible trace elements within the Cochran pegmatite. The data also show distinctive trace element characteristics for the Holly Springs Field, the beryl-bearing pegmatites of the Ball Ground field, and the tourmaline-bearing, but beryl-poor pegmatites of the Ball Ground field.

Figure 4 shows the frequency distribution of Rb(ppm)/K% ratios in muscovite analyses throughout the district. The horizontal bars illustrate the range in the data for each of the indicated groups of pegmatite deposits. The data indicate that the pegmatites from the Holly Springs field have a restricted range of relatively low Rb/K ratios. The low Rb/K ratios correlate with low Rb values rather than exceptionally high K values. The Ball Ground field of pegmatites shows a wider range in Rb/K ratios with the beryl-bearing pegmatites being most enriched in Rb. The Cochran deposit exhibits Rb/K ratios similar to other beryl-bearing deposits in the district. The data imply that Rb/K ratios provide a means of identifying barren pegmatites and beryl-bearing pegmatites of the district.

Figure 5 displays plots of several trace elements relative to Rb(ppm)/K%. In general, as the value of Rb increases in muscovite, other incompatible trace elements tend to increase. Muscovite from the Cochran deposit typically exhibits anomalous enrichment in Li, F, and Nb. The only exception to the Cochran trace element signature is found in border zone muscovite (P-10) which has relatively low Rb(ppm)/K% ratio and corresponding low values for Nb and Cs.

Other beryl-bearing pegmatites of the district show significant enrichment in Rb and Nb, but are not particularly enriched in F, Li, and Cs relative to the other pegmatites of the district. Only the Cochran deposit exhibits consistent enrichment for the entire suite of incompatible trace elements.

Figure 6 demonstrates the negative correlation between Ba and Rb/K in the pegmatitic muscovite. There is a significant increase in the Rb(ppm)/K(%) as Ba values decrease below 300 ppm. The reason for this trend is related to the crystallochemical features of these two elements which are in competition for the same interlayer site. Shamakin (1984) reports a similar negative correlation for these two elements, depending upon the type of pegmatite. Ba is highest in muscovite pegmatites and lowest in rare element pegmatites; whereas, the reverse holds for Rb. Whole rock analyses of granitic rocks exhibit a similar negative correlation between these two elements as a function of granite differentiation (El Bouseily and El Sokkary, 1975). In general, Ba decreases with differentiation; whereas, Rb increases as a function of differentiation.

The Ba/Rb ratio provides an index to pegmatite differentiation. A compilation of Ba/Rb values for muscovite from a variety of locations throughout the world indicates that the Ba/Rb ratio in muscovite pegmatites is in the range 0.3-0.7; whereas, the ratio in rare element pegmatites is in the range 0.002-0.02 (Shmakin, 1984). Within the Cherokee-Pickens district, muscovite from the Cochran deposit is the most depleted in Ba and enriched in Rb, resulting in an average Ba/Rb ratio of about 0.1. This value is between those given for the muscovite class and those of the rare element class. The above trace element values and ratios corroborate other data which indicate that the Cochran deposit is the most differentiated pegmatite in the district. The fact that this pegmatite is also one of the largest and most productive in terms of muscovite and rare element mineralization indicates that detailed trace element chemistry of muscovite may provide a convenient and useful geochemical method for identifying the largest pegmatites within the district.

Similar trace element characteristics observed in other pegmatite districts have prompted Cerny and Burt (1984) to distinguish barren pegmatites, muscovite pegmatites, and rare element pegmatites on the basis of

Table 6. Trace element characteristics of muscovite from the pegmatite deposits of the Cherokee-Pickens district (all values in ppm unless otherwise indicated).

Sample #	Deposit	Interlayer Site Rb	Cs	Ba	Octahedral Site Li	Nb	Tetrahedral Site Be	B	Hydroxyl Site F	Rb(ppm) /K (%)	Comments
	- Holly Springs field -										
P-46	Wacaster	320	<10	420	28	50	7	-	1100	42	
P-47	Wacaster	310	<10	1521	42	40	5	<20	2000	37	
P-48	Wacaster	230	10	1430	46	<20	4	-	1000	29	
P-50	Cole	270	<10	483	32	70	3	<20	770	30.7	
P-51	Hillhouse	240	<10	2775	37	<20	3	<20	880	30	
P-56	Toonigh Cr.	340	<10	653	46	65	<2	-	960	42	
P-108	Cook	292	10	1513	18	45	5	<20	820	36	
	- Ball Ground field (Beryl-Poor) -										
P-26	Cagle	580	20	134	121	40	19	-	1900	80	
P-26A	Cagle	760	20	161	9	40	24	165	600	94	
P-36	Howell	380	10	985	84	80	12	-	1100	46	
P-37	Jones (North)	480	50	1430	74	20	24	-	1100	54	
P-40A	Jones (North)	310	10	1700	79	50	12	-	1500	41	
P-54	Amphlett	260	<20	590	32	<20	4	45	950	32	
P-55	Amphlett	450	10	188	37	40	18	55	960	58	
P-76	Marblehill	530	<10	98	84	20	9	-	920	62	Border Zone
P-77	Marblehill	520	<10	116	84	<20	9	-	870	62	Core Zone
P-81	Jones-Howell*	311	<10	1430	70	<20	8	<50	310	38	
P-82A	Jones-Howell*	330	<10	1611	40	<20	10	-	460	39	
P-82B	Jones-Howell*	750	60	850	696	70	9	-	1400	106	Biotite
P-90	Carney	470	<10	54	23	30	13	-	860	52	
P-95B	Amphlett	320	<10	27	37	<20	4	-	860	37	
P-98A	Amphlett	300	<10	680	28	<20	5	<20	560	37	
P-98B	Amphlett	730	30	510	320	45	4	<20	1700	99	Biotite
	- Ball Ground field (Beryl-bearing) -										
P-1	Cochran	1370	50	143	603	345	28	-	5700	184	
P-5	Cochran	1460	50	125	603	380	30	115	5200	187	
P-10	Cochran	420	<10	250	556	< 20	14	25	4700	51	Border Zone
P-12	Cochran	1100	40	385	343	290	24	-	3800	157	
P-14	Cochran	2830	270	134	315	360	40	-	3500	363	
P-16	Cochran	1280	40	63	162	380	32	70	2900	154	
P-49B	Cochran	1830	50	-	510	-	-	-	5500	186	
P-49	Cochran	1460	50	54	510	340	32	80	7300	216	
P-44A	Jones (South)	1010	70	1700	65	215	24	-	820	121	
P-44B	Jones (South)	1119	60	250	79	280	28	-	1100	137	
P-85	Denson	1830	60	54	5	240	30	245	1100	218	
P-87	Denson	1460	40	27	<5	235	32	250	680	175	
P-88A	Denson	1920	60	36	9	250	34	285	1000	233	Center of Crystal
P-88B	Denson	2290	550	205	32	220	30	-	1900	267	Edge of Crystal
P-95G	Denson	800	60	63	14	235	30	200	1300	94	
P-100	Mullinax	1460	50	206	33	260	42	75	1100	183	
P-106B	Hendrix	1460	30	187	264	260	28	90	4300	187	
P-107	Hendrix	3107	10	98	158	280	42	175	3600	374	

*Area between the Jones and Howell Mines.
- = not determined.

Table 7. Microprobe analyses of micas, Cherokee-Pickens district. (Analyst: S. Whitney, University of Georgia)

Sample #	Location	Type	Rb(ppm)	K%	Rb(ppm)/K%
P-7	Cochran	Disseminated muscovite. (In pegmatite).	920	8.11	113
P-11	Cochran	Muscovite in mica schist. (Contact zone).	470	5.9	80
P-11b	Cochran	Biotite in mica schist. (Contact zone).	150	3.7	40
P-17	Cochran	Muscovite in mica schist. (50 meters from pegmatite).	150	9.76	15
P-17b	Cochran	Biotite in mica schist. (50 meters from pegmatite).	80	5.9	16
P-19	Cochran	Muscovite in mica schist. (100 meters from pegmatite).	<150	7.88	<19
P-19b	Cochran	Biotite in mica schist. (100 meters from pegmatite).	110	4.40	25
P-33	Cochran	Muscovite veinlet in tourmaline. (In pegmatite).	670	8.96	75
85-13-79	Marblehill	Muscovite at a contact between pegmatite and hornblende schist.	560	7.95	71
85-13-79	Marblehill	Biotite at a contact between pegmatite and hornblende schist.	460	7.70	60

muscovite chemistry. Cerny and Burt (1984) have determined trace element fields for each of these pegmatite classes and their results verify incompatible element enrichment and Ba depletion in the muscovites of the rare element class. A modification of one of their diagrams is shown in Figure 7. Within the designated fields the average trace element value for the major groups of pegmatites within the Cherokee-Pickens district is plotted. The results demonstrate that the Holly Springs pegmatites and the beryl-poor pegmatites of the Ball Ground field plot closest to the muscovite class. Only the Be-enriched pegmatites of the Ball Ground field show an affinity with the rare element class. The trace element characteristics of micas from some of the most significant rare element pegmatites in North America are shown for comparison. Micas from these deposits exhibit extreme enrichment in Rb and Li (Rinaldi and others, 1972; Jahns and Ewing, 1976).

Although the trace element chemistry of muscovite provides an important tool to distinguish between barren, rare element-enriched and rare element pegmatites, the role of pegmatite zonation and mineral zonation must be considered. The results from the Cherokee-Pickens study provide several insights concerning these factors.

Trace Element Chemistry of Mica as a Function of Pegmatite Zonation

The Cochran deposit provides an excellent location to investigate trace element variations in muscovite as a function of pegmatite zoning or hydrothermal alteration. Samples of muscovite were collected from core, intermediate, and border zones of the Cochran deposit (Appendix A). Analyses of these samples indicate that all micas within the core or intermediate zones consistently exhibit high values for Li, Rb, Be, Cs and Nb regardless of muscovite paragenesis. In contrast, border zone muscovite, characterized by a distinctive dark gray coloration, exhibits relatively low values for Rb, Cs, Be, and Nb. Li is the only incompatible trace element in anomalous concentrations (>300 ppm Li) for border zone muscovite. These trace element characteristics are probably the result of pegmatite-host rock reactions. The relatively high Li content of border zone muscovite may be attributed to high mobility of Li from pegmatite into the surrounding host rocks. This interpretation is supported by comparing results from whole rock analyses of mica schist within the contact zone (P-11) and 100 meters (P-19) from the pegmatite contact (Table 8). These samples confirm whole rock enrichment in Li near the contact (810 ppm) relative to the more distant sample location (90 ppm). These trends are further supported by the findings of Shearer and others (1986), which indicate relatively high mobility of lithium in exocontact zones of pegmatite. Other elements which exhibit significant decreases in trace element values with distance from the Cochran deposit include fluorine (2200 ppm to 90 ppm) and boron (5,250 ppm to <20 ppm).

Trace element ratios from muscovite analyses

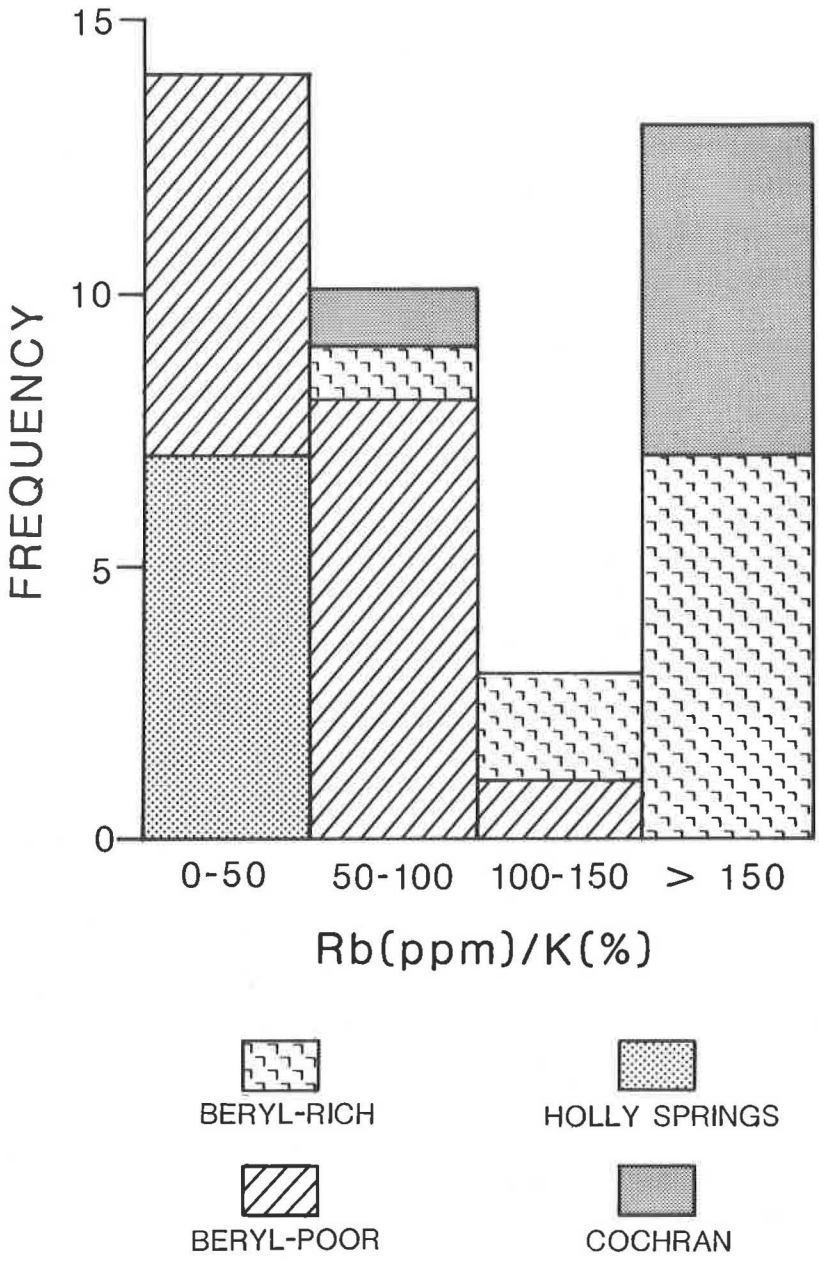

Figure 4. Histogram of Rb(ppm)/K(%) for muscovite samples from pegmatites within the Cherokee-Pickens district. Muscovite from the Holly Springs field and muscovite from beryl-poor pegmatites of the Ball Ground field exhibit relatively low Rb/K values. Muscovite from beryl-rich pegmatites and muscovite from the Cochran Mine have relatively high Rb/K ratios.

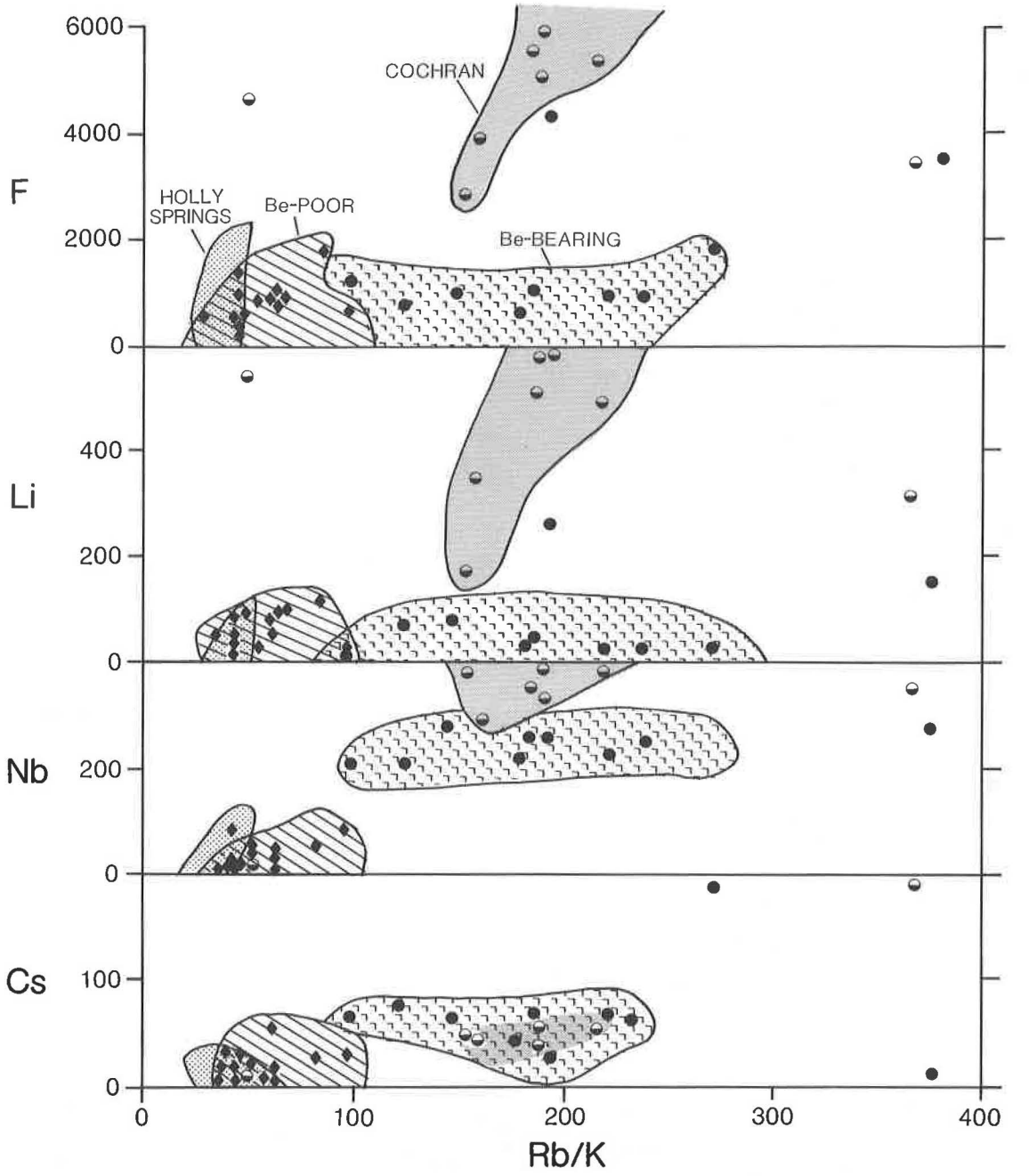

Figure 5. Plot of selected trace elements as a function of Rb(ppm)/K(%) for pegmatitic muscovite. Muscovite from the Holly Springs field (HS) exhibits consistently low values for incompatible trace elements. Muscovite from the Cochran deposit exhibits significant enrichment in incompatible elements. The beryl-bearing pegmatites typically show enrichment in several trace elements relative to beryl-poor pegmatites.

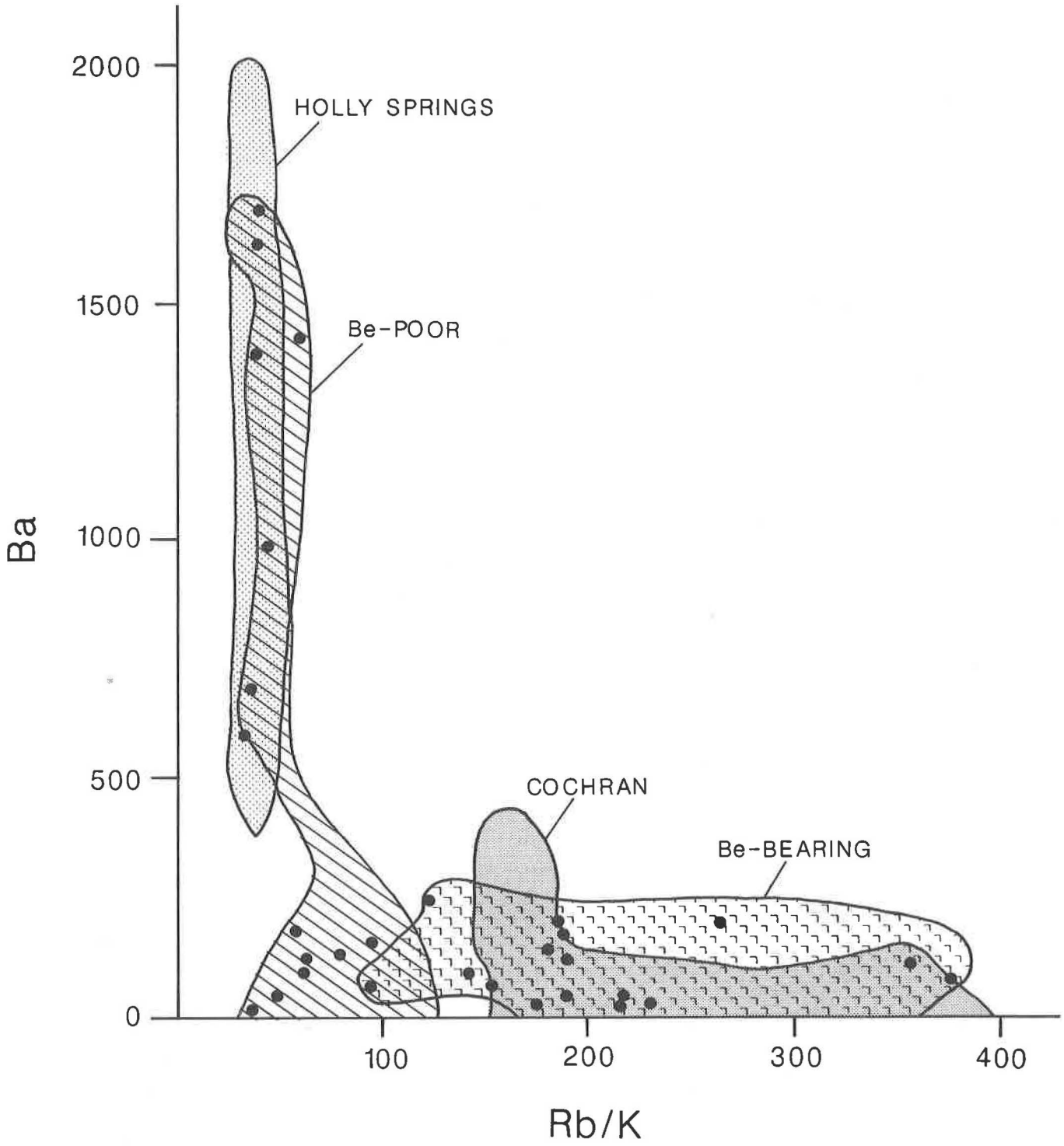

Figure 6. Correlative plot of barium (ppm) as a function of Rb(ppm)/K(%) for pegmatitic muscovite. Muscovite from the Holly Springs field and muscovite from the Be-poor pegmatites of the Ball Ground field exhibit a large range in Ba values. Muscovite from the Be-bearing pegmatites and the Cochran pegmatite exhibit uniformly low Ba values (< 300 ppm). The non-linear distribution shown in this diagram can be attributed to the mutual competition of Ba and Rb for the same K ion site, and suggests that Ba is preferentially incorporated into the mica structure (less incompatible than Rb) during relatively early stages of pegmatite differentiation.

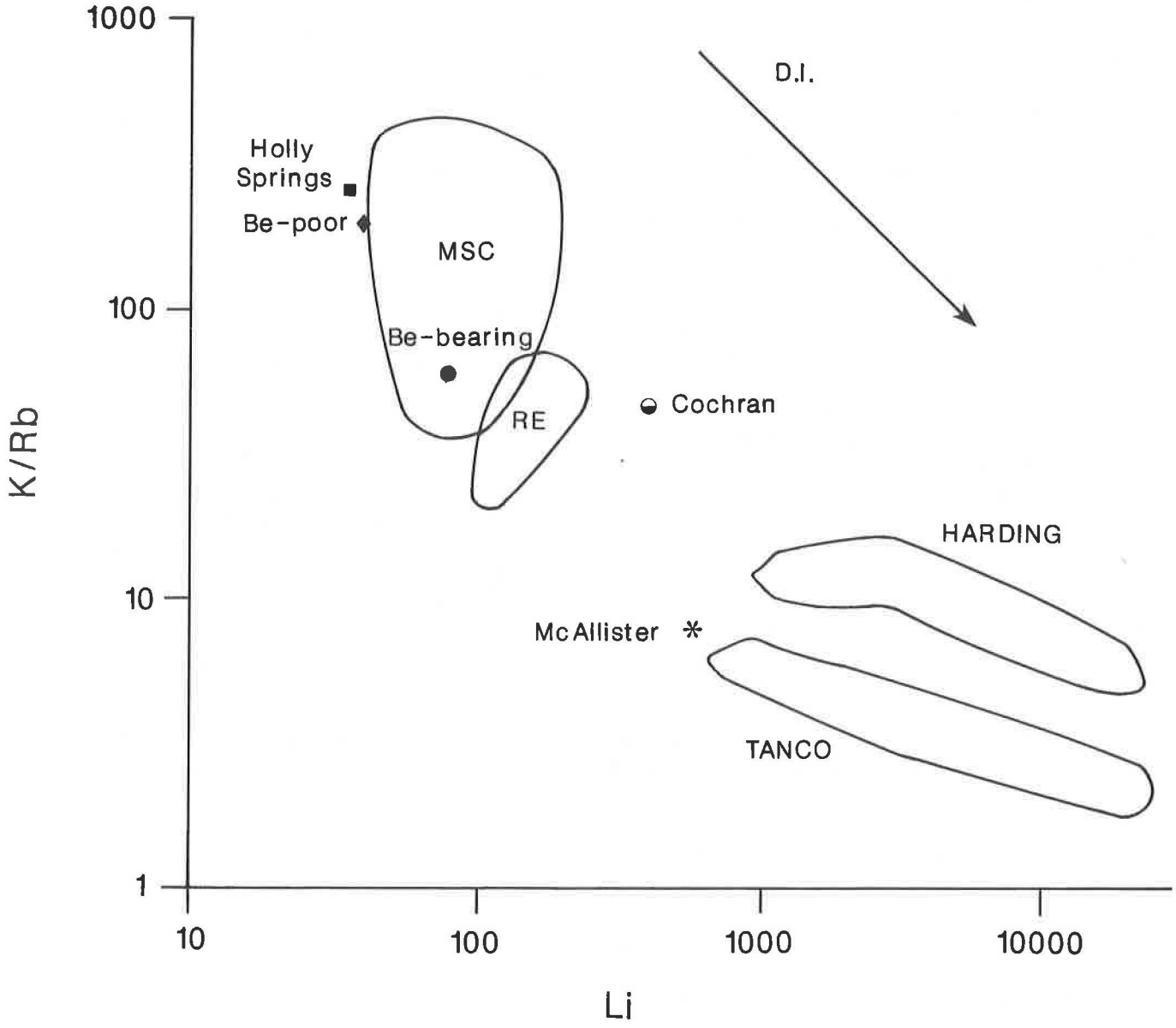

Figure 7. Plot of K/Rb versus Li (all values in ppm) for pegmatitic muscovite from the Cherokee-Pickens district, in comparison with muscovite from other major pegmatites and pegmatite groups. MSC refers to muscovite pegmatites and RE refers to rare element enriched pegmatites (after Cerny and Burt, 1984). Data for the Harding pegmatite, the Tanco pegmatite and the McAllister pegmatite from Jahns and Ewing, 1976; Rinaldi and others, 1972; and Cook and Foord, in press. The direction of increasing differentiation (D.I.) is indicated by the arrow in the upper right of the diagram.

within the Cochran pegmatite and within the host rocks also indicate significant incompatible trace element diffusion outward from the pegmatite. The ratio of Rb ppm/K% decreases from 130-360 within the pegmatite to about 50-80 in the border zone and in tourmalinized mica schist and to < 30 outward from the tourmalinized zone.

The above trace element relations suggest steep trace element gradients adjacent to the pegmatite contact and within the tourmalinized zone. The reasons for these gradients within this aureole may be related to activity gradients, mass balance effects, compositional interdependencies or any combination of these factors. For example, consider the significance of mass balance in controlling the boron distribution in the border zone of the Cochran pegmatite. Although whole rock analyses of the tourmalinized zone indicate significant boron enrichment, (Table 8, P-11), mica from this zone contains less boron than mica associated with the interior of the pegmatite (compare P-10, P-5, P-16, and P-49; Table 6). Here partitioning and mass balance effects appear to have strongly partitioned boron in tourmaline, yielding an associated muscovite with a relatively low boron content. The above trace element trends indicate that a boron and incompatible trace element-enriched fluid evolved from the pegmatite into the hanging wall schists. Thus, the interpretation of muscovite chemistry is complicated by the consideration of wall rock-pegmatite reactions. Despite these complications, trace element gradients within an alteration aureole may be inferred by comparing relative trace element values of a given mineral species from various portions of the aureole.

Chemical Zonation in Color-Zoned Muscovite

The Denson deposit provides an excellent location to study trace element variation within a color-zoned muscovite. A sample of zoned muscovite from the Rock Creek segment of the Denson pegmatite (sample 88 and 88b, Figure 8) was split into central and edge portions according to mica color (central = green, edge = brown). The results of the trace element chemistry for each of these fractions is given in Table 6.

The edge portions of the zoned muscovite exhibit nearly identical major element chemistry relative to the central zone; only MgO and TiO_2 are enriched in the edge (900 ppm vs > 7000 ppm mgO; 200 ppm vs > 5000 ppm TiO_2). However, the trace element differences between these two zones indicate significant incompat-

Table 8. Whole-rock analyses of unaltered and tourmalinized mica schist. Formation from the Cochran mine area, Cherokee County.

	P - 19 100 meters from contact (unaltered)	P -11 Contact zone (Tourmalinized)
SiO_2	56.10 wt. %	65.7 wt. %
Al_2O_3	21.30	15.8
TiO_2	4.7	4.8
Fe_2O_3	5.95	5.53
FeO	0.54	0.93
MnO	0.04	0.02
MgO	1.30	0.98
CaO	0.04	0.06
Na_2O	0.21	0.47
K_2O	6.60	3.90
LOl	4.9	2.8
Li_2O	0.01	0.08
BaO	0.14	0.12
Rb_2O	0.02	0.03
SrO	0.003	0.003
Cs(ppm)	10	20
Nb(ppm)	20	20
Be(ppm)	7	10
B(ppm)	20	5250
F(ppm)	1000	2200
Total	101.87	101.97

Figure 8. Zoned muscovite associated with the Rock Creek segment of the Denson pegmatite; sample 88. Interior zone of the crystal is clear, possesses few inclusions, and has a distinct green coloration (88A). The exterior portion of the crystal is more reflective, contains a greater abundance of mineral inclusions, and has a distinctive dark green or brown coloration (88B).

ible element enrichment in the rim of the color-zoned muscovite (Rb, Cs, F, and Li; Table 6). These trace element variations may be due to microscopic mineral inclusions within the rim, post-crystallization cation diffusion, or to changes in trace element activity within the melt during crystal growth. Considering the crystal-chemical affinity of the above incompatible element suite for the mica structure, it is not necessary to account for the observed trace element zonation as due to differences in the abundance or variety of exotic mineral inclusions. The favored interpretation is that the trace element and color zonation in muscovite at the Denson deposit is due to changes in trace element activities of the pegmatite melt during muscovite crystallization or to processes involving post-crystallization cation diffusion. Assuming this interpretation is correct, the zoned muscovite crystals at the Denson Mine record a differentiation trend at the late stages of pegmatite crystallization.

Trace Element Distribution in Biotite-Muscovite Pairs

Coexisting biotite-muscovite pairs were sampled from the Jones and Amphlett pegmatites (P-82 and P-98, respectively). These pairs provide evidence that incompatible trace elements, Li, Nb, Rb, and Cs are preferentially partitioned into coexisting biotite; whereas, Ca, Ba, and Na are partitioned into coexisting muscovite. This is indicated by the distribution coefficient: Kd (B/M) = Ce_b/Ce_m where Ce_b is the concentration of element(e) in biotite and Ce_m the concentration of element(e) in muscovite. Li appears to exhibit exceptional preference for biotite relative to muscovite, having Kd (B/M) values greater than 10 (Table 9). F exhibits Kd (B/M) values approximately equal to three. The Kd (B/M) values for Rb and Cs are remarkably similar to those obtained by Shearer and others (1986) from pegmatite deposits in the Black Hills, South Dakota.

The role of fluorine in pegmatite is difficult to assess using the F-OH exchange data of Munoz (1984) and Munoz and Gunow (1982). The fluorine values within the micas are too low to adequately quantify the relative fluorine activity associated with each of these deposits. However, based on the lack of fluorite, topaz or other significant fluorine-bearing assemblages within these pegmatites, the activity of fluorine within these pegmatite melts was probably low.

Tourmaline Analyses

Tourmaline has a complex chemistry that can be used to determine trace element signatures of pegmatite deposits. The idealized tourmaline formula is $X\,Y_3\,Z_6\,B_3\,Si_6\,O_{27}\,(O, OH)_3\,(OH, F)$; where X is dominated by Na or

Table 9. K_D values for biotite-muscovite pairs, Cherokee-Pickens district; K_D (biotite/muscovite) = C_e^B / C_e^M where Ce = Concentration of element (e), B = biotite, M = muscovite.

	Amphlett deposit Sample P-98	Jones deposit Sample P-82
Li	11.40	18.80
Nb	> 2.25	> 3.50
Rb	2.42	2.27
Cs	> 3.00	> 6.00
F	3.03	3.04
Ba	0.75	0.53
Na	0.32	0.30

Ca, Y by Fe^{+3}, Fe^{+2}, Mg, Al, or Li; and Z by Al, Fe^{+3}, Mg, or Cr. Individual species are shown with their general formula in Table 10.

Foit and Rosenberg (1977) have suggested that the chemistry of most tourmalines can be plotted on a triangular diagram consisting of the end members schorl/dravite, elbaite, and a hypothetical member dominated by trivalent cations. The hypothetical trivalent end-member contains trivalent cations in both the Y and Z sites (Figure 9). A tourmaline species that fits well with the hypothetical end member is the ferric iron-rich species, buergerite.

A comparison of published tourmaline analyses indicates that tourmaline associated with rare element pegmatites are enriched in Mn, Li, and F; but depleted in Mg, Ti, and Ca (Deer and others, 1962; Kulikov and others, 1976; Foord, 1976; Jolliff and others, 1986). Tourmaline associated with zoned pegmatites tends to become increasingly enriched in the elbaite component toward the core of the pegmatite (Jolliff and others, 1986). These relations suggest that Mn behaves as an incompatible trace element in pegmatites.

The ubiquitous presence of tourmaline within pegmatites of the Ball Ground field provides an opportunity to compare the chemistry of tourmaline associated with beryllium-enriched pegmatites with that associated with beryllium-poor pegmatites. For this reason, several samples of tourmaline were analyzed from the Ball Ground field. The specific analytical methods employed were identical to that outlined for the micas.

Results

The results of the tourmaline analyses for the Ball Ground field show that most are Fe^{+3} enriched (buergerite) and that tourmaline from the Cochran pegmatite is the most enriched in ferric iron (Table 11). With respect to trace element chemistry, the beryllium-enriched pegmatites (Cochran and Hendrix deposits) exhibit the highest content of Mn, Li, and F. The ratio MnO/TiO_2 in tourmaline is utilized as an index of differentiation of the host pegmatite. Most tourmalines from the Ball Ground field have MnO/TiO_2 values less than 0.50; only the tourmalines associated with the beryl-bearing pegmatites exhibit MnO/TiO_2 values that are

Table 10. Chemical formula of tourmaline species.

Name	X	Y	Z	Completed Formula
Buergerite	Na	Fe_3^{3+}	Al_6	$[B_3Si_6O_{27}(O,OH)_3(OH,F)]$
Chromdravite	Na	Mg_3	Cr_5Fe^{3+}	$[B_3Si_6O_{27}(O,OH)_3(OH,F)]$
Dravite	Na	Mg_3	Al_6	$[B_3Si_6O_{27}(O,OH)_3(OH,F)]$
Elbaite	Na	$(Al,Li)_3$	Al_6	$[B_3Si_6O_{27}(O,OH)_3(OH,F)]$
Ferridravite	Na	Mg_3	Fe_6^{3+}	$[B_3Si_6O_{27}(O,OH)_3(OH,F)]$
Liddiocoatite	Ca	$(Li,Al)_3$	Al_6	$[B_3Si_6O_{27}(O,OH)_3(OH,F)]$
Schorl	Na	Fe_3^{2+}	Al_6	$[B_3Si_6O_{27}(O,OH)_3(OH,F)]$
Uvite	Ca	Mg_3	Al_5Mg	$[B_3Si_6O_{27}(O,OH)_3(OH,F)]$

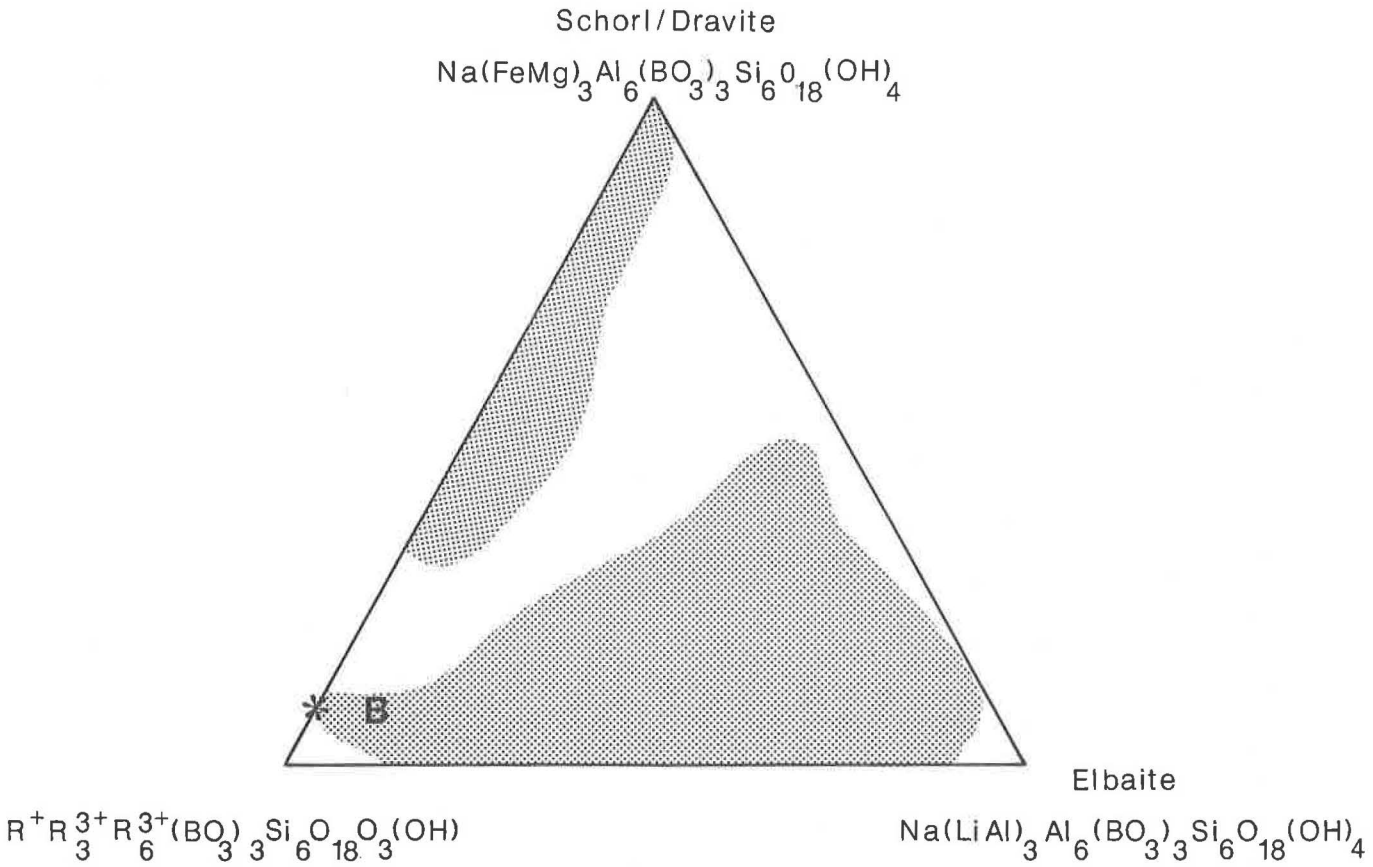

Figure 9. Tourmaline species as a function of cation composition indicating extensive substitution from schorl/dravite and elbaite to the hypothetical R^{3+} end-member. Buergerite (B) plots close to this hypothetical end-member (modified from Dietrich, 1985).

relatively high (> 2.0). Although these trace element compositions and ratios suggest anomalous values at the Cochran deposit, these values are not particularly anomalous relative to other rare element pegmatites. For example, typical MnO/TiO_2 values for tourmaline associated with rare element pegmatites varies between 1.8 to about 30 (Deer and others, 1962; Jolliff and others, 1986).

A few samples of tourmaline were partially analyzed by microprobe techniques (Table 11). The probed samples consist of disseminated tourmaline associated with mica schist host rocks at the Cochran and Cagle deposits. All of these samples have low MnO/TiO_2 ratios (< 0-3) and exhibit unusual enrichment in titanium. Perhaps enrichment in TiO_2 is a characteristic of disseminated tourmaline associated with mica schist host rocks. Alternatively, perhaps, the concentration of these elements are reflecting a difference in the coexisting mineral assemblage or bulk rock compositions.

CLASSIFICATION AND ORIGIN OF PEGMATITES

Tectonic Environment

In order to distinguish between various types of pegmatites, Cerny (1982a, 1986) has classified pegmatites according to their regional tectonic framework at the time of their emplacement. In this respect the principal pegmatite-generating environments are either anorogenic (characterized by bimodal igneous suites with associated peraluminous or alkalic granites) or orogenic (associated with metaluminous or peraluminous granites). The actual relationship between pegmatite and granite may be determined by either direct consanguinity or inferred by the regional geologic setting. Cery (1982a, 1982c, 1986) further classifies pegmatites according to their depth of emplacement (determined primarily on the basis of associated metamorphic

Table 11. Tourmaline analyses from pegmatite deposits of the Cherokee-Pickens district.

	P-33T Cochran Pegmatite	P-102 Cochran Pegmatite	P-68 Foster Pegmatite	P-91 Foster Pegmatite	P-81 Jones Pemgatite	P-94 Amphlett Pegmatite	P-97 Amphlett Pegmatite	P-62 Poole Pegmatite	P-107 Hendrix Pegmatite	P-11* Cochran Mica Schist	P-17* Cochran Mica Schist	P-27* Cagle Mica Schist
SiO_2	33.90	34.40	35.0	35.30	35.50	35.60	36.10	37.1	35.6			
Al_2O_3	32.90	34.0	33.1	34.70	32.70	34.90	32.5	29.6	32.5			
Fe_2O_3	14.20	14.30	10.90	7.8	7.90	8.0	10.5	11.2	10.8	15.3	8.70	9.37
FeO	0.43	0.39	1.00	0.44	1.60	0.48	0.74	0.83	0.87			
MgO	1.81	2.10	3.3	5.10	4.70	5.10	4.10	5.60	3.30			
CaO	0.08	0.08	0.13	0.44	0.43	0.30	0.24	0.42	0.13	0.26	1.11	1.89
Na_2O	1.80	1.90	1.90	1.60	1.90	1.80	2.00	2.10	1.90			
K_2O	0.19	0.19	0.07	0.05	0.21	0.05	0.24	0.29	0.16			
TiO_2	0.12	0.14	0.34	0.45	0.89	0.47	0.87	1.10	0.22	1.20	0.97	1.61
MnO	0.28	0.28	0.16	0.14	0.04	0.07	0.12	0.14	0.51	0.06	0.02	0.46
F	0.12	0.14	0.04	0.08	n.d.	0.04	0.12	0.07	0.13			
LOI	2.00	2.20	2.40	2.70	2.70	2.60	2.30	2.70	2.30			
B_2O_3	9.30	9.70	9.90	9.90	9.20	9.80	9.30	8.80	9.60			
Ce (ppm)	< 40	< 40	< 40	< 40	90	< 40	100	85	< 40			
Y (ppm)	< 40	< 40	< 40	< 40	< 40	< 40	< 40	< 40	< 40			
Li (ppm)	134	134	93	79	37	19	46	5	139			
Cs (ppm)	< 10	< 10	< 10	< 10	< 10	< 10	< 10					
Be (ppm)	< 2	< 2	< 2	< 2	4	< 2	3	3	< 2			
Nb (ppm)	< 40	< 40	< 40	> 40	< 40	< 40	< 40					
Total	97.13	99.82	98.24	98.70	97.77	99.20	99.13	99.95	98.02			
MnO/TiO_2	2.33	2.00	0.47	0.31	0.04	0.15	0.14	0.13	2.32	0.05	0.02	0.29

N.D. = Not determined.

*Microprobe analyses (Analyst: Sandra Whitney); all Fe calculated as Fe_2O_3

assemblages) and according to the pegmatite mineralogy and trace element chemistry.

Examples of anorogenic pegmatites include the topaz and fluorite-bearing pegmatites of the Sawtooth Batholith, Idaho (Boggs, 1986), the Mt. Antero pegmatite in Colorado (Switzer, 1939), and the fluorite-topaz-phenakite-bearing pegmatites of the Sawtooth Batholith (Boggs, 1986; Eckel, 1961). Enrichment in F, Nb, and Y is a common signature of anorogenic pegmatites, regardless of depth of emplacement (Cerny, 1986).

The pegmatites of the Cherokee-Pickens district do not possess this mineralogy or these trace element signatures. Furthermore, they are clearly associated within an orogenic framework. Based upon field relations and the apparent K-Ar ages determined for the Cochran and the Hillhouse pegmatites (356± 20 my and 338± 5 my, respectively), the Cherokee-Pickens pegmatites appear to have been emplaced subsequent to or near the peak of regional metamorphism, a characteristic of orogenic pegmatites (Cerny, 1982a).

Metamorphic Environment

Assuming that pegmatitic melt generation in an orogenic environment is temporally related to peak regional metamorphism, it is likely that pegmatitic melts are generated in a deeper environment than that indicated by the regional metamorphic grade of the enclosing host rocks. Thus, the regional metamorphic grade of the host rocks provides a minimum estimate of the depth of formation of the pegmatite melt. This line of reasoning is the basis for the depth-zone classification of pegmatites developed by Ginsburg (1960), and provides an important concept that relates tectonics and metamorphism to pegmatite genesis. These relations form the basis for the classification of granitic pegmatites presented by Cerny (1982a). Following this reasoning, the depth of melt generation (formation) should not be confused with the depth of pegmatite crystallization or emplacement. If melt generation is at a greater depth than the position of the host rock and if emplacement and crystallization significantly post dates the peak of regional metamorphism, then the metamorphic grade of the host rocks places constraints on the upper bounds for the depth of melt generation. However, if emplacement is penecontemporaneous with the peak of metamorphism and if most crystallization occurs after emplacement, then the metamorphic grade of the host rock defines the depth of emplacement of the pegmatite.

Utilizing data from Winkler (1967), Figure 10 illustrates a P-T diagram modified from Cerny (1986) showing the stability fields for kyanite, sillimanite, and andalusite superimposed with the granite solidus. Included are isograds for biotite, sillimanite, and staurolite, and geothermals for low and high gradient environments (25-50°C/km). The arrows represent the direction of differentiation for various types of orogenic pegmatites and the length of the arrow schematically represents the relative extent of differentiation possible within the various pegmatite classes. According to Cerny's (1986) classification, the orogenic pegmatites intrude into a metamorphosed crust of metaluminous or peraluminous composition. Depending upon depth, pegmatites belong to the abyssal (AB), muscovite (MSC), rare element (RE), or miarolitic classes (MI).

Pegmatites of the abyssal class (AB) and muscovite class (MSC) are produced in orogenic environments of low to moderate geothermal gradients. Each of these classes are formed in distinct metamorphic terrains and have distinctive mineral associations.

The abyssal class (AB) is associated with granulite facies or sillimanite-bearing facies which form at a depth of 20-35 km. Abyssal pegmatites are not typically associated with parental granites and are characterized by U and REE mineralization.

In contrast, the muscovite class (MSC) pegmatites are associated with kyanite-almandine-muscovite subfacies of the almandine-amphibolite facies and found in shallower metamorphic terrains (17-27 km). Associated parental granites are of the biotite or two-mica types, peraluminous, and syntectonic or late tectonic. The muscovite class pegmatites are subdivided by Cerny (1986) according to the associated mineral potential. These groupings consist of ceramic pegmatites, muscovite pegmatites, and complex pegmatites. The ceramic pegmatites contain potentially economic feldspar, whereas the muscovite pegmatites of this class contain potentially economic feldspar or muscovite, and the complex pegmatites contain potentially economic feldspar and muscovite +/-Be, REE, and U.

In regions of high geothermal gradients, pegmatites of the rare element (RE) or miarolitic (MI) class are produced at respective depths of 10-17 km and < 10 km. Both of these pegmatites are related to parental granites at various stages of differentiation. Typically, the extent of differentiation within the parental granite correlates with that of the associated pegmatite (Cerny and Meintzer, in press).

The rare element class of pegmatites (RE) is characterized by an association with andalusite-cordierite-muscovite subfacies and can further be classified according to pegmatite mineralogy. Specific examples of rare element pegmatites in the Southeast include the albite-spodumene type at Kings Mountain, North Carolina (Kesler, 1976), the Amelia district, Virginia (Glass, 1935) and the complex albite-tantalite-spodumene type at the recently discovered McAllister pegmatite in Alabama (Cook and Foord, 1986). As this list indicates, some of the most economically significant orogenic pegmatites in the Southeast belong to the rare element class. Any viable geochemical program for pegmatite explo-

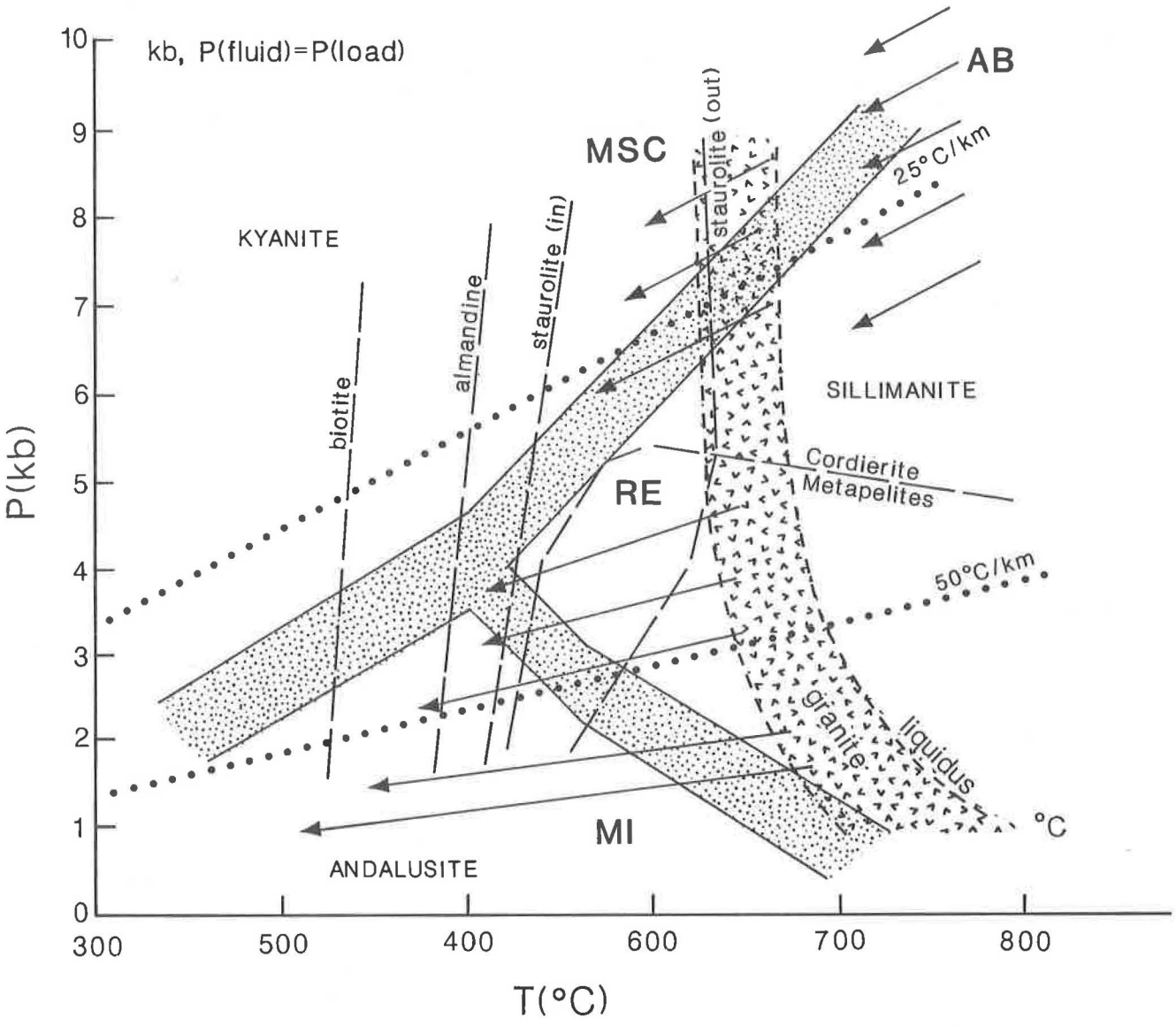

Figure 10. Metamorphic environment of the four classes of orogen-related granitic pegmatites after Cerny (1986). AB = abyssal class, MSC = muscovite class, RE = rare element class, MI = miarolitic class.

ration must have the capability to distinguish between barren, muscovite and rare element-pegmatites.

The miarolitic class of pegmatites (MI) is associated with greenschist facies metamorphism and is further classified on the basis of mineralogy. The most common MI class pegmatites include gem-bearing types containing tourmaline (elbaite and rubellite), topaz, and lepidolite; and the gem-bearing, optical quartz varieties containing beryl and topaz.

For all classes of pegmatites there is a general trend of incompatible trace element enrichment toward shallower emplacement levels. The extent of enrichment is controlled by a variety of differentiation processes and structural conditions affecting the emplacement of the pegmatite.

Within the Cherokee-Pickens district, constraints regarding the grade of regional metamorphism are imposed by the absence of sillimanite and andalusite, the lack of granulite facies, and the presence of kyanite-muscovite or staurolite-garnet subfacies in the host rocks. These features, together with related mineralization within the district, and the trace element characteristics of the associated muscovite indicate that pegmatites of the Cherokee-Pickens district generally belong to the muscovite class. The Be-enriched pegmatites, including the Cochran pegmatite, are more differen-

tiated, suggesting either a shallower level of emplacement or a protracted and more efficient differentiation history. The Be-enriched pegmatites of the district are tentatively placed between the muscovite class and the rare element class of pegmatites.

An important question arises: what is the cause of variation in the extent of differentiation among pegmatites? This question is partially answered by investigating the relationship of pegmatites to parental granites and investigating the causes of trace element partitioning in silicate melts.

Pegmatites and Granites

The possible relationship between pegmatite and parental granite in the southeastern United States has been a source of debate by several authors. Early studies by Jahns and others (1952) note that pegmatite and granite intrusions are closely associated in the southeastern United States, both locally and on a regional scale. Later studies by Griffitts and Olson (1953) conclude that the pegmatites of the Hartwell district show no obvious relation to a parent granite and that the origin of pegmatites is uncertain. Heinrich and others (1953) suggest that the parental material for the pegmatites of the Thomaston-Barnesville district is uncertain due to lack of any exposed large masses of granitic rock within the area. However, assuming a parental granitic mass at depth, they suggest that the mass would have a monzonitic or granodioritic composition due to the abundance of these rocks in the Piedmont.

Many of the suggestions presented above are refutable as the result of more recent geologic studies. Several granitic stocks in the Southeast contain multiple intrusive phases, with many containing true granite intrusions (Whitney and Wenner, 1980; Grant and others, 1980; Atkins, in review). Furthermore, some of these are distinctly associated with pegmatite dikes that possess mineral characteristics similar to the parental granite (Grant and others, 1980). Perhaps even more significant is that the postmetamorphic age of these granitic masses correlates well with the known apparent ages for the pegmatites within the Piedmont (Table 12). This is a general correlation and no specific relationship is implied. For example, the Cochran pegmatite, the Hillhouse pegmatite and the granitic intrusions shown in Table 12 all occur within different thrust sheets relative to each other. The overall geologic and chronologic data indicates that a significant postmetamorphic event(s) involved granite and pegmatite emplacement.

Although there are no known postmetamorphic granite outcrops within the Cherokee-Pickens district, the simple Bouger gravity data of Georgia (Long and others, 1972) show a general correlation between the location of pegmatite districts and a region of negative anomalies (-40 to -80 milligals). This region has traditionally been interpreted as a zone of significant crystal thickening. The anomalies may also indicate a region that is underlain by significant masses of low density granitic rocks. If so, the pegmatites of the district may represent dikes derived by tapping cupolas of underlying granitic melt. Thus, a pegmatite would typically form in a zoned aureol above the parental granite. These spatial relations have been well documented in several pegmatite districts in North America (Cerny, in press).

An alternative hypothesis is that pegmatites are not related to parental granite melts but are the result of in situ anatexis of metapelitic source rocks. However, this alternative is untenable for the Be-enriched pegmatites because it is difficult to envision in situ anatectic processes that could produce a significant enrichment in a suite of incompatible trace elements. A process involving differentiation and presumably a large volume of melt would be required. If this is so, such a melt would be considered a parental granite source. The actual correlation between pegmatites and granites will probably not be resolved in the Southeast until several deep holes are drilled. However, assuming that a large, unexposed parental granite underlies the Cherokee-Pickens district, the parental material may have originated by anatexis of middle and upper crustal source rocks or by magmatic injection from lower crustal environments. A review of known postmetamorphic granites within Georgia indicates that some of these granites were derived from upper crustal sources and others from lower crustal sources (Grant and others, 1980; Atkins and others, 1980; Fullager and Butler, 1979). By analogy, the actual depth of melt generation for an unexposed parental granite is open to conjecture.

Incompatible Trace Elements and Pegmatite Evolution

The nature of incompatible trace element enrichment in each of the pegmatite classes probably involves several processes including partial melting of source rocks (Arth, 1976); crystal fractionation and liquid state diffusion in parental granites (Groves and McCarthy, 1978); and, perhaps, vapor fractionation and thermogravitational diffusion in regions of high geothermal gradients (Shaw and others, 1976; Hildreth, 1981). All of these processes, either acting in concert or separately, can produce significant incompatible trace element enrichment in the roof zone of a differentiating magma chamber; and provide a physiochemical basis for the generation of rare element enrichment in derived pegmatites. Most pegmatites probably represent roof zone portions of a magma chamber tapped at various stages of differentiation. During injections into the host rock differentiation may continue; perhaps, by trace element fractionation at the pegmatite-wall rock interface.

Table 12. Relative age dates for some post-metamorphic pegmatites and granites in Georgia.

Granite	Age Date	Method	Source	Pegmatite	Age Date	Method	Source
Greater Atlanta Region:							
1) Stone Mountain Granite	291±7 m.y. 325 m.y.	Rb/Sr U/Pb Zircon	Whitney and others (1976) Atkins and others (1980)	Cochran Mine	350±20 m.y.	K-Ar	This study
2) Panola Granite	300±15 293±15	K-Ar Rb-Sr	Pinson and others (1957) Pinson and others (1958)	Hillhouse	338±5 m.y.	K-Ar	This study
3) Palmetto Granodiorite	325 m.y.	U/Pb Zircon	Higgins and Atkins (1981)				
4) Ben Hill Granite	342±34 325 m.y.	K-Ar U/Pb Zircon	Pinson and others (1957) Higgins and Atkins (1981)				
Troup and Thomaston-Barnesville Districts:							
					296±16 m.y.	Rb/Sr	Deuser and Herzog (1962)
1) Hollonville Granite	Upper Paleozoic	Rb/Sr	Atkins (in review)	Mauldin	256±m.y.	Rb/Sr	Deuser and Herzog (1962)

A key consideration is the role of volatiles in the differentiation process. An excellent means of enhancing differentiation is by lowering the solidus temperature through depolymyerization of a silicate melt. Depolymerization is enhanced by enrichment in volatiles including F, H_20, and B. As noted by Bailey (1977) and Manning (1981), F can greatly increase the solubility of water in a melt and thereby lower melt viscosity, modify melt structure, and lower the solidus temperature. All of these factors enhance differentiation by promoting crystal settling, liquid state diffusion and volatile complexing (Gunow, 1982).

Bailey (1977) documents that the crystallization temperature for granite may be depressed by about 35°C with the addition of 1.0 wt.% HF. Based on the muscovite compositions given in this study (Appendix B), fluorine appears to have been only a minor constituent of the pegmatites within the Cherokee-Pickens district. However, results reported by Charlton and Martin (1978) indicate that boron may behave in a similar manner as fluorine by depressing the granite solidus by 60°C with the addition of 2 wt% B_2O_3. This may account for the correlation of tourmaline with beryl-bearing pegmatites of the Cherokee-Pickens district.

Depression of the pegmatite solidus by boron enrichment involving anatectic wall rock reactions may promote differentiation during early stages of pegmatite evolution. Perhaps this process explains the correlation of differentiated and rare element enriched pegmatites with the tourmaline-enriched host rocks of the Great Smoky thrust sheet. As indicated in the discussion of the geologic setting for the Cherokee-Pickens district, rocks of the Great Smoky Group and the Murphy belt group contain disseminated tourmaline. During magmatic injection or pegmatite emplacement, granitic melt may have encountered host rocks enriched in tourmaline. If so, it is possible that boron derived from tourmaline would partition into the melt resulting in enhanced differentiation. As the pegmatite migrates up through the crust, volatiles such as boron and fluorine may eventually be expelled by exsolution processes, resulting in pegmatite crystallization and wall rock metasomatism. If this model is accurate, then the observed differences in mineral composition and rare element enrichment between the Holly Springs and Ball Ground fields may be, in part, a function of melt-wall rock reactions.

CONCLUSIONS

Pegmatites of the Cherokee-Pickens district occur in two pegmatite fields, each separated by northeast-trending thrust faults. The Holly Springs Field is characterized by a simple quartz-feldspar-muscovite mineralogy, whereas the pegmatites of the Ball Ground field contain tourmaline ± beryl in addition to the above minerals.

Based on the trace element characteristics of muscovite from pegmatites within the district, the beryl-bearing pegmatites of the Ball Ground field are the most differentiated, whereas those in the Holly Springs field are the least differentiated. The Cochran and Hendrix pegmatites of the Ball Ground field in Cherokee County exhibit anomalous enrichment in rare elements.

All of the pegmatites throughout the district belong to the muscovite class of pegmatites as defined by Cerny (1982a). However, the beryl-bearing pegmatites exhibit an affinity with the rare element class and are distinctly enriched in incompatible trace elements and may have formed in a slightly shallower or boron-enriched environment relative to the other pegmatites of the district. The beryl-bearing pegmatites may have been produced by tapping a more differentiated part of an underlying magma chamber.

The origin of pegmatites with respect to a parental granite is open to conjecture. The preferred interpretation is that the Be-enriched pegmatites (and probably most other pegmatites of the district) are derived from an underlying granite source or sources. This granite source may have been derived from partial melting in either moderate to deep crustal environments. The observed fractionation of trace elements may have been produced by a variety of differentiation processes and melt host rock reactions.

Regardless of origin, the trace element characteristics of pegmatitic muscovite within the district provides useful criteria for: (1) classification of pegmatites, (2) the determination of differentiation trends and (3) the preliminary assessment of the economic potential of the pegmatites within the district.

Favorable features associated with pegmatites having economic potential include:

1. **The development of distinct pegmatite zones.**
   For most pegmatites of the Southeast this includes an interior quartz zone, an intermediate zone and a thin border zone.
2. **Evidence of internal veining and hydrothermal alteration.**
   This is indicated by the presence of quartz veins or replacement minerals within the interior of the pegmatite.
3. **The mineralogy of the pegmatite.**
   (a) The presence of B-, F- or OH-bearing minerals such as tourmaline, muscovite and lepidolite provide evidence for volatile enrichment within a given pegmatite.
   (b) The presence of rare element minerals such as beryl, spodumene, lepidolite and columbite-tantalite are evidence for rare element pegmatites or rare element enriched pegmatites.

4. **Exocontact Features.**
   Evidence for volatile saturation within a given pegmatite is provided by the presence of tourmalinization, albitization or sericitization haloes in the contact zone of the pegmatite.
5. **Muscovite and tourmaline geochemistry.**
   These minerals provide a uniform media for sampling and analysis, and can ultimately be used to classify a given pegmatite. Rare element pegmatites are indicated by micas containing anomalously high values for Rb, Li, Nb, F, Be and Rb/K ratios. Favorable characteristics of tourmaline in rare element pegmatites include Mn/TiO_2 ratios greater than 2.0 and enrichment in Li (>100ppm).
6. **The overall size and orientation of the pegmatite.**
   Only those pegmatites having a significant near-surface exposure are likely to have economic potential. Each pegmatite must be evaluated on an individual basis depending upon the type and distribution of mineralization.
7. **Weathering (saprolitization).**
   Some pegmatites will be favored if they are deeply weathered resulting in amenable rock for mineral extraction and mine development.

Based on the above criteria, the region with the best potential for containing rare element-enriched pegmatites occurs in the Ball Ground area, in the general vicinity between the Hendrix Mine and Cochran Mine, Cherokee County.

REFERENCES

Abrams, C.E., and McConnell, K.I., 1981, Emplacement of the Austell Gneiss: implications regarding the timing of metamorphism and deformation in the Piedmont of Georgia: Geological Society of America Abstracts with Programs, v. 13, p. 1.

Arth, J.G., 1976, Behavior of trace elements during magmatic processes — a summary of theoretical models and their applications: U.S.G.S. Journal of Research, v. 4, p. 41-47.

Atkins, R.L., (in review), Geology of the Cedar Rock Complex: Ph.D. Thesis, Emory University, Atlanta, Georgia.

Atkins, R.L., Higgins, M.W., and Gottfried, D., 1980, Geochemical data bearing on the origin of the Stone Mountain Granite, Panola Granite, and Lithonia Gneiss near Atlanta, Georgia: Geological Society of America Abstracts with Programs, v. 12, p. 170.

Bailey, J.C., 1977, Fluorine in granitic rocks and melts, a review: Chemical Geology, v. 19m, p. 1-42.

Bailey, S.W., 1984, Structures, classification, and crystal chemistry of micas, *in* Bailey, S.W., ed., The Micas: Mineralogical Society of America, Reviews in Mineralogy v. 13, p. 1-57.

Bailey, W.S., 1928, Geology of the Tate Quadrangle, Georgia: Geologic Survey of Georgia Bulletin 43, p. 170.

Beck, W.A., 1948, Georgia mica spots, Cherokee, Upson, Lamar and Monroe Counties, U.S. Bureau of Mines Report of Investigations 4239, p. 29.

Belyankina, Y. D., and Petrov, V.P., 1983, Geochemical role of micas in mineral associations: classification chemistry, and genesis of micas: Int. Geol. Rev., v. 25, p. 993-1003.

Bloss, F.D., 1971, *Crystallography and crystal chemistry: an introduction:* New York, Holt, Rinehart and Winston.

Boggs, R.C., 1986, Pegmatite mineralogy of the Tertiary anorogenic granites of Idaho, *in:* Modreski, P.J. and others, eds., Colorado Pegmatites, Abstracts, Short Papers, and Field Guides from the Colorado Pegmatite Symposium, 1986, p. 48-49.

Brock, K.J., 1974, Zoned lithium-aluminum mica crystals from the Pala pegmatite district: American Mineralogist, v. 59, p. 1242-1248.

Cameron, E.N., Jahns, R.H., McNair, A. and Page, L.R., 1949, Internal Structure of Granitic Pegmatites: Econ. Geol. Monogr. 2, 115 p.

Cerny, P., 1982a, Anatomy and classification of granitic pegmatites, *in*: Cerny, P., ed., Short Course in Granitic Pegmatites in Science and Industry, Mineraological Association of Canada, v. 8, p. 1-39.

Cerny, P., 1982b, The Tanco pegmatite at Bernice Lake, southeastern Manitoba, *in*: Cerny, P., ed., Short Course in Granitic Pegmatites in Science and Industry, Minerological Association of Canada, v. 8, p. 527-543.

Cerny, P., 1982c, Petrogenesis of granitic pegmatites, *in*: Cerny, P., ed., Short Course in Granitic Pegmatites in Science and Industry, Mineralogical Association of Canada, v. 8, p. 405-571.

Cerny, P., 1986, Classification of granitic pegmatites, *in*: Modreski, P.J. and others, eds., Colorado Pegmatites, Abstracts, Short Papers and Field Guides from the Colorado Pegmatite Symposium, 1986, p. 16-19.

Cerny, P., and Burt, D.M., 1984, Paragenesis, crystallochemical characteristics and geochemical evolution of micas in granite pegmatites *in* Bailey, S.W., ed., Micas: Mineralogical Society of America, Reviews in Mineraology, v. 13, p. 257-297.

Cerny, P., Goad, B.E., Hawthorne, F.C., and Chapman, R., 1986, Fractionation trends of the Nb- and Ta-bearing oxide minerals in the Greer Lake pegmatitc granite and its pegmatite aureole, southeastern Manitoba: American Mineralogist, v. 71, p. 501-517.

Cerny, P. and Meintzer, R.E., (in press), Fertile granites in the archean and proterozoic fields of rare element pegmatites: crustal environment, geochemistry, and petrogenetic relationships: Canadian Inst., Mining and Metallurgy, Special Volume #39.

Charlton, L.B., and Martin, R.F., 1978, The effect of boron on the granite solidus: Canadian Mineralogist, v. 16, p. 239-244.

Cook, R.B., Jr., 1978, Minerals of Georgia, their properties and occurrences: Georgia Geologic Survey Bulletin 92, 189 p.

Cook, R.B., Jr., and Foord, E.E., 1986, Geology and Mineralogy of the McAllister Sn-Ta deposit, Coosa County, Alabama, USA: Abstracts of Proceedings, 7th IAGOD symposium, Luela, Sweden.

Costello, J.O., 1978, Shear zones in the Corbin Gneiss of Georgia, *in*: Short contributions to the geology of Georgia: Georgia Geologic Survey Bulletin 92, p. 32-37.

Costello, J.O., and McConnell, K.I., 1980, Stratigraphy of the southwestern Blue Ridge and northernmost Piedmont of Georgia: Geological Society of America, Abstracts with Programs, v. 12, p. 175.

Dallmeyer, R.D., 1978, $^{40}Ar/^{40}Ar$ incremental-release ages of hornblende and biotite across the Georgia Inner Piedmont; Their bearing on late Paleozoic-early Mesozoic tectonothermal history: American Journal of Science, v. 278, p. 124-149.

Dalrymple, G.B., Gromme, C.S., and White, R.W., 1975, Potassium-argon age and paleomagnetism of diabase dikes in Liberia; Initiation of Central Atlantic rifting: Geological Society of America, Bulletin v. 86, p. 399-411.

Deer, W.A., Howie, R.A., and Zussman, J., 1962, *Rock-forming minerals,* New York, John Wiley and Sons, v. 1-5, 371 p.

Deuser, W.G., and Herzog, L.F., 1962, Rubidium-Strontium age determinations of muscovites and biotites from pegmatites of the Blue Ridge and Piedmont, Journal of Geophysical Research, v. 67, p. 1998-2003.

Dietrich, R.V., 1985, *The tourmaline group:* Van Nordstrom — Rhinehart, New York, 300 p.

Dooley, R.E., and Wampler, J.M., 1983, Potassium-argon relations in diabase dikes of Georgia — The influence of excess ^{40}Ar on the geochronology of early Mesozoic igneous and tectonic events: U.S.G.S Professional Paper 1313-M, p. 20-22.

Eckel, E.B., 1961, Minerals of Colorado: a 100-year record: U.S.G.S. Bulletin 1114, 399 p.

El Bouseily, R.M., and El Sokkary, A.A., 1975, The relation between Rb, Ba, and Sr in granitic rocks: Chem. Geology, v. 16, p. 207-219.

Fairley, W.M., 1965, The Murphy syncline in the Tate quadrangle, Georgia: Georgia Geologic Survey Bulletin 75, 71 p.

Fairley, W.M., 1969, Stratigraphy and structure of the Murphy Marble Belt in parts of northern Georgia: Georgia Geological Survey Bulletin 80, p. 89-120.

Foit, F.F., and Rosenberg, P.E., 1977, Coupled substitutions in the tourmaline group: Contributions to Mineralogy and Petrology, v. 62, p. 109-127.

Foord, E.E., 1976, Mineralogy and petrogenesis of layered pegmatite aplite dikes in the Mesa Grande district, San Diego County California: Ph.D. Thesis, Stanford University, Stanford, California.

Foord, E.E., 1986, Crystal chemistry and origin of the color of amazonite, particularly that from the Pikes Peak Batholith, Colorado, *in*: Modreski, P.J. and others, eds., Colorado Pegmatites, Abstracts, Short Papers and Field Guides from the Colorado Pegmatite Symposium, 1986, p. 77-83.

Foord, E.E., and Cook, R.B., Jr., (in press), The Mineralogy and Paragenesis of the McAllister Sn-Ta deposit, Coosa County, Alabama: Canadian Mineralogist.

Foord, E.E., and Martin, R.F., 1979, Amazonite from the Pikes Peak Batholith: Mineralogical Record, v. 10, p. 373-382.

Foster, M.D., 1960, Interpretation of the composition of lithium micas: U.S.G.S. Professional Paper 354-E, p. 115-147.

Fullager, P.D., and Butler, R.J., 1979, 325 to 265 M.Y.-old granitic plutons in the Piedmont of the southeastern Appalachians, American Journal of Science, v. 279, p. 161-185.

Furcron, A.S., 1959, Beryl in Georgia: Georgia Mineral Newsletter, v. 12, p. 91-95.

Furcron, A.S., and Teague, K.H., 1943, Mica-bearing pegmatites of Georgia: Georgia Geological Survey Bulletin 48, 192 p.

Galpin, S.L., 1915, A preliminary report on the feldspar and mica deposits of Georgia: Geological Survey of Georgia Bulletin 30, 190 p.

German, J.M., 1985, The geology of the northeastern portion of the Dahlonega Gold Belt: Georgia Geologic Survey Bulletin 100, 41 p.

Ginsburg, A.I., 1960, Specific geochemical features of the pegmatitic process: Report of the 21st Session of the International Geological Congress, Rept. #17, p. 111-121.

Glass, J.J., 1935, The pegmatite minerals from near Amelia, Virginia: American Mineralogist, v. 20, p. 741-768.

Gordiyenko, V.V., 1971, Concentrations of Li, Rb and Cs in potash feldspar and muscovite as criteria for assessing the rare-metal mineralization in granite pegmatites: Int. Geol. Rev., v. 13, p. 134-141.

Grant, W.H., Size, W.B., and O'Connor, B.J., 1980, Petrology and structure of the Stone Mountain Granite and Mount Arabia migmatite, Lithonia, Georgia: *in* Frey, R.W., ed., Excursions in Southeastern Geology: American Geological Institute, v. 1, p. 41-57.

Griffitts, W.R., 1954, Beryllium resources of the tin-spodumene belt, North Carolina: U.S.G.S. Circular 309, 12 p.

Griffitts, W.R., 1973, Beryllium, *in* Brobst, D.A. and Pratt, W.P., eds., United States Mineral Resources: U.S.G.S. Professional Paper 820, p. 85-93.

Griffitts, W.R., and Olson, J.C., 1953, Mica deposits of the Southeastern Piedmont, part 7, Hartwell district, Georgia and South Carolina: U.S.G.S. Professional Paper 248-E, p. 293-315.

Groves, D.I., and McCarthy, T.S., 1978, Fractional crystallization and the origin of tin deposits in granitoids: Mineral Deposits, v. 13, p. 11-26.

Guidotti, C.V., 1984, Micas in metamorphic rocks: *in* Bailey, S.W., ed., Micas: Mineralogical Society of America, Reviews in Mineralogy, v. 13, p. 357-467.

Gunow, A.J., 1982, Trace element mineralogy in the porphyry molybdenum environment: unpub. Ph.D. Thesis, University of Colorado, 265 p.

Gunow, A.J., Ludington, S., and Munoz, J.L. 1980, Fluorine in micas from the Henderson deposit, Colorado: Economic Geology, v. 75, p. 1122-1137.

Hanley, J.B., Heinrich, E.W., and Page, L.R., 1950, Pegmatite investigations in Colorado, Wyoming, and Utah, 1942-1944, U.S.G.S. Professional Paper 227, 125 pp.

Hayes, C.W., 1901, Geological relations of the iron-ores in the Cartersville district, Georgia: American Institute of Mining Engineers Transactions, v. 30, p. 403-419.

Hazen, R.M., and Burnham, C.W., 1973. The crystal structure of one-layer phlogopite and annite: American Mineralogist, v. 58, p. 889-900.

Heinrich, E.W., 1953, Chemical differentiation of multigeneration pegmatite minerals [abs.]: American Mineralogist, v. 38, p. 343.

Heinrich, E.W., 1962, Geochemical prospecting for beryl and columbite; Economic Geology, v. 57, p. 616-619.

_____, 1967, Micas of the Brown Derby pegmatites, Gunnison County, Colorado: American Mineraologist, v. 52, p. 1110-1121.

Heinrich, E.W., Klepper, M.R., and Jahns, R.H., 1953, Mica deposits of the southeastern Piedmont, part 9: Thomaston-Barnesville District, Georgia, Part 10: Outlying deposits in Georgia: U.S.G.S. Professional Paper 248-F, p. 327-400.

Higgins, M.W., and Atkins, R.L., 1981, The stratigraphy of the Piedmont southeast of the Brevard zone in the Atlanta, Georgia, area, *in*: Wigley, P.B., ed., Latest thinking on the stratigraphy of selected areas in Georgia: Georgia Geologic Survey Information Circular 54-A, p. 3-40.

Hildreth, W., 1981, Gradients in silicic magma chambers: Implications for lithospheric magmatism: Journal Geophysical Research, v. 86, p. 10153-10192.

Hurst, V.J., 1955, Stratigraphy, structure and mineral resources of the Mineral Bluff Quadrangle, Georgia: Georgia Geologic Survey Bulletin 63, 137 p.

_____, 1973, Geology of the southern Blue Ridge belt: American Journal of Science, v. 273, p. 643-670.

Jahns, R.H., 1955, The study of pegmatites; Economic Geology 50th Anniversary, v. 1, p. 1025-1130.

Jahns, R.H., 1982, Internal evolution of pegmatite bodies, *in*: Cerny, P., ed., Short Course in Granitic Pegmatites in Science and Industry, Mineralogical Association of Canada, v. 8, p. 293-327.

Jahns, R.H., and Lancaster, R.W., 1950, Physical characteristics of commercial sheet muscovite in the southeastern United States: U.S.G.S. Professional Paper 225, 110 p.

Jahns, R.H., Griffitts, W.R., and Heinrich, E.W., 1952, Mica Deposits of the Southeastern Piedmont, Part 1, General Features, U.S.G.S. Professional Paper 248-A, 99 p.

Jahns, R.H., and Ewing, R.C., 1976, The Harding mine, Taos County, New Mexico: N. Mex. Geol. Soc. Guidebook, 27th Field Conf., Vermejo Park, p. 263-276.

Jolliff, B.L., Papike, J.J., and Shearer, C.K., 1986, Tourmaline as a recorder of pegmatite evolution: Bob Ingersoll pegmatite, Black Hills, South Dakota: American Mineralogist, v. 71, p. 472-500.

Kesler, T.L., 1961, Exploration of the Kings Mountain Pegmatites: Mining Engineering, v. 13, p. 1062-1068.

Kesler, T.L., 1976, Occurrence, development, and long-range outlook of lithium-pegmatite ore in the Carolinas, U.S.G.S. Professional Paper 1005, p. 45-50.

Kulikov, I.V., Petrov, M.G., Royzenman, F.M., and Glebov, M.P., 1976, Rare-metal rebullite-quartz-feldspar pegmatite veins and their importance in exploration: Int. Geol. Rev., v. 18, p. 205-208.

LaForge, L., and Phalen, W.C., 1913, Ellijay Folio: U.S.G.S. Geologic Atlas of the United States, Folio 187, 22 p.

Landes, K.K., 1933, Origin and classification of pegmatites, American Mineralogist, v. 18, p. 33-56, 95-103.

London, D., 1986, Formation of tourmaline-rich gem pockets in miarolitic pegmatites: American Mineralogist, v. 71, p. 396-405.

London, D., and Burt, D.W., 1982, Lithium minerals in pegmatites: *in* Cerny, P., ed., Mineralogical Association of Canada, Short Course in Granitic Pegmatites in Science and Industry, v. 8, p. 99-1133.

Long, T.L., Bridges, S.R., and Dorman, L.M., 1972, Simple Bouger gravity map of Georgia: Georgia Geological Survey Map.

Makrygina, V.A., 1977, Role of metamorphic zonation in distribution of pegmatites and migmatites of different composition: Int. Geol. Rev., v. 19, p. 1133-1141.

Manning, D.A.C., 1981, The effect of fluorine on liquidus phase relationships in the system Qz-Ab-Or with excess water at 1 kb: Contr. Mineralogy and Petrology, v. 76, p. 206-215.

Martin, B.F., 1974, The petrology of the Corbin Gneiss: (unpubl.) M.S. Thesis, University of Georgia, Athens, 133 p.

McCallie, S.W., 1926, Mineral resources of Georgia: Geological Survey of Georgia Bulletin 23, 164 p.

McConnell, K.I., and Abrams, C.E., 1982, Geology of the New Georgia Group and associated massive sulfide and gold deposits: West-central Georgia: Guidebook, Exploration for Metallic Resources in the Southeast Symposium, University of Georgia Center for Continuing Education, p. 143-170.

_____, 1984, The geology of the Greater Atlanta Region: Georgia Geologic Survey Bulletin 96, 127 p.

McConnell, K.I., and Costello, J.O., 1979, Large scale crustal shortening in the southwest Georgia Blue Ridge and adjacent Piedmont: Geological Society of America Abstracts with Programs, v. 11, p. 205.

_____, 1980, Guide to geology along a traverse through the Blue Ridge and Piedmont Provinces of north Georgia: *in* Frey, R.W., ed., Excursions in Southeastern Geology, American Geological Institute, v. 1, p. 241-258.

_____, 1984, Basement-cover rock relationships along the western edge of Blue Ridge thrust sheet in Georgia: *in* Bartholomew, M.J., ed., The Grenville event in the Appalachians and related topics: Geological Society of America Special Paper 194, p. 263-279.

Muñoz, J.L., 1984, F-OH and C1-OH exchange in micas with applications of hydrothermal ore deposits *in*: Bailey, S.W., ed., Micas: Mineralogical Society of America, Reviews in Mineralogy, v. 13, p. 469-490.

Munoz, J.L. and Gunow, A.J., 1982, Fluorine index: A simple guide to high fluorine environments: Geological Society of American, Abstracts with Programs, v. 14, p. 573.

Nemec, D., 1969, Fluorine in pegmatitic muscovites: Geochem. Int., v. 6, p. 58-68.

Nieva, A.M.R., 1975, Geochemistry of muscovite in the pegmatites of northern Portugal: Fortschr. Mine., v. 52, p. 303-315.

Norton, J.R., 1973, Lithium, cesium and rubidium — the rare alkali metals, *in*: Brobst, D.A. and Pratt, W.P., eds., United States Mineral Resources: U.S.G.S. Professional Paper 820, p. 365-378.

Norton, J.J., Page, R.L. and Brobst, D.A., 1962, Geology of the Hugo pegmatite, Keystone, Dakota, U.S.G.S. Professional Paper 297-B, p. 49-128.

Odom, A.L., Kish, S. and Leggo, P., 1973, Extension of "Grenville basement" to the southern extremity of the Appalachians, U-Pb ages of zircons: Geological Society of America Abstracts with Programs, v. 5, p. 425.

Page, L.E., Adams, J.W., Erickson, M.P., Hall, W.E., Hanley, J.B., Joralemon, P., Norton, J.J., Pray, L.C., Steven, T.A., Stoll, W.C., and Stopper, R.F., 1953, Pegmatite investigations, 1942-1945, Black Hills, South Dakota: U.S.G.S. Professional Paper 247, 228 pp.

Pinson, W.H., Fairburn, H.W., Hurley, P.M., Herzog, L.F., and Cormier, R.F., 1958, Age study of some crystalline rocks of the Georgia Piedmont, *in* Variations in isotopic abundances of strontium, calcium and argon and related topics: U.S. Atomic Energy Commission Report NYO-3938, p. 58-60.

Pinson, W.H., Herzog, L.F., and Cormier, R.F., 1957, Age study of some crystalline rocks of Georgia Piedmont, *in* Variations in isotopic abundances of strontium, calcium, and argon and related topics: U.S. Atomic Energy Commission Report NYO-3937, p. 58-61.

Power, W.R., 1978, Economic geology of the Georgia Marble District, *in* Twelfth forum on the geology of industrial minerals: Georgia Geologic Survey Information Circular 49, p. 59-67.

Power, W.R. and Forrest, J.T., 1973, Stratigraphy and paleogeography in the Murphy Marble Belt: American Journal of Science, v. 273, p. 698-711.

Reno, H.C., 1956, Beryllium, *in* Mineral Facts and Problems: U.S. Bureau of Mines Bulletin 556, p. 95-102.

Rinaldi, R., Cerny P., and Ferguson, R.B., 1972, The Tanco pegmatite at Bernic Lake, Manitoba. VI Lithium-rubidum-cesium micas: Canadian Mineralogist, v. 11, p. 690-707.

Shaw, H.R., Smith, R.L. and Hildreth, W., 1976, Thermogravitational mechanism for chemical variations in zoned magma chambers; Geological Society of America, Abstracts with Programs, v. 8, p. 1102.

Shearer, C.K., Papike, J.J., Simon, S.B., and Laul, J.C., 1986, Pegmatite-wallrock interactions, Black Hills, South Dakota: Interaction between pegmatite derived fluids and quartz-mica schist wallrock: American Mineralogist, v. 71, p. 518-539.

Shamakin, B.M., 1984, Geochemistry and origin of granitic pegmatites: Geochemistry Int., v. 21, p. 1-8.

Smith, J.W., Wampler, J.M., and Green, M.A., 1969, Isotopic dating and metamorphic isograds of the crystalline rocks of Georgia, *in* Precambrian-Paleozoic Appalachian problems: Georgia Geological Survey Bulletin 80, p. 121-139.

Speer, J.A., 1984, Micas in igneous rocks, *in* Bailey, S.W., ed., Micas: Mineralogical Society of America, Reviews in Mineralogy, v. 13, p. 299-356.

Staatz, M.H., Murata, K.J. and Glass, J.J., 1955, Variation in composition and physical properties of tourmaline with its position in the pegmatite: American Mineralogist, v. 40, p. 789-804.

Staatz, M.H., Griffitts, W.R., and Barnett, P.R., 1965, Differences in the minor element composition of beryl in various environments: American Mineralogist, v. 50, p. 1783-1795.

Staatz, M.H., and Trites, A.F., 1955, Geology of the Quartz Creek pegmatite district, Gunnison County, Colorado, U.S.G.S. Professional Paper 265, 111 p.

Stern, L.A., Brown, G.E., Bird, Jr., D.K., and Jahns, R.H. 1986, Mineralogy and geochemical evolution of the Little Three pegmatite aplite layered intrusive, Ramona, California: American Mineralogist, v. 71, p. 406-427.

Sterrett, D.B., 1923, Mica deposits of the United States: U.S.G.S. Bulletin 740, 342 p.

Switzer, G., 1939, Granite pegmatites of the Mt. Antero Region, Colorado: American Mineralogist, v. 24, p. 791-809.

Trueman, D.L. and Cerny, P., 1982, Exploration for rare-element granitic pegmatites, *in*: Cerny, P., ed., Short Course in Granitic Pegmatites in Science and Industry, Mineralogical Association of Canada, v. 8, p. 463-494.

Turner, F.J., and Verhoogen, J., 1960, *Igneous and metamorphic petrology*: New York, New York, McGraw-Hill Book Company, 694 p.

Whitney, J.A., Jones, L.M. and Walker, R.L., 1976, Age and origin of the Stone Mountain Granite, Lithonia district, Georgia: Geological Society of America Bulletin, v. 87, p. 1067-1077.

Whitney, J.A., and Wenner, D.B., 1980, Petrology and structural setting of post-metamorphic granites of Georgia; *in* Frey, R.W., ed., Excursions in Southeastern Geology: American Geological Institute, v. 2, p. 351-378.

Winkler, H.G.F., 1967, *Petrogenesis of Metamorphic Rocks*; 2nd ed., Springer-Verlag, New York, 334 p.

APPENDIX A
SELECTED PEGMATITE DEPOSITS

The Cochran Mine

The Cochran Mine is located within the Great Smoky thrust sheet, 4 km N 78°E of Ball Ground and 1.4 km east of Long Swamp Creek, within northeastern Cherokee County. The most comprehensive report concerning this pegmatite is that of Furcron and Teague (1943).

The earliest reported mining activity at the Cochran Mine occurred in 1933 by the Georgia Mineral Products Company at Holly Springs, Georgia for the production of sheet and scrap mica. As the demand for beryllium rose during World War II, the Cochran Mine became a source for beryl ore. From 1942-1945 over 4,000 lbs of beryl were mined from this location (Furcron, 1959). In 1985 minor scrap mica, sheet mica and 10-12 tons of beryl were removed and sold as the result of a small-scale, hand-cobbing operation. The Georgia Geologic Survey drilled 5 diamond drill holes along the strike of the pegmatite to test the continuity of the pegmatite at depth. The pegmatite is currently owned by Jack Parkman of Atlanta, Georgia.

The Cochran pegmatite averages greater than 25 meters in width and has a strike length of at least 500 meters. The pegmatite has been mined in two separate areas along its strike, forming a lower pit and an upper pit (Figure 11).

The lower pit incorporates the early pit and most of the small shafts mentioned by Furcron and Teague (1943). At present the lower pit measures approximately 60 meters long, 20 meters wide and trends N 36°E. The pit walls are composed of deeply saprolitized medium- to fine-grained pegmatite consisting of weathered feldspar, perthite, muscovite and quartz. Accessory minerals include tourmaline, beryl, and weathered garnet. Individual crystals of tourmaline, beryl and muscovite up to 15 cm across are common. Local zones containing massive quartz are exposed on the northeast side of the pit.

The upper pit is located in the area described by Furcron and Teague (1943) as the open cut. This portion of the pegmatite trends N70-N75°E and dips 48-53° southeast. Present exposures of the pegmatite within the upper pit measure 100 meters by 10 meters. Although deeply saprolitized, the pegmatite from this area exhibits a wide variety of textures including perthitic, graphic, and coarse-to fine-grained pegmatite. Individual crystals of tourmaline, muscovite and beryl (up to 0.5 meters long) are present within the saprolitized feldspar, muscovite and quartz matrix.

X-ray analyses of two samples of strongly saprolitized feldspar from the upper pit indicates that at least some of the feldspar is microline. When rubbed between the fingers, the white, powdery microline, which looks nearly identical to kaolinite, has a slightly gritty feel. Other X-ray analyses of saprolitized feldspar indicate the presence of kaolinite in the most intensely weathered portion of the pegmatite.

The host rocks of the Cochran pegmatite consist of garnet and tourmaline-bearing, quartz-muscovite-biotite schists, metaarkose, metasandstone and garnet-bearing biotite gneiss of the Dean Formation, Ocoee Supergroup. Muscovite-biotite schists predominate south of the pegmatite and within the hanging wall of the pegmatite, whereas biotite gneiss, metaarkose, and metasandstone predominate as outcrops on the footwall side of the pegmatite.

Several excellent outcrop exposures of a schist-pegmatite contact are located at the south side of the upper pit. Here the foliation of the schist trends N 75°E and dips 51°E and the pegmatite is concordant. The contacts between the red saprolitized schists and the white pegmatite are sharp and distinct (Figure 12).

The Cochran pegmatite is a zoned pegmatite characterized by at least three zones. These include a hanging wall border zone, an intermediate zone and a core zone. The hanging wall border zone is a narrow 5-15 cm band of quartz-muscovite-tourmaline in which muscovite crystals are oriented perpendicular to the contact. Muscovite is typically less than 4 cm wide and is a dark gray color, which is distinctive relative to muscovite from all other zones within the pegmatite. Feldspar is relatively abundant adjacent to the intermediate zone.

The intermediate zone constitutes the bulk of the pegmatite and consists of fine- to coarse-grained feldspar-quartz-muscovite with accessory tourmaline, beryl and weathered garnet. The tourmaline occurs as black euhedral crystals exhibiting a length/width ratio of 3/1. In thin section, the tourmaline interior to the border zone exhibits a light blue-dark blue pleochroism whereas the tourmaline from the border zone and the surrounding mica schist exhibit a muddy brown to green pleochroism. The beryl occurs as euhedral, light buff, pale yellow, light apple green or bluish-green crystals that are typically fractured. Manganese oxides are commonly observed filling fracture surfaces of many of the crystals.

The large muscovite crystals occur as faint greenish-yellow euhedral books up to 25 cm wide and 20 cm thick. Most of this sheet mucovite splits well, is relatively free of mineral impurities (less than 1%), and only occassionally exhibits ruling. Mineral inclusions observed in these large muscovite crystals include manganese oxides, iron oxides, rutile, kaolinite and tourmaline.

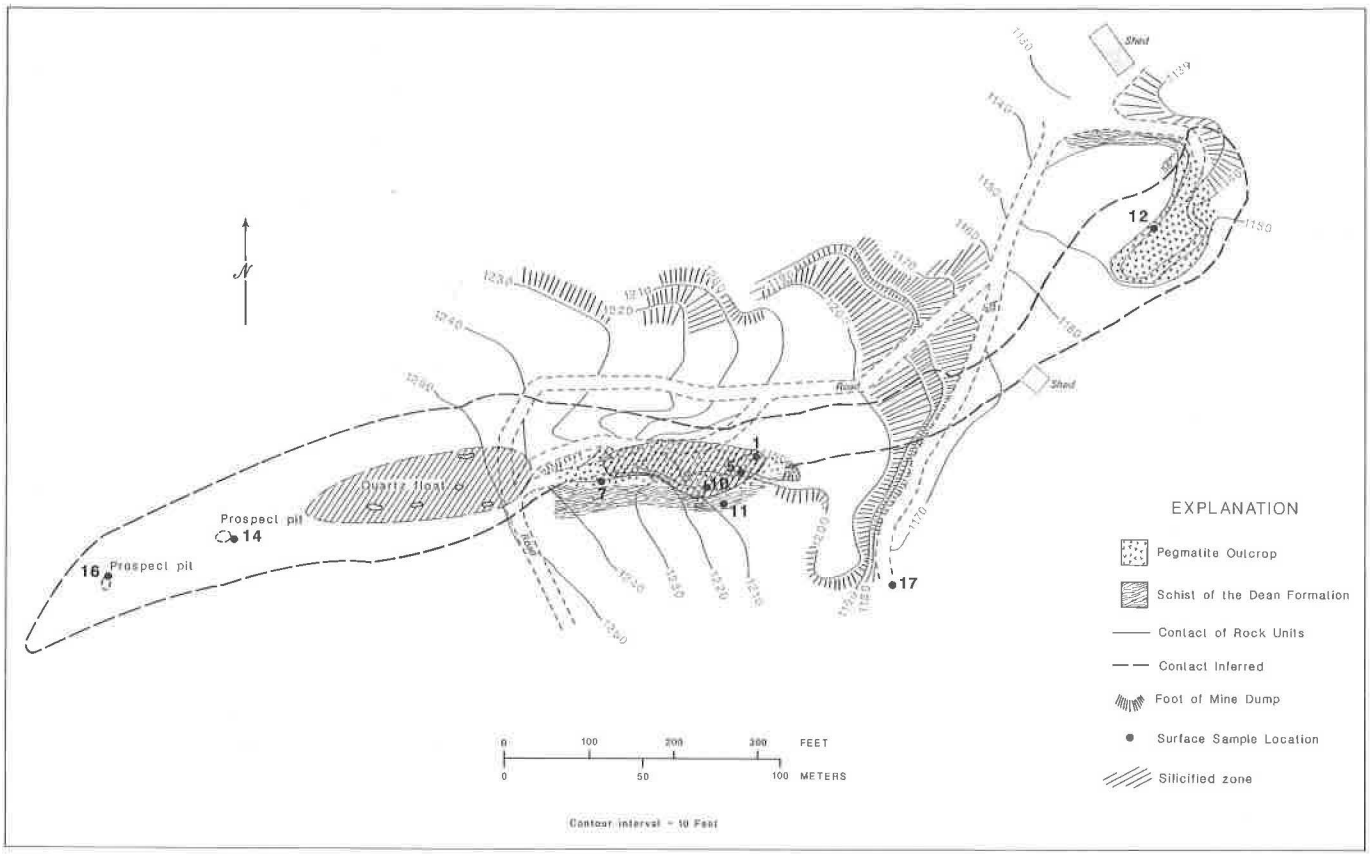

Figure 11. Geologic Map of the Cochran Pegmatite, Cherokee County, Georgia.

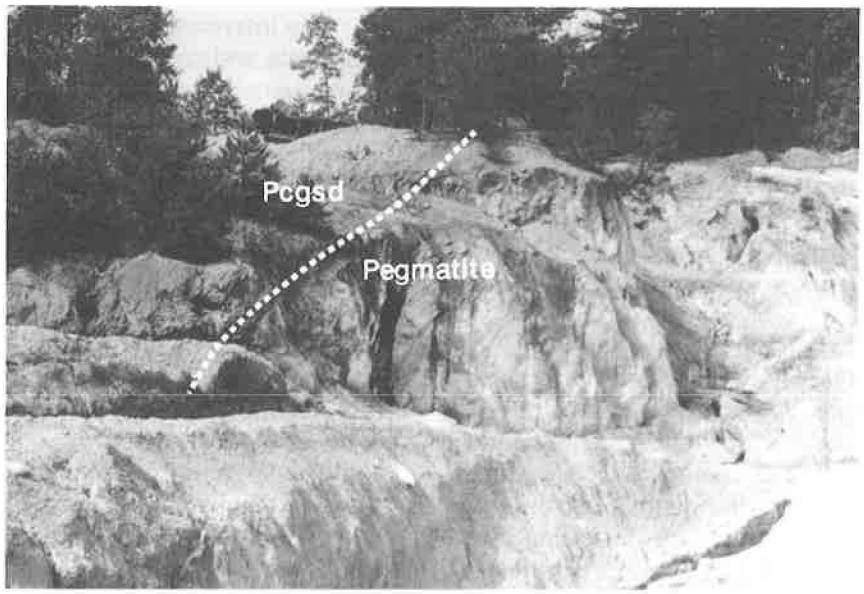

Figure 12. Contact between mica schist of the Dean Formation (Pcgsd) and the Cochran pegmatite. View is to the southeast, south hanging wall, upper pit.

A sample of muscovite from the intermediate zone has been dated by K-Ar methods yielding an age date of 356 ± 20 m.y. (J.M. Wampler, personal communications, 1986).

A second variety of muscovite in this intermediate zone occurs as colorless, randomly oriented crystal aggregates, up to 5 cm wide, enveloping large tourmaline crystals. This variety of muscovite typically exhibits numerous striations, herringbone structure and curved facies, resulting in muscovite that splits poorly. This muscovite forms as either a replacement of the tourmaline or as a selected replacement of feldspar adjacent to tourmaline during late-stage hydrothermal alteration. The late-stage development of this muscovite is indicated by the occurrence of muscovite veinlets crosscutting disseminated tourmaline (Figures 13 and 14).

The core zone of this pegmatite is arbitrarily defined as a zone composed of greater than 25% quartz over a 3 meter interval. The quartz from the core zone consists of massive quartz lenses, clear quartz and smoky quartz veins, and intergranular quartz. Euhedral beryl and tourmaline crystals are found as either dissemination or as accessory minerals in smoky quartz veins. Beryl is typically associated with the quartz veins. Vein-related beryl is nearly of gem quality exhibiting exceptional euhedral forms and a light-green coloration (Figure 15). The extent of the exposed quartz core is shown in Figure 11. The existence of abundant massive quartz float to the west of the present workings on the upper pit suggests that the quartz core may be more extensive, possibly occurring as multiple bifurcating lenses.

Disseminated beryl occurs as crystals up to 0.5 meters long and is commonly cut by quartz-potassium feldspar veins up to 1 cm wide. Both white and pink varieties of potassium feldspar are associated with these veins.

An unusual banded quartz zone occurs between the core and intermediate zone. The banded zone consists of distinct blocks up to 5 meters long characterized by 1 mm-1 cm wide bands of quartz alterating with pegmatite layers up to 1 cm wide. The edges of these banded zones are abruptly terminated by fine-grained to coarse-grained pegmatite. Bands within the banded rock are approximately parallel with the foliation of the host rock. The origin of banded rock within the Cochran Mine pegmatite is unknown.

Tourmalinization is commonly observed in the hanging wall mica schist within 10 meters of the pegmatite contact. This alteration is characterized by the development of quartz-muscovite-tourmaline lenses, up to 0.2 meters wide and elongate parallel to the foliation of the schist. Individual crystals of tourmaline from this zone are generally less than 1 cm long occurring as aggregates within the podiform lenses. In thin section this tourmaline has a brownish-green pleochroism and appears to form as an alteration of biotite (Figures 16 and 17). Modal and chemical analyses of relatively fresh and tourmalized mica schist are shown in Table 8. The locations for these samples are indicated in Figure 11.

Due to the large size of this pegmatite and the abundance of beryl relative to other pegmatite within the district, the Cochran pegmatite should be evaluated in more detail for its economic potential as a source for sheet muscovite, scrap muscovite, feldspar, beryl, and possibly, kaolinite. Field relations indicate that the Cochran pegmatite is probably continuous from the lower pit through the upper pit and extends at least 200 meters west of the present upper pit workings. Assuming an average mineable pegmatite width of 35 meters with a hanging wall dip of 50° and a footwall dip of 35°, the following reserves are estimated:

Proven reserves:	250,000 tons of pegmatite (8 meter depth)
Probable reserves:	550,000 tons of pegmatite (16 meter depth)

These estimates also assume a maxium of 3 meters of overburden and that the pegmatite averages 2670 kg/cubic meter.

If one allows for an extension of the pegmatite to the northwest of the present working, in a zone delineated by quartz float, the possible reserves of this pegmatite are estimated at 1.2 million tons of pegmatite. The actual percentage of recoverable minerals would have to be determined by a more detailed study.

The Marblehill Pegmatite

The Marblehill pegmatite is an example of a boron-enriched but beryllium-poor pegmatite within the Great Smoky thrust sheet. This pegmatite includes the Foster prospect described by Furcron and Teague (1943) and several outcrop exposures southwest of the prospect. It is located in southeastern Pickens County near the town of Marblehill. The pegmatite extends from a small knob approximately 1200 meters N30°W of Marblehill and has intermittent exposures for 700 meters along a N60°E-N75°E, S60°W-S75°W trend (Figure 18). The pegmatite dips 18°-24° to the southeast nearly parallel to the hill slopes of this region. The pegmatite varies from less than 0.5 meters to up to 1.5 meters in thickness and consists of a fine-grained to medium-grained pegmatite assemblage of microcline-quartz-plagioclase-muscovite and tourmaline. Garnet and biotite are common accessory minerals. The garnets occur as 1 mm to 1 cm wide, red, euhedral crystals which vary from clear, gem quality crystals to deeply weathered, oxidized crystals. The host rocks consist of tourmaline and garnet-bearing muscovite schists of the Brasstown formation (Fairley, 1969).

Biotite is found as brownish-black to golden-brown pseudohexagonal intergrowths in muscovite up

Figure 13. Late-stage muscovite forming an alteration rim on tourmaline, and fracture-fillings within the tourmaline crystal; Cochran pegmatite, Cherokee County.

Figure 14. Late-stage muscovite (M) forming a fracture-filling within tourmaline (T); transmitted light, 64X. Width of field is 1.42 mm.

Figure 15. Vein-related beryl associated with smoky quartz at the Cochran pegmatite, Cherokee County.

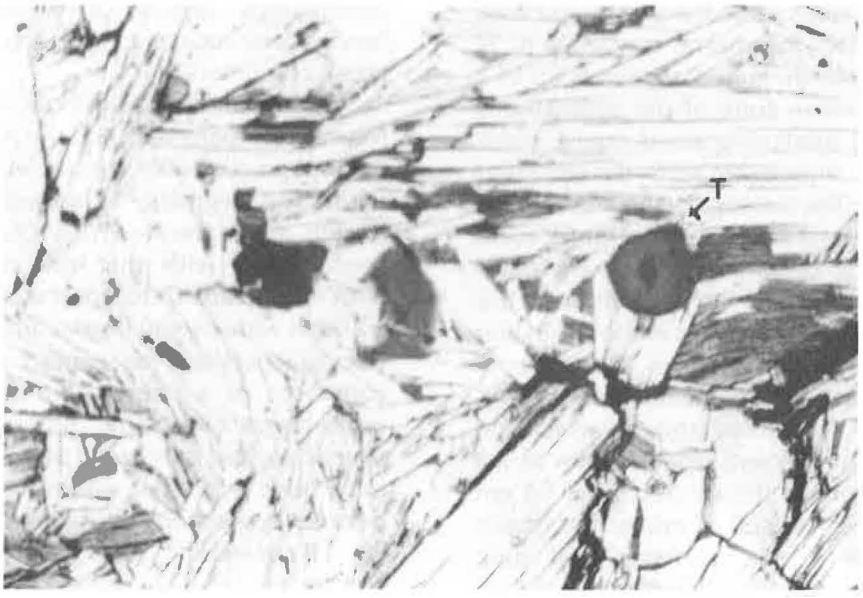

Figure 16. Example of relatively fresh, tourmaline (T)-bearing mica schist from the Dean Formation, Cochran Mine. Sample P-17, transmitted light, 190X. Width of field is .48 mm.

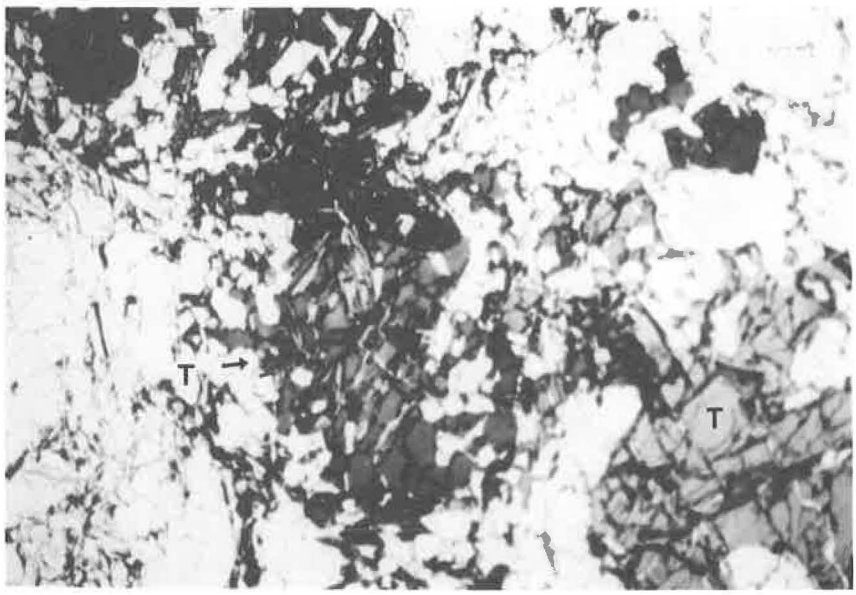

Figure 17. Example of tourmalinized mica schist from the Dean Formation containing an abundance of coarse-grained tourmaline (T), Cochran Mine, Sample P-11, transmitted light, 30X. Width of field is 3 mm.

to 10 cm wide. The tourmaline is schorl, varying from less than 1 mm up to 10 cm in length and exhibits brown to green pleochroism in thin section.

The Marblehill pegmatites are generally conformable to host rock foliation and are only weakly zoned in the widest portions of the pegmatite. The zoning is characterized by a 0.5 meter wide massive quartz core containing euhedral black tourmaline crystals up to 10 cm long and dark red, fresh, euhedral garnets up to 1 cm wide. The intermediate zone of the pegmatite is composed of fine- to medium-grained equigranular feldspar, quartz and muscovite with disseminated tourmaline and garnet. The cleavage of the muscovite is oriented parallel to the foliation of the country rock. Inclusions of tourmaline-bearing mica schist are found within the intermediate zone of the pegmatite and it is typical to see tourmaline segregations in the pegmatite adjacent to the schist inclusions (Figures 19 and 20).

The contact between the pegmatite and the schist is characterized by an 8 cm wide zone in which the tourmaline in the schist coarsens from 0.2 mm to 2-8 mm adjacent to the contact (Figure 21). Local 1-3 cm wide pegmatite pods composed of microcline quartz and plagioclase appear to have been emplaced along foliation planes of the tourmaline-bearing schist. Adjacent to these pods the foliation of the schist appears to have been warped as if to accommodate the pegmatite during emplacement.

Fracture-filling and host rock alteration are rare within the Marblehill pegmatites. Only at the Foster prospect has veining been observed. These veins consist of 1mm-2cm wide smoky quartz that cut potassium feldspar within the pegmatite. Muscovite from the Marblehill pegmatites is relatively free of mineral inclusions, typically exhibits curved plates and herringbone structure, and is characterized by a silvery-green coloration.

Recent drilling (drill hole 85-13) by the Georgia Marble Company revealed the presence of a 0.3 meter thick pegmatite dike cutting Marble Hill hornblende schist. This pegmatite is located 0.2 km south of East Branch, above the New York Quarry. This pegmatite is conformable with the host rock foliation, trends N78°W, and dips 17-18° southwest. It is characterized by a 2-3 cm wide biotite border zone in which the biotite cleavage parallels the contact and an interior zone composed of a fine-grained (0.6-1.2 cm) pegmatite assemblage of quartz, potassium feldspar, sodic plagioclase and muscovite. Minor 1-2 mm disseminated tourmaline is present within the interior zone of this pegmatite, occurring in angular clusters and aggregates up to 1 cm wide.

Denson-Cagle Pegmatite

The Denson and Cagle pegmatites are located in southern Pickens County, approximately 2000 meters

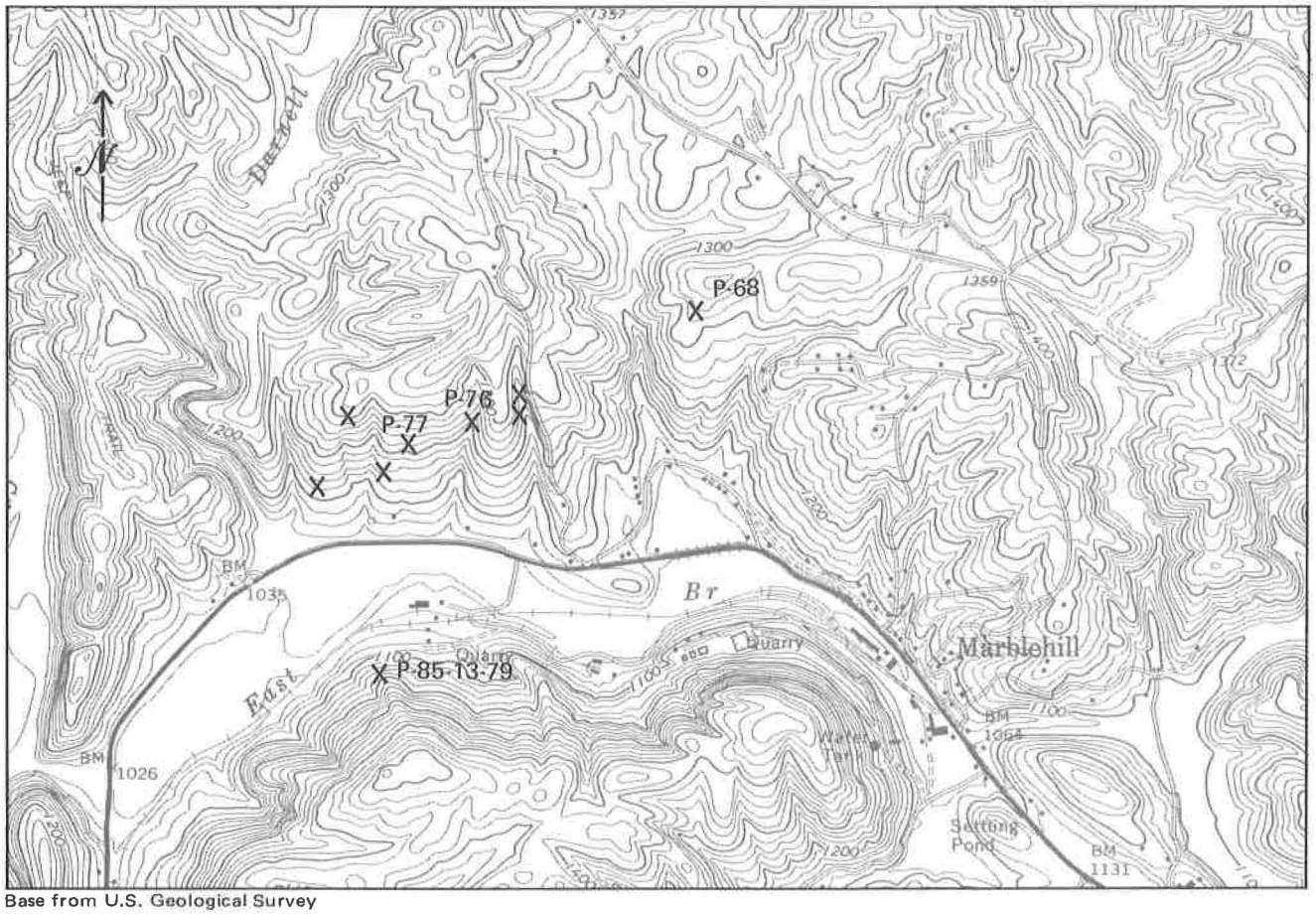

Figure 18. Location of the Marblehill pegmatite in southeastern Pickens County (U.S. Geological Survey, Nelson, Georgia; 1:24,000 topographic quadrangle).

east of Bethany Church (Figure 22). The principal outcrops of the pegmatite sampled in the present study are from the Rock Creek locality. The Rock Creek segment of the Denson pegmatite joins the Denson Mine as reported by Furcron and Teague (1943). Due to their proximity, the Rock Creek and Cagle localities are considered in this report as individual segments of the same pegmatite.

The Denson Pegmatite (Rock Creek Segment)

The Rock Creek segment of the Denson pegmatite occurs as a northeast-trending, 1.5 meter thick, concordant pegmatite hosted by biotite gneiss and mica schist of the Ocoee Supergroup. Several outcrops and prospect pit exposures are present along the steep slopes immediately south of Rock Creek. The pegmatite dips 43-48° to the southeast and is characterized by a massive quartz core up to 0.5 meters wide. This core is persistent throughout the outcrop exposure of the Rock Creek segment.

The core zone is bordered on both sides by a 0.5-1.0 meter wide intermediate zone characterized by relatively fresh medium-grained pegmatite consisting of granular intergrowths of quartz, feldspar, muscovite, garnet, beryl, and tourmaline. Most of the beryl is found between the core and the intermediate zone and varies from honey-yellow to yellow-green and pale green in color.

Muscovite crystals within the intermediate zone occur as individual books up to 10 cm wide. This muscovite is only weakly ruled, and weakly striated, but distinctively zoned (Figure 8). The mineral zoning is char-

Figure 19. Lenses of mica schist containing coarse-grained tourmaline; the schist is an inclusion within a pegmatite at Marblehill. The coarse-grained tourmaline probably developed by recrystallization of fine-grained tourmaline within the schist.

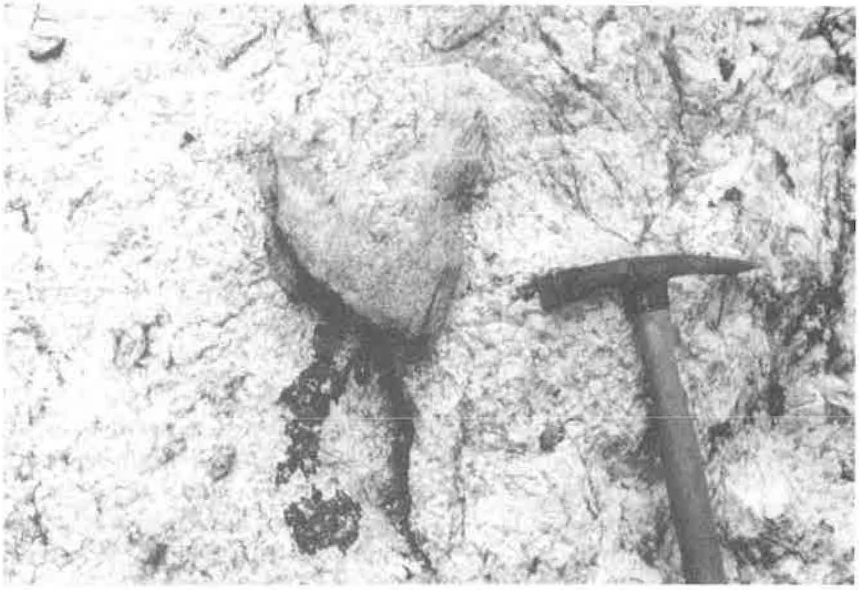

Figure 20. Inclusions of mica schist in the Marblehill pegmatite. Tourmaline forms within the pegmatite in close proximity to the inclusions. The schist may have provided a source for boron by pegmatite-wall rock reactions.

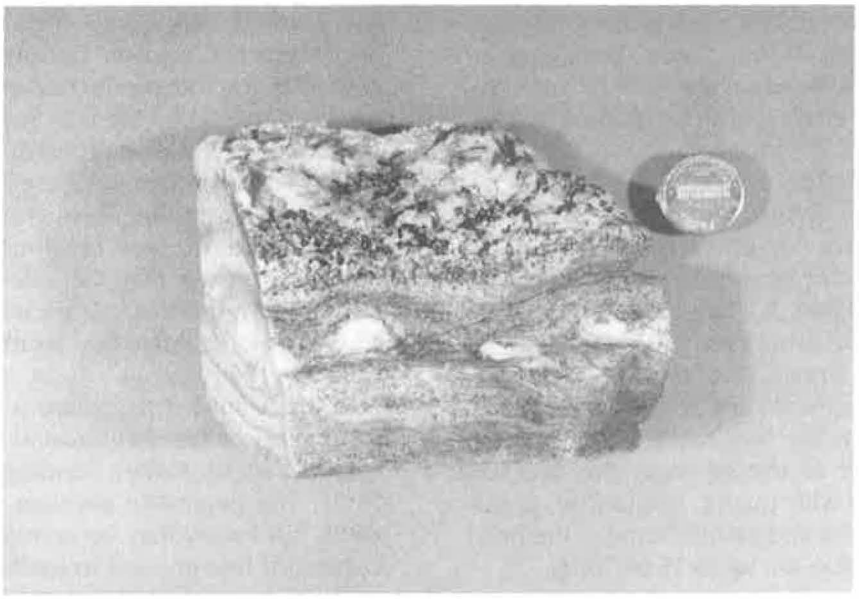

Figure 21. Contact between mica schist and the Marblehill pegmatite illustrating the coarsening of tourmaline from the schist and into the pegmatite. Note the presence of feldspar lenses in the schist adjacent to the pegmatite. The feldspar growth appears to have contorted the foliation, suggesting emplacement of this pegmatite rather than simple in situ anatexis.

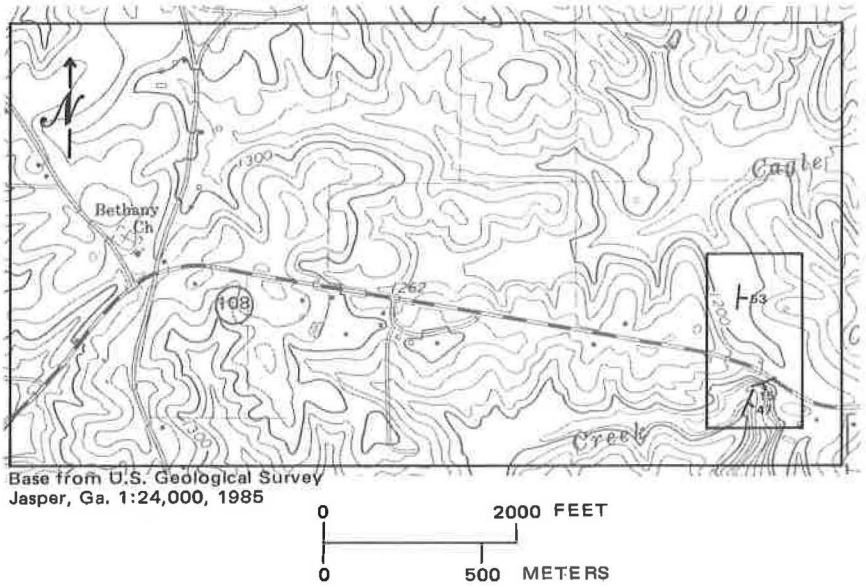

Figure 22. Location of the Denson (Rock Creek segment) and Cagle pegmatites in southern Pickens County (U.S. Geological Survey, Jasper, Georgia; 1:24,000 topographic quadrangle).

acterized by pseudohexagonal sheets of light yellowish-green muscovite bordered by a 5 mm wide light brown to greenish-brown rim of muscovite containing an abundance of opaque inclusions (> 0.7% by volume), including rutile, iron oxides, and manganese oxides. Striations and ruling of the zoned muscovite cut across both the central and border zones.

Toward the north, immediately adjacent to Rock Creek and on the north side of the creek, the schists, gneisses and concordant pegmatite dip at a shallow angle (15°) to the southeast. A 1.5 meter wide pegmatite is exposed at the base of some overhanging ledges near the water level of the stream. Both massive quartz and intermediate zone pegmatite are present. Locally, the massive quartz borders the host rocks. Furcron (1959) describes aquamarine recovered from this location where it is associated with quartz, plagioclase, potassium feldspar, muscovite and garnet. Some of the beryl crystals from this location are up to 15 cm long.

The Cagle Mine

The Cagle Mine segment of the Denson pegmatite crops out approximately 200 meters north of Ga. Highway 108 along a N 20°E strike. A shaft, crosscut, and several prospect pits expose various portions of this pegmatite. The Cagle pegmatite was worked to a depth of 6 to 8 meters. The pegmatite is generally concordant to host rock foliation but some exposures indicate that at least some of the pegmatite transects foliation at a slight angle. The Cagle pegmatite averages approximately 2 meters in width and dips 53° east. Host rocks include biotite gneiss and muscovite schist which are strongly tourmalinized up to one meter away from the pegmatite.

The pegmatite contains clear quartz, milky quartz, smoky quartz, kaolinite, feldspar, tourmaline and garnet. Some of the garnets occur as aggregate crystals up to 10 cm wide and are moderately oxidized to limonite/goethite and hematite. The tourmaline in the Cagle deposit is brownish-green in thin section. Muscovite crystals up to 25 cm across have been reported from this property (Furcron and Teague, 1943). Most of the larger crystals are strongly striated, exhibit herringbone structure and split poorly. Beryl is not reported and was not observed within this segment of the pegmatite.

The Amphlett Mine

The Amphlett pegmatite is one of the larger pegmatites within the district, having an intermittent exposure length of over 600 meters. It is one of the most thoroughly studied pegmatites in the Cherokee-Pickens district. Reports pertaining to it include those of Furcron and Teague (1943), Heinrich and others (1953) and Beck (1948). The Amphlett pegmatite is located within the Blue Ridge Province, 6.9 kilometers S 86°E of Ball Ground and 3.9 kilometers S 42°W of Mica in northeastern Cherokee County. It was worked from 1942-1945 for the production of sheet mica and was explored in 1944 by the U.S. Bureau of Mines during a subsurface exploration program. This program involved drilling and core recovery from five diamond drill holes at various locations throughout the pegmatite to determine subsurface continuity. None of the drill holes was greater than 70 meters long. The pegmatite was mined in three separate areas, respectively referred to as the North, Main and South Workings (Figure 23; Plate 2).

The Amphlett pegmatite is similar to many of the pegmatites of the Ball Ground field. It is concordant with host rock foliation, trending N50°E and dipping 30-55°SE. The pegmatite averages only 1 to 2 meters in width but locally may be as much as 7 meters wide. It consists of fine-grained to medium-grained pegmatite containing interlocking crystals of plagioclase, potassium feldspar, quartz, muscovite and abundant black tourmaline.

At least three distinct varieties of muscovite are present at the Amphlett pegmatite. Most of the muscovite is cinnamon brown and relatively free of inclusions, striations, and ruling. However, a second variety of muscovite is observed at the South Workings, associated with a quartz core zone. Here the muscovite has a distinct greenish tinge, is strongly striated, and exhibits A-structure and herringbone structure. Some of this muscovite is color zoned and appears nearly identical to the zoned muscovite associated with the Rock Creek segment of the Denson pegmatite. A third variety of muscovite is a fine-grained pale green sericite coating on feldspar. This mineral is most noticeable from samples collected from the Main Workings.

Tourmaline occurs as idiomorphic black crystals or crystal splays up to 20 cm in length. The most common accessories include garnet and biotite; rare accessories include apatite, beryl, pyrrhotite, chalcopyrite, columbite, autunite, calcite and malachite. According to Heinrich and others (1953), the rare accessories occur as granular minerals or mineral coatings within a 1 to 2 meter pod of massive quartz at the north workings of the pegmatite.

The Amphlett pegmatite is poorly zoned, consisting of a weakly defined border, an intermediate zone and a locally developed core zone. The border zone is characterized by a 5 cm wide intermittent zone of medium to coarse-grained muscovite or quartz-muscovite ± tourmaline selvages. The intermediate zone is composed of fine- to medium-grained pegmatite consisting of interlocking crystals of quartz, potassium feldspar, muscovite and tourmaline. The core is composed of massive quartz ± perthite and typically contains muscovite garnet and tourmaline crystals, all up to 12

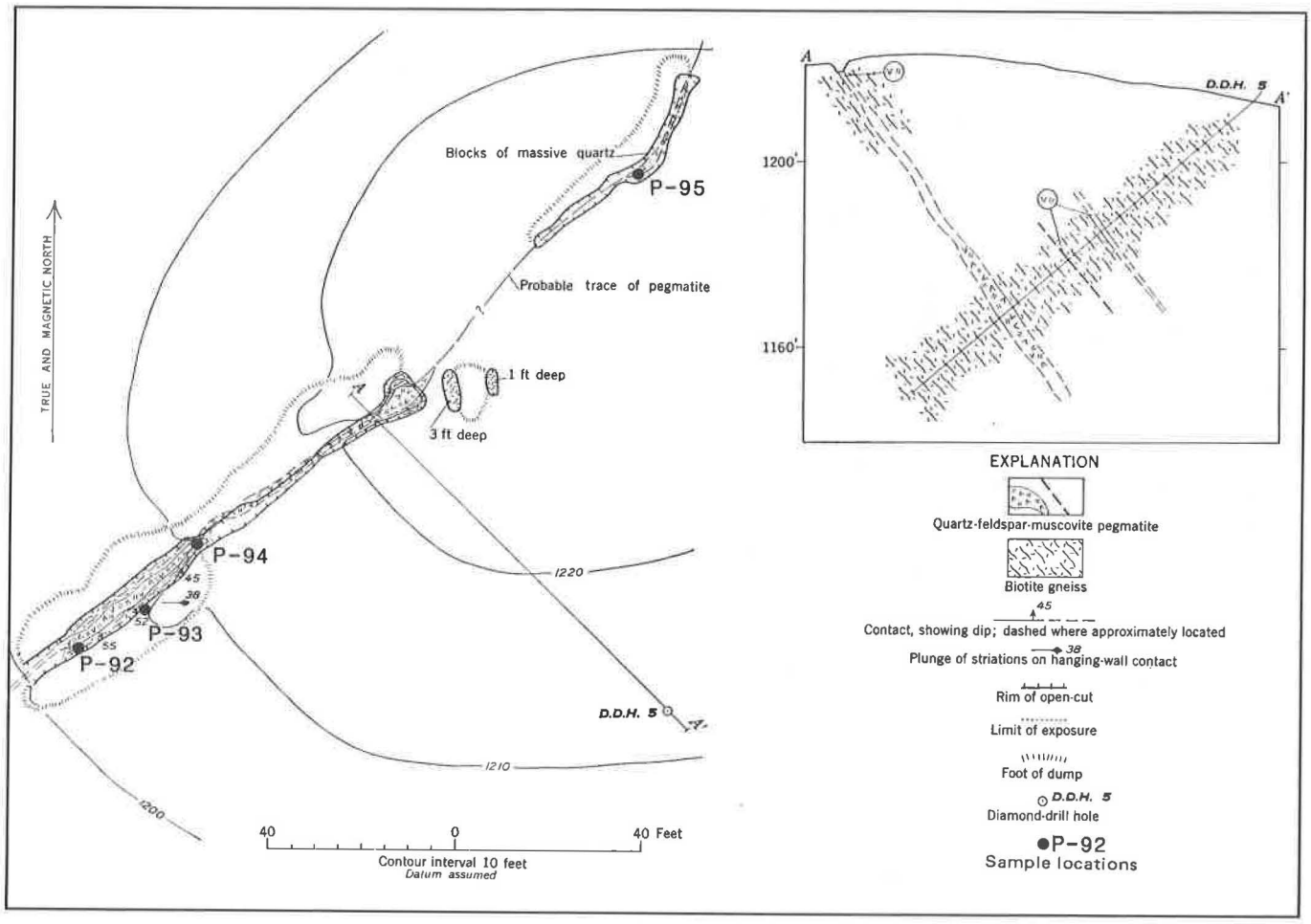

Figure 23. Geologic map and section of the South Amphlett prospect, Cherokee County, (modified from Heinrich and others, 1953).

cm across. Excellent outcrops of core material are observed at the South Workings. All of the above pegmatite zones are discontinuous. The host rocks consist of garnet-bearing biotite gneiss and mica schists of the Etowah Formation of the Ocoee Supergroup. The dominant foliation trends N 50°E and dips 30-55°SE; the steepest dips are found at the South Workings.

The Amphlett pegmatite is one of the least saprolitized pegmatites of the district, and plagioclase shows evidence of strong clay alteration, but the potassium feldspar is generally fresh throughout the pegmatite, and the rock is fairly competent. The pegmatite shows evidence of minor hydrothermal alteration and fracture-filling by the development of sericite on feldspar and local quartz veins up to 1/8" wide cutting feldspar. Alteration within the host rocks is indicated by the development of chlorite veinlets, or chlorite or muscovite as pseudomorphic replacements of biotite within 3 meters of the pegmatite-biotite gneiss contact.

A bifurcating diabase dike up to 2 meters wide cuts the Amphlett pegmatite near the north cut of the Main Workings (Plate 2). Here the dark gray, fine-grained diabase trends N 25°-45°W and dips 70° to the west. Assuming that the diabase dike has a similar age as that of other diabase dikes within the state, (180 m.y.), and assuming a late Precambrian to early Paleozoic age for the Etowah Formation, the age of the Amphlett pegmatite must be between 180 m.y. and 600 m.y. These rough constraints are in agreement with the K-Ar age date obtained from the Cochran Mine (350 m.y.) assuming the two deposits related to the orogenic events.

The Wacaster Mine

In contrast to all of the preceding pegmatites, the Wacaster deposit is associated with the Chattahoochee thrust sheet and belongs to the Holly Springs pegmatitic field. This deposit is located 1.9 kilometers S 40°W of

Holly Springs and 2.4 kilometers N 20°W of Toonigh in southeastern Cherokee County.

Furcron and Teague (1943) report that the mine was opened in 1920 and worked until 1926. The underground workings, which are now completely filled, consisted of a 20 meter vertical shaft and an 8 meter long northeast-trending crosscut. A 20 meter wide pit, up to 7 meters deep, remains as evidence of this past activity.

The exposed pegmatite along the pit walls is strongly saprolitized but relief textures indicate that the pegmatite consists of a fine-grained to medium-grained pegmatite composed of an interlocking aggregate or feldspar, quartz and muscovite. Most of the muscovite occurs as "burr rock" with individual crystals less than 3 cm wide. The muscovite is generally light grayish brown in color and contains numerous opaque oxide and brown pleochoric biotite inclusions (Figure 19).

The pegmatite is poorly zoned and the only evidence for internal structure is the existence of a quartz-rich zone on the southwest side of the pit described by Furcron and Teague (1943) as a "quartz blowout." The Wacaster pegmatite is typical of other pegmatites of the Holly Springs field in that tourmaline and beryl are not present.

APPENDIX B
MUSCOVITE ANALYSES

Holly Springs Field

P-46 WACASTER

ELEMENT	WT PCT	OXIDE	WT PCT	CATION/ANION OCCUPANCY FULL OCTAHEDRAL LAYER	
Si	24.020	SiO_2	51.400	Si	3.441
Al	15.830	Al_2O_3	29.900	Al4	0.559
				Al6	1.800
Ti	0.174	TiO_2	0.290	Ti	0.015
Fe^{+3}	1.259	Fe_2O_3	1.800	Fe^{+3}	0.091
Fe^{+2}	0.389	FeO	0.500	Fe^{+2}	0.028
Mn	0.020	MnO	0.026	Mn	0.001
Mg	0.386	MgO	0.640	Mg	0.064
Li	0.003	Li_2O	0.006	Li	0.002
		SUM OCTAHEDRAL CATIONS		=	2.000
Ca	0.057	CaO	0.080	Ca	0.006
Na	0.586	Na_2O	0.790	Na	0.103
K	7.720	K_2O	9.300	K	0.794
Ba	0.042	BaO	0.047	Ba	0.001
Rb	0.032	Rb_2O	0.035	Rb	0.002
Cs	0.000	Cs_2O	0.000	Cs	0.000
F	0.110	F	0.110	F	0.023
Cl	0.000	Cl	0.000	Cl	0.000
*	0.000	OH	0.000	OH	1.977
		SUM	94.88		
		=			

* H_2O+ Calculated From OH (SUM+ = 22) = 4.49.
Corrected SUM Oxides = 99.36

P-47 WACASTER

ELEMENT	WT PCT	OXIDE	WT PCT	CATION/ANION OCCUPANCY FULL OCTAHEDRAL LAYER	
Si	21.687	SiO_2	46.400	Si	3.119
Al	16.991	Al_2O_3	32.100	Al4	0.881
				Al6	1.662
Ti	0.360	TiO_2	0.600	Ti	0.030
Fe^{+3}	2.238	Fe_2O_3	3.200	Fe^{+3}	0.162
Fe^{+2}	0.668	FeO	0.860	Fe^{+2}	0.048
Mn	0.033	MnO	0.043	Mn	0.002
Mg	0.555	MgO	0.920	Mg	0.092
Li	0.004	Li_2O	0.009	Li	0.002
		SUM OCTAHEDRAL CATIONS		=	2.000
Ca	0.019	CaO	0.026	Ca	0.002
Na	0.475	Na_2O	0.640	Na	0.084
K	8.219	K_2O	9.900	K	0.851
Ba	0.152	BaO	0.170	Ba	0.004
Rb	0.031	Rb_2O	0.034	Rb	0.001
Cs	0.000	Cs_2O	0.000	Cs	0.000
F	0.200	F	0.200	F	0.043
Cl	0.000	Cl	0.000	Cl	0.000
*	0.000	OH	0.000	OH	1.957
		SUM	95.018		
		=			

* H_2O+ Calculated From OH (SUM+ = 22) = 4.36.
Corrected SUM Oxides = 99.37

Holly Springs Field

P-48 WACASTER

ELEMENT	WT PCT	OXIDE	WT PCT	CATION/ANION OCCUPANCY FULL OCTAHEDRAL LAYER	
Si	23.230	SiO_2	49.700	Si	3.342
Al	15.456	Al_2O_3	29.200	Al4	0.658
				Al6	1.657
Ti	0.372	TiO_2	0.620	Ti	0.032
Fe^{+3}	1.714	Fe_2O_3	2.450	Fe^{+3}	0.125
Fe^{+2}	0.583	FeO	0.750	Fe^{+2}	0.043
Mn	0.027	MnO	0.035	Mn	0.002
Mg	0.531	MgO	0.880	Mg	0.089
Li	0.005	Li_2O	0.010	Li	0.003
		SUM OCTAHEDRAL CATIONS		=	2.000
Ca	0.064	CaO	0.090	Ca	0.007
Na	0.527	Na_2O	0.710	Na	0.093
K	7.804	K_2O	9.400	K	0.814
Ba	0.143	BaO	0.160	Ba	0.004
Rb	0.023	Rb_2O	0.025	Rb	0.001
Cs	0.001	Cs_2O	0.001	Cs	0.000
F	0.100	F	0.100	F	0.021
Cl	0.000	Cl	0.000	Cl	0.000
*	0.000	OH	0.000	OH	1.979
		SUM	94.089		
		=			

* H_2O+ Calculated From OH (SUM+ = 22) = 4.41.
Corrected SUM Oxides = 98.50

Holly Springs Field

P-50 COLE

ELEMENT	WT PCT	OXIDE	WT PCT	CATION/ANION OCCUPANCY FULL OCTAHEDRAL LAYER	
Si	21.267	SiO_2	45.500	Si	3.101
Al	16.567	Al_2O_3	31.300	Al4	0.899
				Al6	1.615
Ti	0.192	TiO_2	0.320	Ti	0.016
Fe^{+3}	2.588	Fe_2O_3	3.700	Fe^{+3}	0.190
Fe^{+2}	0.855	FeO	1.100	Fe^{+2}	0.063
Mn	0.035	MnO	0.045	Mn	0.003
Mg	0.663	MgO	1.100	Mg	0.112
Li	0.003	Li_2O	0.007	Li	0.002
		SUM OCTAHEDRAL CATIONS		=	2.000
Ca	0.009	CaO	0.013	Ca	0.001
Na	0.453	Na_2O	0.610	Na	0.081
K	8.800	K_2O	10.600	K	0.922
Ba	0.048	BaO	0.054	Ba	0.001
Rb	0.027	Rb_2O	0.030	Rb	0.001
Cs	0.000	Cs_2O	0.000	Cs	0.000
F	0.077	F	0.077	F	0.017
Cl	0.000	Cl	0.000	Cl	0.000
*	0.000	OH	0.000	OH	1.983
		SUM	94.423		
		=			

* H_2O+ Calculated From OH (SUM+ = 22) = 4.35.
Corrected SUM Oxides = 98.78

P-51 HILLHOUSE

ELEMENT	WT PCT	OXIDE	WT PCT	CATION/ANION OCCUPANCY FULL OCTAHEDRAL LAYER	
Si	21.267	SiO_2	45.500	Si	3.105
Al	16.567	Al_2O_3	31.300	Al4	0.895
				Al6	1.624
Ti	0.240	TiO_2	0.400	Ti	0.021
Fe^{+3}	2.728	Fe_2O_3	3.900	Fe^{+3}	0.200
Fe^{+2}	0.668	FeO	0.860	Fe^{+2}	0.049
Mn	0.035	MnO	0.045	Mn	0.003
Mg	0.603	MgO	1.000	Mg	0.102
Li	0.004	Li_2O	0.008	Li	0.002
		SUM OCTAHEDRAL CATIONS		=	2.000
Ca	0.019	CaO	0.026	Ca	0.002
Na	0.556	Na_2O	0.750	Na	0.099
K	7.804	K_2O	9.400	K	0.819
Ba	0.278	BaO	0.310	Ba	0.008
Rb	0.024	Rb_2O	0.026	Rb	0.001
Cs	0.000	Cs_2O	0.000	Cs	0.000
F	0.088	F	0.088	F	0.019
Cl	0.000	Cl	0.000	Cl	0.000
*	0.000	OH	0.000	OH	1.981
		SUM	93.576		
		=			

* H_2O+ Calculated From OH (SUM+ = 22) = 4.33.
Corrected SUM Oxides = 97.91

P-56 TOONIGH

ELEMENT	WT PCT	OXIDE	WT PCT	CATION/ANION OCCUPANCY FULL OCTAHEDRAL LAYER	
Si	21.220	SiO_2	45.400	Si	3.063
Al	16.726	Al_2O_3	31.600	Al4	0.937
				Al6	1.576
Ti	0.276	TiO_2	0.460	Ti	0.023
Fe^{+3}	3.007	Fe_2O_3	4.300	Fe^{+3}	0.218
Fe^{+2}	0.777	FeO	1.000	Fe^{+2}	0.056
Mn	0.039	MnO	0.050	Mn	0.002
Mg	0.724	MgO	1.200	Mg	0.121
Li	0.005	Li_2O	0.010	Li	0.003
		SUM OCTAHEDRAL CATIONS		=	2.000
Ca	0.013	CaO	0.018	Ca	0.001
Na	0.378	Na_2O	0.510	Na	0.067
K	8.053	K_2O	9.700	K	0.835
Ba	0.065	BaO	0.073	Ba	0.002
Rb	0.034	Rb_2O	0.037	Rb	0.002
Cs	0.000	Cs_2O	0.006	Cs	0.000
F	0.096	F	0.096	F	0.020
Cl	0.000	Cl	0.000	Cl	0.000
*	0.000	OH	0.000	OH	1.980
		SUM	94.413		
		=			

* H_2O+ Calculated From OH (SUM+ = 22) = 4.36.
Corrected SUM Oxides = 98.77

P-108 COOK

ELEMENT	WT PCT	OXIDE	WT PCT	CATION/ANION OCCUPANCY FULL OCTAHEDRAL LAYER	
Si	23.650	SiO_2	50.600	Si	3.391
Al	15.879	Al_2O_3	30.000	Al4	0.609
				Al6	1.760
Ti	0.282	TiO_2	0.470	Ti	0.024
Fe^{+3}	1.539	Fe_2O_3	2.200	Fe^{+3}	0.111
Fe^{+2}	0.529	FeO	0.680	Fe^{+2}	0.038
Mn	0.010	MnO	0.013	Mn	0.001
Mg	0.392	MgO	0.650	Mg	0.065
Li	0.002	Li_2O	0.004	Li	0.001
		SUM OCTAHEDRAL CATIONS		=	2.000
Ca	0.050	CaO	0.070	Ca	0.005
Na	0.608	Na_2O	0.820	Na	0.105
K	7.887	K_2O	9.500	K	0.812
Ba	0.152	BaO	0.170	Ba	0.004
Rb	0.029	Rb_2O	0.032	Rb	0.001
Cs	0.001	Cs_2O	0.001	Cs	0.000
F	0.082	F	0.082	F	0.017
Cl	0.000	Cl	0.000	Cl	0.000
*	0.000	OH	0.000	OH	1.877
		SUM	99.458		
		=			

* H_2O+ Calculated From OH (SUM+ = 22) = 4.36.
Corrected SUM Oxides = 97.39

Ball Ground Field (Beryl-Poor)

P-26 CAGLE

ELEMENT	WT PCT	OXIDE	WT PCT	CATION/ANION OCCUPANCY FULL OCTAHEDRAL LAYER	
Si	22.809	SiO_2	48.800	Si	3.304
Al	15.985	Al_2O_3	30.200	Al4	0.696
				Al6	1.714
Ti	0.096	TiO_2	0.160	Ti	0.008
Fe^{+3}	0.979	Fe_2O_3	1.400	Fe^{+3}	0.071
Fe^{+2}	1.321	FeO	1.700	Fe^{+2}	0.096
Mn	0.033	MnO	0.042	Mn	0.002
Mg	0.603	MgO	1.000	Mg	0.101
Li	0.012	Li_2O	0.026	Li	0.007
		SUM OCTAHEDRAL CATIONS		=	2.000
Ca	0.622	CaO	0.870	Ca	0.063
Na	0.712	Na_2O	0.960	Na	0.126
K	7.223	K_2O	8.700	K	0.751
Ba	0.013	BaO	0.015	Ba	0.000
Rb	0.058	Rb_2O	0.063	Rb	0.003
Cs	0.002	Cs_2O	0.002	Cs	0.000
F	0.190	F	0.190	F	0.013
Cl	0.000	Cl	0.000	Cl	0.000
*	0.000	OH	0.000	OH	1.987
		SUM	94.048		
		=			

* H_2O+ Calculated From OH (SUM+ = 22) = 4.36.
Corrected SUM Oxides = 98.41

Ball Ground Field (Beryl-Poor)

P-26A CAGLE

ELEMENT	WT PCT	OXIDE	WT PCT	CATION/ANION OCCUPANCY FULL OCTAHEDRAL LAYER	
Si	22.155	SiO_2	47.400	Si	3.202
Al	17.732	Al_2O_3	33.500	Al4	0.798
				Al6	1.870
Ti	0.054	TiO_2	0.090	Ti	0.005
Fe^{+3}	0.594	Fe_2O_3	0.850	Fe^{+3}	0.043
Fe^{+2}	0.777	FeO	1.000	Fe^{+2}	0.057
Mn	0.029	MnO	0.037	Mn	0.002
Mg	0.139	MgO	0.230	Mg	0.023
Li	0.001	Li_2O	0.002	Li	0.001
		SUM OCTAHEDRAL CATIONS		=	2.000
Ca	0.031	CaO	0.043	Ca	0.003
Na	0.638	Na_2O	0.860	Na	0.113
K	8.053	K_2O	9.700	K	0.836
Ba	0.016	BaO	0.018	Ba	0.000
Rb	0.076	Rb_2O	0.083	Rb	0.004
Cs	0.002	Cs_2O	0.002	Cs	0.000
F	0.060	F	0.060	F	0.013
Cl	0.000	Cl	0.000	Cl	0.000
*	0.000	OH	0.000	OH	1.987
		SUM	93.850		
		=			

* H_2O+ Calculated From OH (SUM+ = 22) = 4.43.
Corrected SUM Oxides = 98.28

Ball Ground Field (Beryl-Poor)

P-36 HOWELL

ELEMENT	WT PCT	OXIDE	WT PCT	CATION/ANION OCCUPANCY FULL OCTAHEDRAL LAYER	
Si	21.454	SiO_2	45.900	Si	3.051
Al	18.790	Al_2O_3	35.500	Al4	0.949
				Al6	1.832
Ti	0.150	TiO_2	0.250	Ti	0.012
Fe^{+3}	0.650	Fe_2O_3	0.930	Fe^{+3}	0.047
Fe^{+2}	0.466	FeO	0.600	Fe^{+2}	0.033
Mn	0.011	MnO	0.014	Mn	0.001
Mg	0.428	MgO	0.710	Mg	0.070
Li	0.008	Li_2O	0.018	Li	0.005
		SUM OCTAHEDRAL CATIONS		=	2.000
Ca	0.014	CaO	0.019	Ca	0.001
Na	0.734	Na_2O	0.990	Na	0.128
K	8.302	K_2O	10.000	K	0.848
Ba	0.099	BaO	0.110	Ba	0.003
Rb	0.038	Rb_2O	0.042	Rb	0.002
Cs	0.001	Cs_2O	0.001	Cs	0.000
F	0.110	F	0.110	F	0.023
Cl	0.000	Cl	0.000	Cl	0.000
*	0.000	OH	0.000	OH	1.977
		SUM	95.148		
		=			

* H_2O+ Calculated From OH (SUM+ = 22) = 4.45.
Corrected SUM Oxides = 99.59

Ball Ground Field (Beryl-Poor)

P-37 JONES

ELEMENT	WT PCT	OXIDE	WT PCT	CATION/ANION OCCUPANCY FULL OCTAHEDRAL LAYER	
Si	21.173	SiO_2	45.300	Si	3.007
Al	17.573	Al_2O_3	33.200	Al4	0.993
				Al6	1.606
Ti	0.282	TiO_2	0.470	Ti	0.023
Fe^{+3}	2.658	Fe_2O_3	3.800	Fe^{+3}	0.190
Fe^{+2}	0.777	FeO	1.000	Fe^{+2}	0.056
Mn	0.036	MnO	0.046	Mn	0.003
Mg	0.724	MgO	1.200	Mg	0.119
Li	0.007	Li_2O	0.016	Li	0.004
		SUM OCTAHEDRAL CATIONS		=	2.000
Ca	0.015	CaO	0.021	Ca	0.001
Na	0.564	Na_2O	0.760	Na	0.098
K	8.883	K_2O	10.700	K	0.906
Ba	0.143	BaO	0.160	Ba	0.004
Rb	0.048	Rb_2O	0.053	Rb	0.002
Cs	0.004	Cs_2O	0.005	Cs	0.000
F	0.110	F	0.110	F	0.023
Cl	0.000	Cl	0.000	Cl	0.000
*	0.000	OH	0.000	OH	1.977
		SUM	96.794		
		=			

* H_2O+ Calculated From OH (SUM+ = 22) = 4.44.
Corrected SUM Oxides = 101.23

Ball Ground Field (Beryl-Poor)

P-40A JONES

ELEMENT	WT PCT	OXIDE	WT PCT	CATION/ANION OCCUPANCY FULL OCTAHEDRAL LAYER	
Si	22.996	SiO_2	49.200	Si	3.328
Al	15.350	Al_2O_3	29.000	Al4	0.672
				Al6	1.640
Ti	0.414	TiO_2	0.690	Ti	0.035
Fe^{+3}	2.308	Fe_2O_3	3.300	Fe^{+3}	0.168
Fe^{+2}	0.692	FeO	0.890	Fe^{+2}	0.050
Mn	0.033	MnO	0.043	Mn	0.003
Mg	0.597	MgO	0.990	Mg	0.100
Li	0.008	Li_2O	0.017	Li	0.005
		SUM OCTAHEDRAL CATIONS		=	2.000
Ca	0.050	CaO	0.070	Ca	0.005
Na	0.645	Na_2O	0.870	Na	0.114
K	7.638	K_2O	9.200	K	0.794
Ba	0.170	BaO	0.190	Ba	0.005
Rb	0.031	Rb_2O	0.034	Rb	0.001
Cs	0.001	Cs_2O	0.001	Cs	0.000
F	0.150	F	0.150	F	0.032
Cl	0.000	Cl	0.000	Cl	0.000
*	0.000	OH	0.000	OH	1.968
		SUM	94.582		
		=			

* H_2O+ Calculated From OH (SUM+ = 22) = 4.39.
Corrected SUM Oxides = 98.97

Ball Ground Field (Beryl-Poor)

P-54 AMPHLETT

ELEMENT	WT PCT	OXIDE	WT PCT	CATION/ANION OCCUPANCY FULL OCTAHEDRAL LAYER	
Si	22.435	SiO_2	48.000	Si	3.215
Al	17.626	Al_2O_3	33.300	Al4	0.785
				Al6	1.844
Ti	0.162	TiO_2	0.270	Ti	0.014
Fe^{+3}	0.608	Fe_2O_3	0.870	Fe^{+3}	0.044
Fe^{+2}	0.396	FeO	0.510	Fe^{+2}	0.029
Mn	0.012	MnO	0.015	Mn	0.001
Mg	0.404	MgO	0.670	Mg	0.067
Li	0.003	Li_2O	0.007	Li	0.002
		SUM OCTAHEDRAL CATIONS		=	2.000
Ca	0.034	CaO	0.048	Ca	0.003
Na	0.675	Na_2O	0.910	Na	0.118
K	7.887	K_2O	9.500	K	0.812
Ba	0.059	BaO	0.066	Ba	0.002
Rb	0.026	Rb_2O	0.028	Rb	0.001
Cs	0.000	Cs_2O	0.000	Cs	0.000
F	0.095	F	0.095	F	0.020
Cl	0.000	Cl	0.000	Cl	0.000
*	0.000	OH	0.000	OH	1.980
		SUM	94.249		
		=			

* H_2O+ Calculated From OH (SUM+ = 22) = 4.45.
Corrected SUM Oxides = 98.70

Ball Ground Field (Beryl-Poor)

P-55 AMPHLETT

ELEMENT	WT PCT	OXIDE	WT PCT	CATION/ANION OCCUPANCY FULL OCTAHEDRAL LAYER	
Si	22.996	SiO_2	49.200	Si	3.305
Al	17.255	Al_2O_3	32.600	Al4	0.695
				Al6	1.887
Ti	0.126	TiO_2	0.210	Ti	0.011
Fe^{+3}	0.518	Fe_2O_3	0.740	Fe^{+3}	0.037
Fe^{+2}	0.334	FeO	0.430	Fe^{+2}	0.024
Mn	0.011	MnO	0.014	Mn	0.001
Mg	0.229	MgO	0.380	Mg	0.038
Li	0.004	Li_2O	0.008	Li	0.002
		SUM OCTAHEDRAL CATIONS		=	2.000
Ca	0.046	CaO	0.065	Ca	0.005
Na	0.742	Na_2O	1.000	Na	0.129
K	7.721	K_2O	9.300	K	0.797
Ba	0.019	BaO	0.021	Ba	0.001
Rb	0.045	Rb_2O	0.049	Rb	0.002
Cs	0.001	Cs_2O	0.001	Cs	0.000
F	0.096	F	0.096	F	0.020
Cl	0.000	Cl	0.000	Cl	0.000
*	0.000	OH	0.000	OH	1.980
		SUM	94.074		
		=			

* H_2O+ Calculated From OH (SUM+ = 22) = 4.46.
Corrected SUM Oxides = 98.53

Ball Ground Field (Beryl-Poor)

P-76 MARBLEHILL (Border Zone)

ELEMENT	WT PCT	OXIDE	WT PCT	CATION/ANION OCCUPANCY FULL OCTAHEDRAL LAYER	
Si	21.220	SiO_2	45.400	Si	3.072
Al	18.261	Al_2O_3	34.500	Al4	0.933
				Al6	1.815
Ti	0.240	TiO_2	0.400	Ti	0.020
Fe^{+3}	0.846	Fe_2O_3	1.210	Fe^{+3}	0.062
Fe^{+2}	0.259	FeO	0.333	Fe^{+2}	0.019
Mn	0.022	MnO	0.028	Mn	0.002
Mg	0.452	MgO	0.750	Mg	0.076
Li	0.013	Li_2O	0.028	Li	0.008
		SUM OCTAHEDRAL CATIONS		=	2.000
Ca	0.005	CaO	0.007	Ca	0.001
Na	0.571	Na_2O	0.770	Na	0.101
K	8.551	K_2O	10.300	K	0.888
Ba	0.010	BaO	0.011	Ba	0.000
Rb	0.053	Rb_2O	0.058	Rb	0.003
Cs	0.005	Cs_2O	0.006	Cs	0.000
F	0.092	F	0.092	F	0.020
Cl	0.000	Cl	0.000	Cl	0.000
*	0.000	OH	0.000	OH	1.980
		SUM	93.848		
		=			

* H_2O+ Calculated From OH (SUM+ = 22) = 4.39.
Corrected SUM Oxides = 98.24

Ball Ground Field (Beryl-Poor)

P-77 MARBLEHILL (Core Zone)

ELEMENT	WT PCT	OXIDE	WT PCT	CATION/ANION OCCUPANCY FULL OCTAHEDRAL LAYER	
Si	21.080	SiO_2	45.100	Si	3.062
Al	18.155	Al_2O_3	34.300	Al4	0.938
				Al6	1.806
Ti	0.258	TiO_2	0.430	Ti	0.022
Fe^{+3}	0.853	Fe_2O_3	1.220	Fe^{+3}	0.062
Fe^{+2}	0.350	FeO	0.450	Fe^{+2}	0.026
Mn	0.021	MnO	0.027	Mn	0.002
Mg	0.446	MgC	0.740	Mg	0.075
Li	0.013	Li_2O	0.028	Li	0.008
		SUM OCTAHEDRAL CATIONS		=	2.000
Ca	0.006	CaO	0.008	Ca	0.001
Na	0.542	Na_2O	0.730	Na	0.096
K	8.468	K_2O	10.200	K	0.883
Ba	0.012	BaO	0.013	Ba	0.000
Rb	0.052	Rb_2O	0.057	Rb	0.002
Cs	0.000	Cs_2O	0.000	Cs	0.000
F	0.087	F	0.087	F	0.019
Cl	0.000	Cl	0.000	Cl	0.000
*	0.000	OH	0.000	OH	1.981
		SUM	93.353		
		=			

* H_2O+ Calculated From OH (SUM+ = 22) = 4.37.
Corrected SUM Oxides = 97.72

Ball Ground Field (Beryl-Poor)

P-81 JONES - Howell

ELEMENT	WT PCT	OXIDE	WT PCT	CATION/ANION OCCUPANCY FULL OCTAHEDRAL LAYER	
Si	22.061	SiO_2	47.200	Si	3.149
Al	18.155	Al_2O_3	34.300	Al4	0.851
				Al6	1.847
Ti	0.228	TiO_2	0.380	Ti	0.019
Fe^{+3}	0.685	Fe_2O_3	0.980	Fe^{+3}	0.049
Fe^{+2}	0.311	FeO	0.400	Fe^{+2}	0.022
Mn	0.005	MnO	0.007	Mn	0.000
Mg	0.356	MgO	0.590	Mg	0.059
Li	0.007	Li_2O	0.014	Li	0.004
		SUM OCTAHEDRAL CATIONS		=	2.000
Ca	0.024	CaO	0.034	Ca	0.002
Na	0.742	Na_2O	1.000	Na	0.129
K	8.136	K_2O	9.800	K	0.834
Ba	0.143	BaO	0.160	Ba	0.004
Rb	0.031	Rb_2O	0.034	Rb	0.001
Cs	0.000	Cs_2O	0.000	Cs	0.000
F	0.031	F	0.031	F	0.007
Cl	0.000	Cl	0.000	Cl	0.000
*	0.000	OH	0.000	OH	1.993
		SUM	94.074		
		=			

* H_2O+ Calculated From OH (SUM+ = 22) = 4.49.
Corrected SUM Oxides = 99.41

Ball Ground Field (Beryl-Poor)

P-82A JONES - Howell

ELEMENT	WT PCT	OXIDE	WT PCT	CATION/ANION OCCUPANCY FULL OCTAHEDRAL LAYER	
Si	21.313	SiO_2	45.600	Si	3.082
Al	18.261	Al_2O_3	34.500	Al4	0.918
				Al6	1.831
Ti	0.252	TiO_2	0.420	Ti	0.021
Fe^{+3}	0.553	Fe_2O_3	0.790	Fe^{+3}	0.040
Fe^{+2}	0.552	FeO	0.710	Fe^{+2}	0.040
Mn	0.010	MnO	0.013	Mn	0.001
Mg	0.386	MgO	0.640	Mg	0.064
Li	0.004	Li_2O	0.008	Li	0.002
		SUM OCTAHEDRAL CATIONS		=	2.000
Ca	0.011	CaO	0.015	Ca	0.001
Na	0.549	Na_2O	0.740	Na	0.097
K	8.468	K_2O	10.200	K	0.880
Ba	0.161	BaO	0.180	Ba	0.005
Rb	0.033	Rb_2O	0.036	Rb	0.002
Cs	0.000	Cs_2O	0.000	Cs	0.000
F	0.046	F	0.046	F	0.010
Cl	0.000	Cl	0.000	Cl	0.000
*	0.000	OH	0.000	OH	1.990
		SUM	93.879		
		=			

* H_2O+ Calculated From OH (SUM+ = 22) = 4.41.
Corrected SUM Oxides = 98.29

Ball Ground Field (Beryl-Poor)

P-82B JONES (Biotite)

ELEMENT	WT PCT	OXIDE	WT PCT	CATION/ANION OCCUPANCY FULL OCTAHEDRAL LAYER	
Si	17.481	SiO_2	37.400	Si	2.947
Al	10.957	Al_2O_3	20.700	Al4	1.053
				Al6	0.869
Ti	1.559	TiO_2	2.600	Ti	0.154
Fe^{+3}	1.105	Fe_2O_3	1.580	Fe^{+3}	0.094
Fe^{+2}	12.903	FeO	16.600	Fe^{+2}	1.094
Mn	0.026	MnO	0.033	Mn	0.002
Mg	3.800	MgO	6.300	Mg	0.740
Li	0.070	Li_2O	0.150	Li	0.048
		SUM OCTAHEDRAL CATIONS		=	2.000
Ca	0.019	CaO	0.026	Ca	0.002
Na	0.163	Na_2O	0.220	Na	0.034
K	7.057	K_2O	8.500	K	0.854
Ba	0.085	BaO	0.095	Ba	0.003
Rb	0.075	Rb_2O	0.082	Rb	0.004
Cs	0.005	Cs_2O	0.006	Cs	0.000
F	0.140	F	0.140	F	0.035
Cl	0.000	Cl	0.000	Cl	0.000
*	0.000	OH	0.000	OH	1.965
		SUM	94.373		
		=			

* H_2O+ Calculated From OH (SUM+ = 22) = 3.93.
Corrected SUM Oxides = 98.30

Ball Ground Field (Beryl-Poor)

P-90 CARNEY

ELEMENT	WT PCT	OXIDE	WT PCT	CATION/ANION OCCUPANCY FULL OCTAHEDRAL LAYER	
Si	21.313	SiO_2	45.600	Si	3.111
Al	17.679	Al_2O_3	33.400	Al4	0.889
				Al6	1.796
Ti	0.156	TiO_2	0.260	Ti	0.013
Fe^{+3}	0.748	Fe_2O_3	1.070	Fe^{+3}	0.055
Fe^{+2}	0.552	FeO	0.710	Fe^{+2}	0.041
Mn	0.028	MnO	0.036	Mn	0.002
Mg	0.543	MgO	0.900	Mg	0.092
Li	0.002	Li_2O	0.005	Li	0.001
		SUM OCTAHEDRAL CATIONS		=	2.000
Ca	0.006	CaO	0.008	Ca	0.001
Na	0.445	Na_2O	0.600	Na	0.079
K	8.883	K_2O	10.700	K	0.931
Ba	0.005	BaO	0.006	Ba	0.000
Rb	0.047	Rb_2O	0.051	Rb	0.002
Cs	0.000	Cs_2O	0.000	Cs	0.000
F	0.086	F	0.086	F	0.019
Cl	0.000	Cl	0.000	Cl	0.000
*	0.000	OH	0.000	OH	1.981
		SUM	93.396		
		=			

* H_2O+ Calculated From OH (SUM+ = 22) = 4.36.
Corrected SUM Oxides = 97.75

Ball Ground Field (Beryl-Poor)

P-95B AMPHLETT

ELEMENT	WT PCT	OXIDE	WT PCT	CATION/ANION OCCUPANCY FULL OCTAHEDRAL LAYER	
Si	21.407	SiO_2	45.800	Si	3.097
Al	18.208	Al_2O_3	34.400	Al4	0.903
				Al6	1.839
Ti	0.258	TiO_2	0.430	Ti	0.022
Fe^{+3}	0.671	Fe_2O_3	0.960	Fe^{+3}	0.049
Fe^{+2}	0.326	FeO	0.420	Fe^{+2}	0.024
Mn	0.014	MnO	0.018	Mn	0.001
Mg	0.380	MgO	0.630	Mg	0.064
Li	0.004	Li_2O	0.008	Li	0.002
		SUM OCTAHEDRAL CATIONS		=	2.000
Ca	0.008	CaO	0.011	Ca	0.001
Na	0.623	Na_2O	0.840	Na	0.110
K	8.634	K_2O	10.400	K	0.897
Ba	0.029	BaO	0.032	Ba	0.001
Rb	0.032	Rb_2O	0.035	Rb	0.002
Cs	0.000	Cs_2O	0.000	Cs	0.000
F	0.086	F	0.086	F	0.018
Cl	0.000	Cl	0.000	Cl	0.000
*	0.000	OH	0.000	OH	1.982
		SUM	94.034		
		=			

* H_2O+ Calculated From OH (SUM+ = 22) = 4.40.
Corrected SUM Oxides = 98.44

Ball Ground Field (Beryl-Poor)

P-98A AMPHLETT

ELEMENT	WT PCT	OXIDE	WT PCT	CATION/ANION OCCUPANCY FULL OCTAHEDRAL LAYER	
Si	22.155	SiO_2	47.400	Si	3.201
Al	17.573	Al_2O_3	33.200	Al4	0.799
				Al6	1.844
Ti	0.228	TiO_2	0.380	Ti	0.019
Fe^{+3}	0.530	Fe_2O_3	0.758	Fe^{+3}	0.039
Fe^{+2}	0.466	FeO	0.600	Fe^{+2}	0.034
Mn	0.009	MnO	0.011	Mn	0.001
Mg	0.374	MgO	0.620	Mg	0.062
Li	0.003	Li_2O	0.006	Li	0.002
		SUM OCTAHEDRAL CATIONS		=	2.000
Ca	0.022	CaO	0.031	Ca	0.002
Na	0.645	Na_2O	0.870	Na	0.114
K	8.219	K_2O	9.900	K	0.853
Ba	0.068	BaO	0.076	Ba	0.002
Rb	0.030	Rb_2O	0.033	Rb	0.001
Cs	0.000	Cs_2O	0.000	Cs	0.000
F	0.056	F	0.056	F	0.012
Cl	0.000	Cl	0.000	Cl	0.000
*	0.000	OH	0.000	OH	1.988
		SUM	93.917		
		=			

* H_2O+ Calculated From OH (SUM+ = 22) = 4.43.
Corrected SUM Oxides = 98.35

Ball Ground Field (Beryl-Poor)

P-98B AMPHLETT (Biotite)

ELEMENT	WT PCT	OXIDE	WT PCT	CATION/ANION OCCUPANCY FULL OCTAHEDRAL LAYER	
Si	18.462	SiO_2	39.500	Si	3.104
Al	10.057	Al_2O_3	19.000	Al4	0.896
				Al6	0.864
Ti	1.259	TiO_2	2.100	Ti	0.124
Fe^{+3}	1.434	Fe_2O_3	2.100	Fe^{+3}	0.121
Fe^{+2}	12.748	FeO	16.400	Fe^{+2}	1.078
Mn	0.077	MnO	0.100	Mn	0.007
Mg	4.041	MgO	6.700	Mg	0.785
Li	0.032	Li_2O	0.069	Li	0.022
		SUM OCTAHEDRAL CATIONS		=	2.000
Ca	0.034	CaO	0.048	Ca	0.004
Na	0.208	Na_2O	0.280	Na	0.043
K	7.389	K_2O	8.900	K	0.892
Ba	0.051	BaO	0.057	Ba	0.002
Rb	0.073	Rb_2O	0.080	Rb	0.004
Cs	0.003	Cs_2O	0.003	Cs	0.000
F	0.170	F	0.170	F	0.042
Cl	0.000	Cl	0.000	Cl	0.000
*	0.000	OH	0.000	OH	1.958
		SUM	95.385		
		=			

* H_2O+ Calculated From OH (SUM+ = 22) = 3.96.
Corrected SUM Oxides = 99.34

Ball Ground Field (Beryl-bearing)

P-1 COCHRAN

ELEMENT	WT PCT	OXIDE	WT PCT	CATION/ANION OCCUPANCY FULL OCTAHEDRAL LAYER	
Si	21.033	SiO_2	45.000	Si	3.250
Al	15.403	Al_2O_3	29.100	Al4	0.750
				Al6	1.728
Ti	0.132	TiO_2	0.220	Ti	0.012
Fe^{+3}	1.679	Fe_2O_3	2.400	Fe^{+3}	0.130
Fe^{+2}	0.700	FeO	0.900	Fe^{+2}	0.054
Mn	0.056	MnO	0.072	Mn	0.004
Mg	0.187	MgO	0.310	Mg	0.033
Li	0.060	Li_2O	0.130	Li	0.038
		SUM OCTAHEDRAL CATIONS		=	2.000
Ca	1.215	CaO	1.700	Ca	0.132
Na	0.697	Na_2O	0.940	Na	0.132
K	7.472	K_2O	9.000	K	0.829
Ba	0.014	BaO	0.016	Ba	0.000
Rb	0.137	Rb_2O	0.150	Rb	0.007
Cs	0.005	Cs_2O	0.005	Cs	0.000
F	0.570	F	0.570	F	0.130
Cl	0.000	Cl	0.000	Cl	0.000
*	0.000	OH	0.000	OH	1.870
		SUM	90.273		
		=			

* H_2O+ Calculated From OH (SUM+ = 22) = 3.94.
Corrected SUM Oxides = 94.22

Ball Ground Field (Beryl-bearing)

P-5 COCHRAN

ELEMENT	WT PCT	OXIDE	WT PCT	CATION/ANION OCCUPANCY FULL OCTAHEDRAL LAYER	
Si	22.155	SiO_2	47.400	Si	3.271
Al	15.985	Al_2O_3	30.200	Al4	0.729
				Al6	1.727
Ti	0.126	TiO_2	0.210	Ti	0.011
Fe^{+3}	1.539	Fe_2O_3	2.200	Fe^{+3}	0.114
Fe^{+2}	1.010	FeO	1.300	Fe^{+2}	0.075
Mn	0.061	MnO	0.079	Mn	0.005
Mg	0.187	MgO	0.310	Mg	0.032
Li	0.060	Li_2O	0.130	Li	0.036
		SUM OCTAHEDRAL CATIONS		=	2.000
Ca	0.300	CaO	0.420	Ca	0.031
Na	0.697	Na_2O	0.940	Na	0.126
K	7.804	K_2O	9.400	K	0.828
Ba	0.013	BaO	0.014	Ba	0.000
Rb	0.146	Rb_2O	0.160	Rb	0.007
Cs	0.005	Cs_2O	0.005	Cs	0.000
F	0.520	F	0.520	F	0.113
Cl	0.000	Cl	0.000	Cl	0.000
*	0.000	OH	0.000	OH	1.887
		SUM	93.069		
		=			

* H_2O+ Calculated From OH (SUM+ = 22) = 4.12.
Corrected SUM Oxides = 97.19

Ball Ground Field (Beryl-bearing)

P-10 COCHRAN (Border Zone)

ELEMENT	WT PCT	OXIDE	WT PCT	CATION/ANION OCCUPANCY FULL OCTAHEDRAL LAYER	
Si	21.641	SiO_2	46.300	Si	3.154
Al	16.514	Al_2O_3	31.200	Al4	0.846
				Al6	1.660
Ti	0.108	TiO_2	0.180	Ti	0.009
Fe^{+3}	2.378	Fe_2O_3	3.400	Fe^{+3}	0.174
Fe^{+2}	0.715	FeO	0.920	Fe^{+2}	0.052
Mn	0.035	MnO	0.045	Mn	0.003
Mg	0.410	MgO	0.680	Mg	0.069
Li	0.056	Li_2O	0.120	Li	0.033
		SUM OCTAHEDRAL CATIONS		=	2.000
Ca	0.017	CaO	0.024	Ca	0.002
Na	0.453	Na_2O	0.610	Na	0.081
K	8.219	K_2O	9.900	K	0.860
Ba	0.025	BaO	0.028	Ba	0.001
Rb	0.042	Rb_2O	0.046	Rb	0.002
Cs	0.000	Cs_2O	0.000	Cs	0.000
F	0.470	F	0.470	F	0.101
Cl	0.000	Cl	0.000	Cl	0.000
*	0.000	OH	0.000	OH	1.899
		SUM	93.725		
		=			

* H_2O+ Calculated From OH (SUM+ = 22) = 4.16.
Corrected SUM Oxides = 97.89

Ball Ground Field (Beryl-bearing)

P-12 COCHRAN

ELEMENT	WT PCT	OXIDE	WT PCT	CATION/ANION OCCUPANCY FULL OCTAHEDRAL LAYER	
Si	25.3331	SiO_2	54.200	Si	3.658
Al	14.344	Al_2O_3	27.100	Al4	0.342
				Al6	1.818
Ti	0.168	TiO_2	0.280	Ti	0.014
Fe^{+3}	1.469	Fe_2O_3	2.100	Fe^{+3}	0.107
Fe^{+2}	0.575	FeO	0.740	Fe^{+2}	0.042
Mn	0.042	MnO	0.054	Mn	0.003
Mg	0.000	MgO	0.000	Mg	0.000
Li	0.034	Li_2O	0.074	Li	0.020
		SUM OCTAHEDRAL CATIONS		=	2.000
Ca	0.107	CaO	0.140	Ca	0.010
Na	0.683	Na_2O	0.920	Na	0.120
K	6.974	K_2O	8.400	K	0.723
Ba	0.039	BaO	0.043	Ba	0.001
Rb	0.110	Rb_2O	0.120	Rb	0.005
Cs	0.004	Cs_2O	0.004	Cs	0.000
F	0.380	F	0.380	F	0.081
Cl	0.000	Cl	0.000	Cl	0.000
*	0.000	OH	0.000	OH	1.919
		SUM	94.395		
		=			

* H_2O+ Calculated From OH (SUM+ = 22) = 4.36.
Corrected SUM Oxides = 98.75

Ball Ground Field (Beryl-bearing)

P-14 COCHRAN

ELEMENT	WT PCT	OXIDE	WT PCT	CATION/ANION OCCUPANCY FULL OCTAHEDRAL LAYER	
Si	22.388	SiO_2	47.900	Si	3.268
Al	16.673	Al_2O_3	31.500	Al4	0.732
				Al6	1.802
Ti	0.168	TiO_2	0.280	Ti	0.014
Fe^{+3}	1.399	Fe_2O_3	2.000	Fe^{+3}	0.103
Fe^{+2}	0.451	FeO	0.580	Fe^{+2}	0.033
Mn	0.029	MnO	0.038	Mn	0.002
Mg	0.163	MgO	0.270	Mg	0.027
Li	0.032	Li_2O	0.068	Li	0.019
		SUM OCTAHEDRAL CATIONS		=	2.000
Ca	0.041	CaO	0.057	Ca	0.004
Na	0.660	Na_2O	0.890	Na	0.118
K	7.804	K_2O	9.400	K	0.818
Ba	0.013	BaO	0.015	Ba	0.000
Rb	0.283	Rb_2O	0.310	Rb	0.014
Cs	0.026	Cs_2O	0.028	Cs	0.001
F	0.350	F	0.350	F	0.076
Cl	0.000	Cl	0.000	Cl	0.000
*	0.000	OH	0.000	OH	1.924
		SUM	93.539		
		=			

* H_2O+ Calculated From OH (SUM+ = 22) = 4.26.
Corrected SUM Oxides = 97.80

Ball Ground Field (Beryl-bearing)

P-16 COCHRAN

ELEMENT	WT PCT	OXIDE	WT PCT	CATION/ANION OCCUPANCY FULL OCTAHEDRAL LAYER	
Si	21.687	SiO_2	46.400	Si	3.160
Al	17.202	Al_2O_3	32.500	Al4	0.840
				Al6	1.769
Ti	0.240	TiO_2	0.400	Ti	0.020
Fe^{+3}	1.329	Fe_2O_3	1.900	Fe^{+3}	0.097
Fe^{+2}	0.637	FeO	0.820	Fe^{+2}	0.047
Mn	0.027	MnO	0.035	Mn	0.002
Mg	0.326	MgO	0.540	Mg	0.055
Li	0.016	Li_2O	0.035	Li	0.010
		SUM OCTAHEDRAL CATIONS		=	2.000
Ca	0.026	CaO	0.036	Ca	0.003
Na	0.527	Na_2O	0.710	Na	0.094
K	8.302	K_2O	10.000	K	0.869
Ba	0.006	BaO	0.007	Ba	0.000
Rb	0.128	Rb_2O	0.140	Rb	0.006
Cs	0.004	Cs_2O	0.004	Cs	0.000
F	0.000	F	0.290	F	0.062
Cl	0.000	Cl	0.000	Cl	0.000
*	0.000	OH	0.000	OH	1.938
		SUM	93.695		
		=			

* H_2O+ Calculated From OH (SUM+ = 22) = 4.27.
Corrected SUM Oxides = 97.97

Ball Ground Field (Beryl-bearing)

P-49B COCHRAN

ELEMENT	WT PCT	OXIDE	WT PCT	CATION/ANION OCCUPANCY FULL OCTAHEDRAL LAYER	
Si	21.080	SiO_2	45.100	Si	3.068
Al	17.467	Al_2O_3	33.000	Al4	0.932
				Al6	1.713
Ti	0.210	TiO_2	0.350	Ti	0.018
Fe^{+3}	1.748	Fe_2O_3	2.500	Fe^{+3}	0.128
Fe^{+2}	0.855	FeO	1.100	Fe^{+2}	0.063
Mn	0.046	MnO	0.059	Mn	0.003
Mg	0.265	MgO	0.440	Mg	0.045
Li	0.051	Li_2O	0.110	Li	0.030
		SUM OCTAHEDRAL CATIONS		=	2.000
Ca	0.017	CaO	0.024	Ca	0.002
Na	0.564	Na_2O	0.760	Na	0.100
K	8.468	K_2O	10.200	K	0.885
Ba	0.004	BaO	0.004	Ba	0.000
Rb	0.183	Rb_2O	0.200	Rb	0.009
Cs	0.004	Cs_2O	0.005	Cs	0.000
F	0.550	F	0.550	F	0.118
Cl	0.000	Cl	0.000	Cl	0.000
*	0.000	OH	0.000	OH	1.882
		SUM	94.170		
		=			

* H_2O+ Calculated From OH (SUM+ = 22) = 4.13.
Corrected SUM Oxides = 98.30

Ball Ground Field (Beryl-bearing)

P-49 COCHRAN

ELEMENT	WT PCT	OXIDE	WT PCT	CATION/ANION OCCUPANCY FULL OCTAHEDRAL LAYER	
Si	20.940	SiO_2	44.800	Si	3.039
Al	17.679	Al_2O_3	33.400	Al4	0.961
				Al6	1.710
Ti	0.174	TiO_2	0.290	Ti	0.015
Fe^{+3}	1.748	Fe_2O_3	2.500	Fe^{+3}	0.128
Fe^{+2}	0.933	FeO	1.200	Fe^{+2}	0.068
Mn	0.053	MnO	0.068	Mn	0.004
Mg	0.271	MgO	0.450	Mg	0.046
Li	0.051	Li_2O	0.110	Li	0.030
		SUM OCTAHEDRAL CATIONS		=	2.000
Ca	0.012	CaO	0.017	Ca	0.001
Na	0.653	Na_2O	0.880	Na	0.116
K	7.887	K_2O	9.500	K	0.822
Ba	0.005	BaO	0.006	Ba	0.000
Rb	0.146	Rb_2O	0.160	Rb	0.007
Cs	0.005	Cs_2O	0.005	Cs	0.000
F	0.730	F	0.730	F	0.157
Cl	0.000	Cl	0.000	Cl	0.002
*	0.000	OH	0.000	OH	1.841
		SUM	93.824		
		=			

* H_2O+ Calculated From OH (SUM+ = 22) = 4.03.
Corrected SUM Oxides = 97.86

Ball Ground Field (Beryl-bearing)

P-44A JONES (South)

ELEMENT	WT PCT	OXIDE	WT PCT	CATION/ANION OCCUPANCY FULL OCTAHEDRAL LAYER	
Si	22.342	SiO_2	47.800	Si	3.234
Al	16.726	Al_2O_3	31.600	Al4	0.766
				Al6	1.753
Ti	0.156	TiO_2	0.260	Ti	0.013
Fe^{+3}	1.539	Fe_2O_3	2.200	Fe^{+3}	0.112
Fe^{+2}	0.700	FeO	0.900	Fe^{+2}	0.051
Mn	0.018	MnO	0.023	Mn	0.001
Mg	0.392	MgO	0.650	Mg	0.066
Li	0.007	Li_2O	0.014	Li	0.004
		SUM OCTAHEDRAL CATIONS		=	2.000
Ca	0.033	CaO	0.046	Ca	0.003
Na	0.638	Na_2O	0.860	Na	0.113
K	8.302	K_2O	10.000	K	0.863
Ba	0.025	BaO	0.028	Ba	0.001
Rb	0.101	Rb_2O	0.110	Rb	0.005
Cs	0.007	Cs_2O	0.007	Cs	0.000
F	0.082	F	0.082	F	0.018
Cl	0.000	Cl	0.000	Cl	0.000
*	0.000	OH	0.000	OH	1.982
		SUM	94.545		
		=			

* H_2O+ Calculated From OH (SUM+ = 22) = 4.42.
Corrected SUM Oxides = 98.96

Ball Ground Field (Beryl-bearing)

P-44B JONES (South)

ELEMENT	WT PCT	OXIDE	WT PCT	CATION/ANION OCCUPANCY FULL OCTAHEDRAL LAYER	
Si	21.594	SiO_2	46.200	Si	3.119
Al	17.361	Al_2O_3	32.800	Al4	0.881
				Al6	1.729
Ti	0.162	TiO_2	0.270	Ti	0.014
Fe^{+3}	1.748	Fe_2O_3	2.500	Fe^{+3}	0.127
Fe^{+2}	0.777	FeO	1.000	Fe^{+2}	0.056
Mn	0.032	MnO	0.041	Mn	0.002
Mg	0.398	MgO	0.660	Mg	0.066
Li	0.008	Li_2O	0.017	Li	0.005
		SUM OCTAHEDRAL CATIONS		=	2.000
Ca	0.027	CaO	0.038	Ca	0.003
Na	0.653	Na_2O	0.880	Na	0.115
K	8.136	K_2O	9.800	K	0.844
Ba	0.010	BaO	0.011	Ba	0.000
Rb	0.112	Rb_2O	0.130	Rb	0.006
Cs	0.006	Cs_2O	0.006	Cs	0.000
F	0.110	F	0.110	F	0.023
Cl	0.000	Cl	0.000	Cl	0.000
*	0.000	OH	0.000	OH	1.977
		SUM	94.417		
		=			

* H_2O+ Calculated From OH (SUM+ = 22) = 4.38.
Corrected SUM Oxides = 98.80

Ball Ground Field (Beryl-bearing)

P-85 DENSON

ELEMENT	WT PCT	OXIDE	WT PCT	CATION/ANION OCCUPANCY FULL OCTAHEDRAL LAYER	
Si	21.641	SiO_2	46.300	Si	3.113
Al	18.473	Al_2O_3	34.900	Al4	0.887
				Al6	1.880
Ti	0.024	TiO_2	0.040	Ti	0.002
Fe^{+3}	0.920	Fe_2O_3	1.315	Fe^{+3}	0.067
Fe^{+2}	0.389	FeO	0.500	Fe^{+2}	0.028
Mn	0.020	MnO	0.026	Mn	0.001
Mg	0.133	MgO	0.220	Mg	0.022
Li	0.000	Li_2O	0.001	Li	0.000
		SUM OCTAHEDRAL CATIONS		=	2.000
Ca	0.012	CaO	0.017	Ca	0.001
Na	0.616	Na_2O	0.830	Na	0.108
K	8.385	K_2O	10.100	K	0.866
Ba	0.005	BaO	0.006	Ba	0.000
Rb	0.183	Rb_2O	0.200	Rb	0.009
Cs	0.005	Cs_2O	0.006	Cs	0.000
F	0.110	F	0.110	F	0.023
Cl	0.000	Cl	0.000	Cl	0.000
*	0.000	OH	0.000	OH	1.977
		SUM	94.524		
		=			

* H_2O+ Calculated From OH (SUM+ = 22) = 4.42.
Corrected SUM Oxides = 98.94

Ball Ground Field (Beryl-bearing)

P-87 DENSON

ELEMENT	WT PCT	OXIDE	WT PCT	CATION/ANION OCCUPANCY FULL OCTAHEDRAL LAYER	
Si	21.547	SiO_2	46.100	Si	3.092
Al	18.737	Al_2O_3	35.400	Al4	0.908
				Al6	1.890
Ti	0.018	TiO_2	0.030	Ti	0.002
Fe^{+3}	0.730	Fe_2O_3	1.044	Fe^{+3}	0.053
Fe^{+2}	0.466	FeO	0.600	Fe^{+2}	0.034
Mn	0.019	MnO	0.025	Mn	0.001
Mg	0.127	MgO	0.210	Mg	0.021
Li	0.000	Li_2O	0.000	Li	0.000
		SUM OCTAHEDRAL CATIONS		=	2.000
Ca	0.005	CaO	0.007	Ca	0.001
Na	0.601	Na_2O	0.810	Na	0.105
K	8.385	K_2O	10.100	K	0.864
Ba	0.003	BaO	0.003	Ba	0.000
Rb	0.146	Rb_2O	0.160	Rb	0.007
Cs	0.003	Cs_2O	0.004	Cs	0.000
F	0.068	F	0.068	F	0.014
Cl	0.000	Cl	0.000	Cl	0.000
*	0.000	OH	0.000	OH	1.986
		SUM	94.532		
		=			

* H_2O+ Calculated From OH (SUM+ = 22) = 4.44.
Corrected SUM Oxides = 98.97

Ball Ground Field (Beryl-bearing)

P-88A DENSON (Crystal Center)

ELEMENT	WT PCT	OXIDE	WT PCT	CATION/ANION OCCUPANCY FULL OCTAHEDRAL LAYER	
Si	21.220	SiO_2	45.400	Si	3.098
Al	18.420	Al_2O_3	34.800	Al4	0.902
				Al6	1.897
Ti	0.018	TiO_2	0.030	Ti	0.002
Fe^{+3}	0.867	Fe_2O_3	1.240	Fe^{+3}	0.064
Fe^{+2}	0.326	FeO	0.420	Fe^{+2}	0.024
Mn	0.049	MnO	0.063	Mn	0.004
Mg	0.054	MgO	0.090	Mg	0.009
Li	0.001	Li_2O	0.002	Li	0.001
		SUM OCTAHEDRAL CATIONS		=	2.000
Ca	0.010	CaO	0.014	Ca	0.001
Na	0.594	Na_2O	0.800	Na	0.106
K	8.219	K_2O	9.900	K	0.862
Ba	0.004	BaO	0.004	Ba	0.000
Rb	0.192	Rb_2O	0.210	Rb	0.009
Cs	0.005	Cs_2O	0.006	Cs	0.000
F	0.100	F	0.100	F	0.022
Cl	0.000	Cl	0.000	Cl	0.000
*	0.000	OH	0.000	OH	1.978
		SUM	93.036		
		=			

* H_2O+ Calculated From OH (SUM+ = 22) = 4.36.
Corrected SUM Oxides = 97.39

Ball Ground Field (Beryl-bearing)

P-88B DENSON (Crystal Edge)

ELEMENT	WT PCT	OXIDE	WT PCT	CATION/ANION OCCUPANCY FULL OCTAHEDRAL LAYER	
Si	21.828	SiO_2	46.700	Si	3.167
Al	17.255	Al_2O_3	32.600	Al4	0.833
				Al6	1.773
Ti	0.342	TiO_2	0.570	Ti	0.029
Fe^{+3}	0.825	Fe_2O_3	1.180	Fe^{+3}	0.060
Fe^{+2}	0.777	FeO	1.000	Fe^{+2}	0.057
Mn	0.014	MnO	0.018	Mn	0.001
Mg	0.464	MgO	0.770	Mg	0.078
Li	0.003	Li_2O	0.007	Li	0.002
		SUM OCTAHEDRAL CATIONS		=	2.000
Ca	0.011	CaO	0.015	Ca	0.001
Na	0.527	Na_2O	0.710	Na	0.093
K	8.551	K_2O	10.300	K	0.891
Ba	0.021	BaO	0.023	Ba	0.001
Rb	0.229	Rb_2O	0.250	Rb	0.011
Cs	0.049	Cs_2O	0.052	Cs	0.001
F	0.190	F	0.190	F	0.041
Cl	0.000	Cl	0.000	Cl	0.000
*	0.000	OH	0.000	OH	1.959
		SUM	94.305		
		=			

* H_2O+ Calculated From OH (SUM+ = 22) = 4.34.
Corrected SUM Oxides = 98.65

Ball Ground Field (Beryl-bearing)

P-95G (Denson)

ELEMENT	WT PCT	OXIDE	WT PCT	CATION/ANION OCCUPANCY FULL OCTAHEDRAL LAYER	
Si	21.547	SiO_2	46.100	Si	3.122
Al	18.367	Al_2O_3	34.700	Al4	0.878
				Al6	1.891
Ti	0.024	TiO_2	0.040	Ti	0.002
Fe^{+3}	0.790	Fe_2O_3	1.130	Fe^{+3}	0.058
Fe^{+2}	0.311	FeO	0.400	Fe^{+2}	0.023
Mn	0.016	MnO	0.021	Mn	0.001
Mg	0.145	MgO	0.240	Mg	0.024
Li	0.001	Li_2O	0.003	Li	0.001
		SUM OCTAHEDRAL CATIONS		=	2.000
Ca	0.011	CaO	0.015	Ca	0.001
Na	0.608	Na_2O	0.820	Na	0.108
K	8.468	K_2O	10.200	K	0.881
Ba	0.006	BaO	0.007	Ba	0.000
Rb	0.080	Rb_2O	0.087	Rb	0.004
Cs	0.005	Cs_2O	0.006	Cs	0.000
F	0.130	F	0.130	F	0.028
Cl	0.000	Cl	0.000	Cl	0.000
*	0.000	OH	0.000	OH	1.972
		SUM	93.844		
		=			

* H_2O+ Calculated From OH (SUM+ = 22) = 4.38.
Corrected SUM Oxides = 98.22

Ball Ground Field (Beryl-bearing)

P-100 MULLINAX

ELEMENT	WT PCT	OXIDE	WT PCT	CATION/ANION OCCUPANCY FULL OCTAHEDRAL LAYER	
Si	23.323	SiO_2	49.900	Si	3.368
Al	16.620	Al_2O_3	31.400	Al4	0.632
				Al6	1.866
Ti	0.036	TiO_2	0.060	Ti	0.003
Fe^{+3}	0.832	Fe_2O_3	1.190	Fe^{+3}	0.060
Fe^{+2}	0.777	FeO	1.000	Fe^{+2}	0.056
Mn	0.085	MnO	0.110	Mn	0.006
Mg	0.036	MgO	0.060	Mg	0.006
Li	0.003	Li_2O	0.007	Li	0.002
		SUM OCTAHEDRAL CATIONS		=	2.000
Ca	0.037	CaO	0.052	Ca	0.004
Na	0.542	Na_2O	0.730	Na	0.096
K	7.970	K_2O	9.600	K	0.827
Ba	0.021	BaO	0.023	Ba	0.001
Rb	0.146	Rb_2O	0.160	Rb	0.007
Cs	0.004	Cs_2O	0.005	Cs	0.000
F	0.110	F	0.110	F	0.023
Cl	0.000	Cl	0.000	Cl	0.000
*	0.000	OH	0.000	OH	1.977
		SUM	94.360		
		=			

* H_2O+ Calculated From OH (SUM+ = 22) = 4.44.
Corrected SUM Oxides = 98.80

Ball Ground Field (Beryl-bearing)

P-106B HENDRIX

ELEMENT	WT PCT	OXIDE	WT PCT	CATION/ANION OCCUPANCY FULL OCTAHEDRAL LAYER	
Si	23.183	SiO_2	49.600	Si	3.337
Al	16.355	Al_2O_3	30.900	Al4	0.663
				Al6	1.787
Ti	0.162	TiO_2	0.270	Ti	0.014
Fe^{+3}	1.539	Fe_2O_3	2.200	Fe^{+3}	0.111
Fe^{+2}	0.505	FeO	0.520	Fe^{+2}	0.029
Mn	0.051	MnO	0.066	Mn	0.004
Mg	0.235	MgO	0.390	Mg	0.039
Li	0.026	Li_2O	0.028	Li	0.008
		SUM OCTAHEDRAL CATIONS		=	2.000
Ca	0.048	CaO	0.067	Ca	0.005
Na	0.616	Na_2O	0.830	Na	0.108
K	7.804	K_2O	9.400	K	0.807
Ba	0.019	BaO	0.021	Ba	0.001
Rb	0.146	Rb_2O	0.160	Rb	0.007
Cs	0.003	Cs_2O	0.003	Cs	0.000
F	0.430	F	0.430	F	0.091
Cl	0.000	Cl	0.000	Cl	0.000
*	0.000	OH	0.000	OH	1.974
		SUM	99.133		
		=			

* H_2O+ Calculated From OH (SUM+ = 22) = 4.39.
Corrected SUM Oxides = 98.24

Ball Ground Field (Beryl-bearing)

P-107 HENDRIX

ELEMENT	WT PCT	OXIDE	WT PCT	CATION/ANION OCCUPANCY FULL OCTAHEDRAL LAYER	
Si	21.828	SiO_2	46.700	Si	3.175
Al	17.520	Al_2O_3	33.100	Al4	0.825
				Al6	1.827
Ti	0.096	TiO_2	0.160	Ti	0.008
Fe^{+3}	1.539	Fe_2O_3	2.200	Fe^{+3}	0.113
Fe^{+2}	0.326	FeO	0.420	Fe^{+2}	0.024
Mn	0.108	MnO	0.140	Mn	0.008
Mg	0.066	MgO	0.110	Mg	0.011
Li	0.016	Li_2O	0.034	Li	0.009
		SUM OCTAHEDRAL CATIONS		=	2.000
Ca	0.023	CaO	0.032	Ca	0.002
Na	0.549	Na_2O	0.740	Na	0.098
K	8.302	K_2O	10.000	K	0.867
Ba	0.010	BaO	0.011	Ba	0.000
Rb	0.311	Rb_2O	0.340	Rb	0.015
Cs	0.011	Cs_2O	0.012	Cs	0.000
F	0.360	F	0.360	F	0.077
Cl	0.000	Cl	0.000	Cl	0.000
*	0.000	OH	0.000	OH	2.131
		SUM	98.907		
		=			

* H_2O+ Calculated From OH (SUM+ = 22) = 4.41.
Corrected SUM Oxides = 98.29

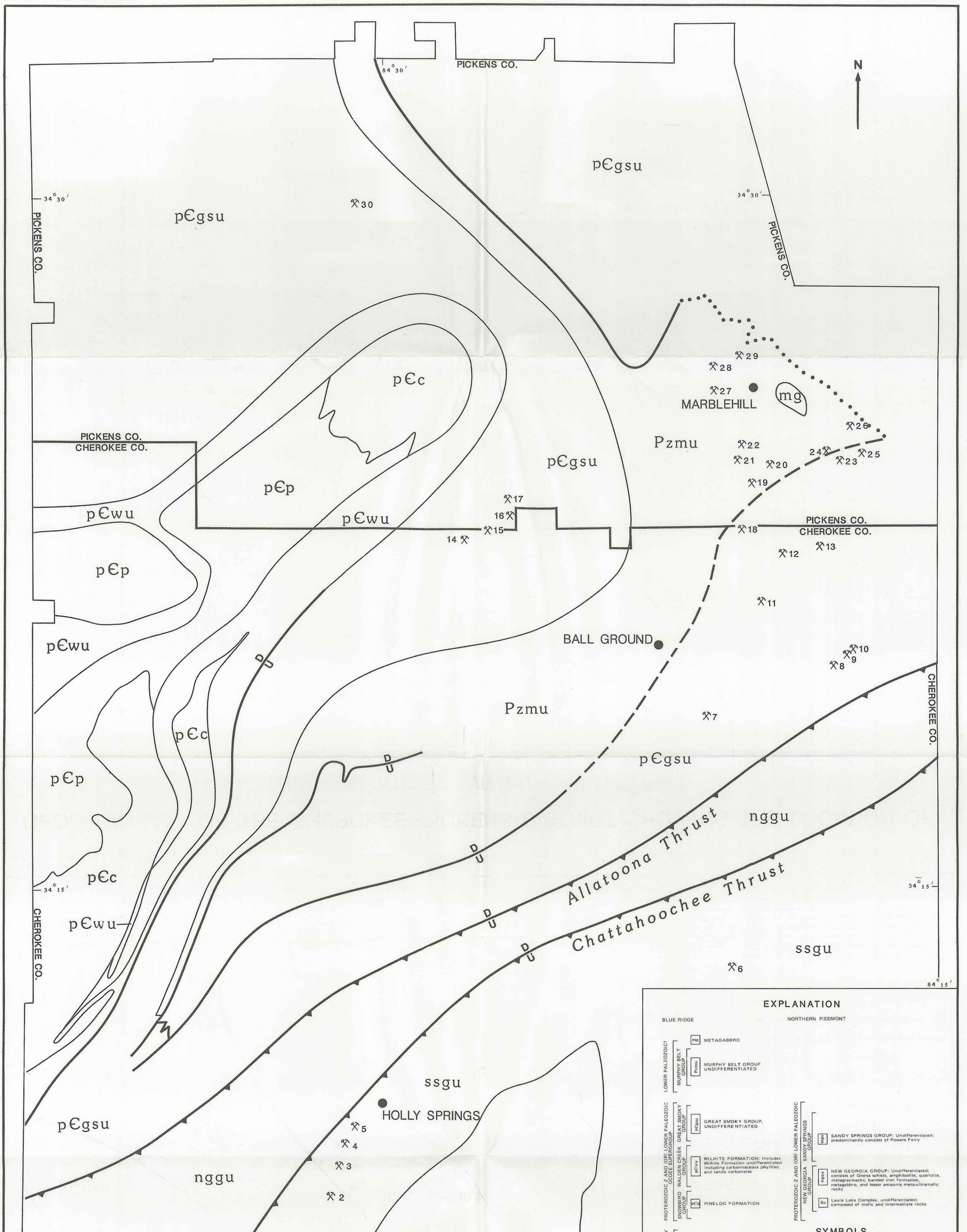

EXPLANATION

BLUE RIDGE — NORTHERN PIEDMONT

LOWER PALEOZOIC?
- MURPHY BELT GROUP
  - mg — METAGABBRO
  - Pzmu — MURPHY BELT GROUP UNDIFFERENTIATED

PROTEROZOIC Z AND (OR) LOWER PALEOZOIC
- OCOEE SUPERGROUP
  - WALDEN CREEK GROUP
    - GREAT SMOKY GROUP
      - pCgsu — GREAT SMOKY GROUP, UNDIFFERENTIATED
    - pCwu — WILHITE FORMATION: Includes Wilhite Formation undifferentiated including carbonnaceous phyllites and sandy carbonates
  - SNOWBIRD GROUP
    - pCp — PINELOG FORMATION

PROTEROZOIC Z AND (OR) LOWER PALEOZOIC
- SANDY SPRINGS GROUP
  - ssgu — SANDY SPRINGS GROUP: Undifferentiated; predominantly consists of Powers Ferry
- NEW GEORGIA GROUP
  - nggu — NEW GEORGIA GROUP: Undifferentiated; consists of Gneiss schists, amphibolite, quartzite, metagraywacke, banded iron formation, metagabbro, and lesser amounts meta-ultramafic rocks
  - llu — Laura Lake Complex, undifferentiated; composed of mafic and intermediate rocks

PROTEROZOIC Y
- pCc — CORBIN GNEISS COMPLEX

SYMBOLS

- PEGMATITE LOCATION
- CONTACT, DASHED WHERE INFERRED
- THRUST FAULT, DASHED WHERE INFERRED,
- D U REVERSE FAULT, DASHED WHERE INFERRED DOTTED WHERE UNCERTAIN

PEGMATITE DEPOSITS: 1) Kuykendall Prospect, 2) Dean Mine, 3) Hause Mine (Toonigh Cr.), 4) Hillhouse Prospect, 5) Wacaster Mine, 6) Cook Mine, 7) Hendrix Prospect, 8) Amphlett Mine (south workings), 9) Amphlett Mine (middle workings), 10) Amphlett Mine (north workings), 11) Cochran Mine, 12) Revis Prospect, 13) Densmore Prospect, 14) Bennett Mine 15) Carney Prospect, 16) Denson Mines (Rock Cr.), 17) Cagle Mine, 18) Fowler-Freeman Mine, 19) Jones Mine, 20) Reynolds Mine, 21) Davis Prospect, 22) Howell Mine, 23) Wilkie Prospect, 24) Worley Prospect, 25) Poole Mine, 26) Partian Prospect, 27) Marblehill Quarry Prospect, 28) Marblehill Prospects, 29) Foster Prospects, 30) Mullinax Prospect

Base from U.S. Geological Survey
Cartersville Georgia, 1:100,000, 1981
and Dalton Georgia, 1:100,000, 1981

Modified after Furcron and Teague, 1947; McConnell and Costello, 1980 and McConnell and Costello, 1982.

GEOLOGIC MAP OF THE CHEROKEE–PICKENS DISTRICT SHOWING THE LOCATION OF THE PEGMATITES WITHIN THE DISTRICT.

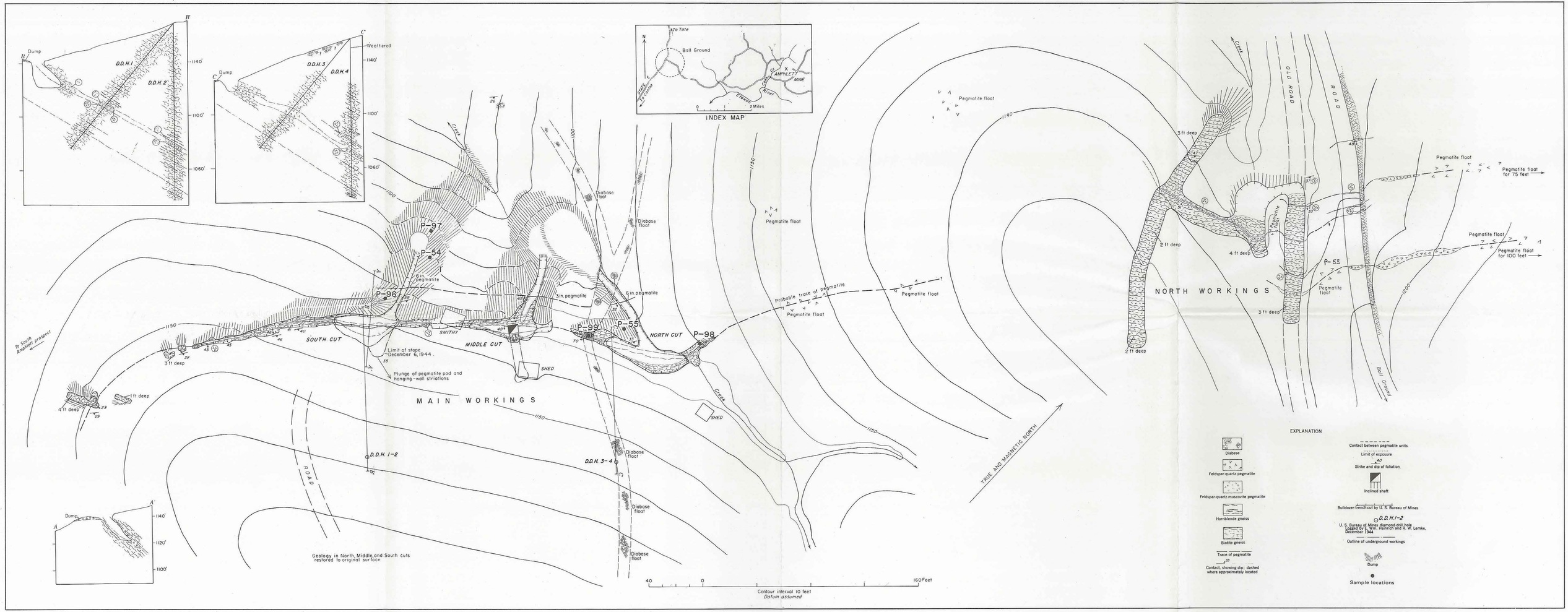
B
B'
Dump
D.D.H. 1
D.D.H. 2
1140'
1100'
1060'
C
C'
Weathered
D.D.H. 3
D.D.H. 4
A
A'
1140'
1120'
1100'
INDEX MAP
To Tate
Ball Ground
Etowah River
AMPHERY MINE
2 Miles
To South Amphery prospect
SOUTH CUT
SMITHY
MIDDLE CUT
NORTH CUT
MAIN WORKINGS
P-97
P-54
P-96
P-98
P-55
Limit of stope December 6, 1944.
Plunge of pegmatite pod and hanging-wall striations
SHED
Diabase float
Pegmatite float
Probable trace of pegmatite
3 ft deep
4 ft deep
2 ft deep
D.D.H. 1-2
D.D.H. 3-4
ROAD
Geology in North, Middle, and South cuts restored to original surface
TRUE AND MAGNETIC NORTH
NORTH WORKINGS
OLD ROAD
Pegmatite float for 75 feet
Pegmatite float for 100 feet
Ball Ground
40 0 160 Feet
Contour interval 10 feet
Datum assumed
EXPLANATION
Diabase
Feldspar-quartz pegmatite
Feldspar-quartz muscovite pegmatite
Hornblende gneiss
Biotite gneiss
Trace of pegmatite
Contact, showing dip; dashed where approximately located
Contact between pegmatite units
Limit of exposure
Strike and dip of foliation
Inclined shaft
Bulldozer-trench cut by U. S. Bureau of Mines
D.D.H.1-2
U. S. Bureau of Mines diamond-drill hole Logged by E. Wm. Heinrich and R. W. Lemke, December 1944
Outline of underground workings
Dump
Sample locations

For convenience in selecting our reports from your bookshelves, they will be color-keyed across the spine by subject as follows:

Red	Valley and Ridge mapping and structural geology
Dk. Purple	Piedmont and Blue Ridge mapping and structural geology
Maroon	Coastal Plain mapping and stratigraphy
Lt. Green	Paleontology
Lt. Blue	Coastal Zone studies
Dk. Green	Geochemical and geophysical studies
Dk. Blue	Hydrology
Olive	Economic geology
	Mining directory
Yellow	Environmental studies
	Engineering studies
Dk. Orange	Bibliographies and lists of publications
Brown	Petroleum and natural gas
Black	Field trip guidebooks
Dk. Brown	Collections of papers

Colors have been selected at random, and will be augmented as new subjects are published.

Editor: Patricia Allgood

$3,584/500